Dictyostelium Chemotaxis studied with Fluorescence Fluctuation Spectroscopy

Ruchira

Promotoren:
Prof. dr. A.J.W.G. Visser
hoogleraar Microspectroscopie in de Biochemie
Wageningen Universiteit

Prof. dr. P.J.M. van Haastert
hoogleraar Biochemie
Universiteit Groningen

Promotiecommissie:
Prof. dr. Y. Engelborghs, Katholieke Universiteit Leuven, België
Dr. G. Gerisch, Max-Planck-Institut für Biochemie, Martinsried, Germany
Prof. dr. H. C. Gerritsen, Universiteit Utrecht
Dr. A.B. Houtsmuller, Erasmus Universiteit Rotterdam
Prof. dr. T. Bisseling, Wageningen Universiteit

Dit onderzoek is uitgevoerd binnen de onderzoekschool EPS.

Dictyostelium Chemotaxis studied with Fluorescence Fluctuation Spectroscopy

Ruchira

Proefschrift
ter verkrijging van de graad van doctor
op gezag van de rector magnificus
van Wageningen Universiteit,
Prof. dr. M. J. Kropff,
in het openbaar te verdedigen
op dinsdag 20 september 2005
des namiddags te half twee in de Aula

ISBN: 90-8504-263-1

Preface

This thesis describes the research that I performed in the Laboratory of Biochemistry at Wageningen University between October 2000 and March 2005. This period has been an educative and enjoyable experience for me and I would like to express my gratitude to all those who have helped in making it so.

It was Ton Visser's confidence in me that made my entry into the fascinating world of molecules, cells and fluorescence microscopy possible. Ton gave me all the independence to pursue the research goals and was always available for discussions and smoothing down obstacles as and when they arose. His encouragement for participating in conferences and presenting my work has helped me remain aware of new developments and gain more self-confidence. I look forward to working with him in my upcoming projects. My introduction to the 'social amoeba' *Dictyostelium* was made possible by Peter van Haastert. His enthusiasm for the happenings in this tiny organism is infectious and consequently the discussions with Peter were always very inspiring and fruitful. Though I regret that the distance between Wageningen and Groningen prevented these discussions from being more frequent.

I am greatly indebted to Mark Hink for teaching me the intricacies of fluorescence fluctuation spectroscopy. Mark's approachable and helpful nature meant that I could go to him with every kind of problem and he would always find time to discuss it. His critical comments on this thesis have also been very helpful. I look forward to continuing a lively interaction with him (though I can assure him that he will never be able to persuade me to take up ice-skating!). Also of great help, especially when I was finding my way around here, was Jan Willem Borst. He introduced me to not only the lab and the instruments but also helped me through the Dutch bureaucracy. His lively presence along with his questions and comments added life to the weekly work-discussions. I would also like to thank Mark and Jan Willem for agreeing to be my paranymphs.

My association with *Dictyostelium* would not have been successful without the constant support and guidance from the Cell Biochemistry group of Groningen University. I would specially like to thank Leonard Bosgraaf for all the help and guidance he provided me in working with *Dictyostelium* cells and for his prompt and informative responses to my e-mail queries. I would also like to thank him for the PH domain-GFP and free GFP expressing cell lines. I would like to acknowledge Mieke Blaauw and Jaco Knol for the GFP-Gβγ and PhLP1-null cell lines and a very fruitful cooperation; Douwe Veltman, Marten Postma, Harriet Loovers and other members of the group for enjoyable discussions.

I would also like to thank Peter Devreotes and Chris Janetopoulos for giving me an opportunity to visit their lab in Baltimore, USA and for generously providing me with cell lines, which unfortunately I was not able to use. I also appreciate the help provided by Victor Skakun with the FCS data processor software.

The pleasant working environment at the laboratory of Biochemistry, Wageningen has contributed much to my enjoyment of the time as an *AIO*. I would like to thank Sacco, Adrie, Mark (Kwaaitaal), Jose, Monique, Niek, Carlo and Sanne (who is also a nice office-mate) for their interest in my work and their critical comments during our weekly work discussions, which helped me to improve myself. I would also like to thank Adrie for the model of GFP tagged G-protein, which appears on the cover of this thesis. Also of immense help was Sjef whose mass-spectrometric/ liquid chromatographic characterization of a fluorescently labelled cAMP analogue ultimately saved me a lot of time. Laura's efficient help with administrative things has saved many a hassle for me. Mariëlle was always at hand for any queries a *foreigner* might have about the Netherlands and actively kept the lunch group going. Yee was able to infect me with her enthusiasm for doing sports and learning the Dutch language, about which I am very glad. The 'lunch time is Dutch time' idea that was carried forward with gusto especially by Mariëlle, Yee and Sjef has helped my Dutch language skills, which I hope will keep improving. The dinners at the *mensa* with Hans were also enjoyable and so was Robert's company as my office-mate in the first year of my PhD.

My coming to Netherlands and taking the first steps towards building a scientific career would not have been possible without the support and encouragement of my family. My parents have nurtured my interest in science and taught me to look beyond conventions and traditions, which has encouraged me to think rationally and contributed to my evolution as a scientist. The long chats and discussions I have had with my sisters on all matters, scientific or otherwise, have been a continuous source of inspiration to me. The visits to Gerty and Fritz and their warmth and affection have been a source of comfort and assurance to me, especially during my first year in the Netherlands, when I was still adjusting to a new culture and lifestyle. The openness and love with which Henry, Ans and Wouter have accepted me as a part of their family has added much to my feeling of being at home here in the Netherlands.

There are not words enough to describe what Maarten has meant to me during this time. He has motivated me when things looked dull, criticized me when I was not at my best and cheered me at every success. With his love and support nothing seems impossible.

Ruchira
Wageningen, August 2005

CONTENTS

1 General Introduction

The movement of cells in the direction of a chemical gradient, also known as chemotaxis, is a vital biological process. Chemotaxis plays a central role in embryogenesis, immune response, wound healing and in progression of diseases such as cancer, artherosclerosis, arthritis and mental retardation (Buehr 1997; Thelen 2001; Balkwill 2004; Martin and Parkhurst 2004). During chemotaxis, minute extracellular signals are translated into complex cellular responses such as change in morphology and motility. This requires the coordination and interaction of various cellular signaling networks composed of a variety of regulatory molecules (Postma *et al.,* 2004). To understand the chemotaxis mechanism at a molecular level it is important to know how, when and where these regulatory molecules get activated and interact. It is essential to *look* into chemotaxing cells and obtain detailed information about the localization and dynamics of the signaling processes. The chemotaxis mechanism in eukaryotic cells is highly conserved, with mammalian cells showing remarkable similarity in chemotaxis to the simple organism *Dictyostelium discoideum* and hence, this organism is used as a model system to study chemotaxis. *Dictyostelium* as a model system has the advantage that it is genetically manageable and easily accessible for biochemical and biological studies (Manahan *et al.,* 2004). In this thesis, information about various regulatory molecules involved in the chemotaxis mechanism of *Dictyostelium* cells has been obtained using fluorescence fluctuation spectroscopy.

1.1 The Chemotaxis Mechanism of *Dictyostelium discoideum*

1.1.1 The Life Cycle

Dictyostelium is a cellular slime mould, often referred to as a social amoeba because of its typical life cycle. The organism grows as free-living amoebae in the soil, feeding on bacteria. Upon exhaustion of the food supply, *Dictyostelium* undergoes a complex developmental cycle, where upto a hundred thousand amoebae aggregate and differentiate to eventually form a multicellular fruiting body (Fig. 1.1). The fruiting body consists of spores embedded in a slime droplet on top of highly vacuolized cells arranged in a stalk. When environmental conditions are suitable the spores germinate to form the single cells again, thereby completing the life cycle.

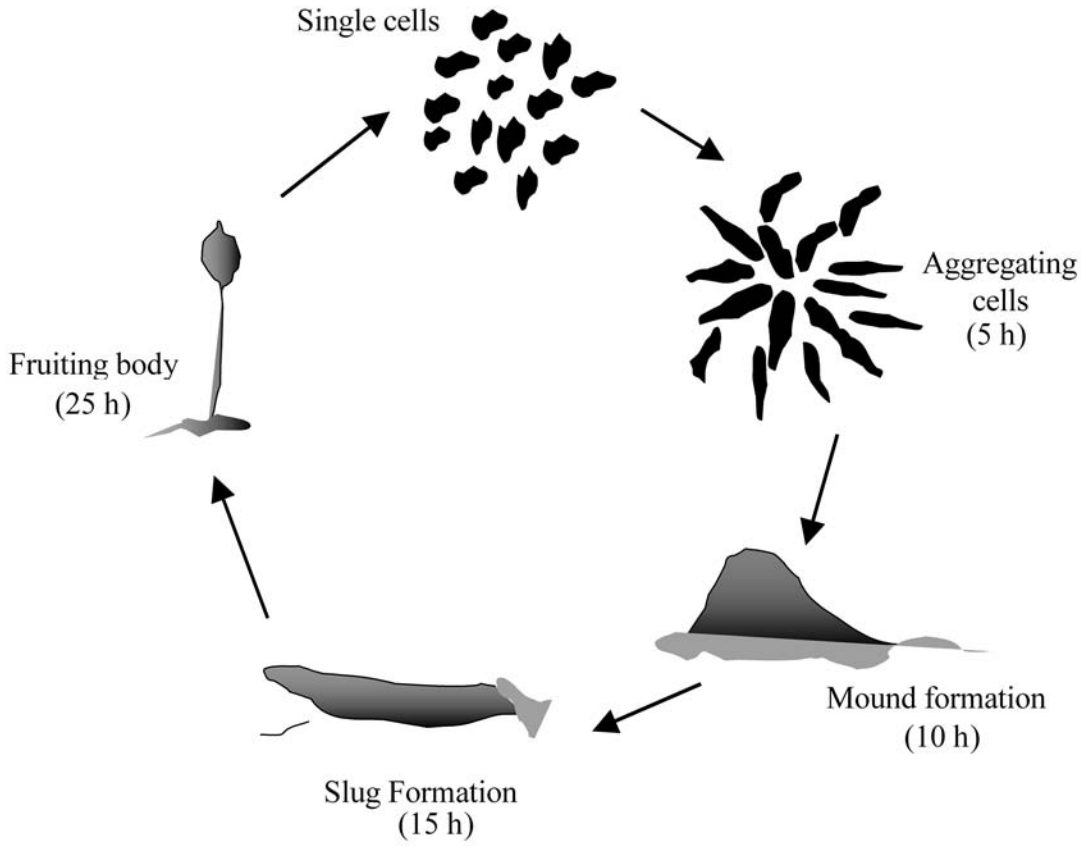

Figure 1.1: Life Cycle of *Dictyostelium discoideum.* Unicellular *Dictyostelium* when faced with starvation undergo a complex developmental cycle to form multicellular fruiting bodies. The formation of a fruiting body from beginning of starvation of single cells takes around 25 hours.

Chemotaxis is necessary for *Dictyostelium* to find bacteria in the vegetative stage and to aggregate when faced with starvation. Aggregation of starving *Dictyostelium* cells occurs in response to a concentration gradient of adenosine 3′,5′-cyclic monophosphate (cAMP). A few cells forming aggregation centers emanate pulses of cAMP, which are detected, amplified and relayed further by the surrounding cells. cAMP thus acts as a chemoattractant to bring the cells together and also as a morphogen to induce genes required for the process. Cells chemotaxing towards aggregation centers extend pseudopods (protrusion of the plasma membrane) preferentially in the direction of rising cAMP concentrations and acquire an elongated, polarized morphology, with a defined anterior and posterior. Chemotaxis of a cell requires the coordination and integration of spatial and temporal information by various signaling networks working together. A detailed description of the various pathways currently known can be found in Kimmel and Parent 2003 and Manahan *et al.,* 2004.

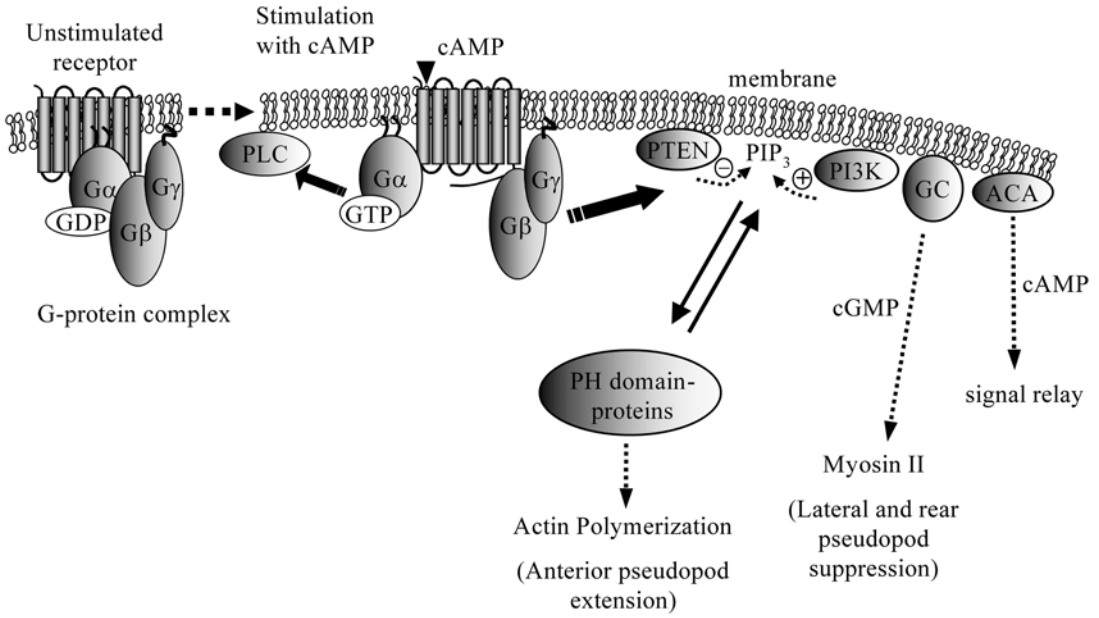

Figure 1.2: Chemotaxis Mechanism. A simplified depiction of the events leading to chemotaxis in *Dictyostelium discoideum*. The extracellular signal is transmitted to the cell interior by means of transmembrane receptors coupled to heterotrimeric G-proteins. Binding of cAMP molecule stimulates the receptor and results in dissociation of the G-protein complex into Gβγ and Gα, which can then activate downstream effectors PLC (phospholipase C), PI3K (phosphoinositide 3-kinase), PTEN (PI3 phosphatase), GC (guanylyl cyclase) and ACA (adenylyl cyclase A). PI3K increases phosphotidylinositol triphosphate (PIP_3) levels at membrane leading to translocation of PH (pleckstrin homology) domain containing proteins from cytoplasm to the membrane. This is thought to be responsible for actin polymerization. PIP_3 is degraded by PTEN. Second messengers cGMP and cAMP produced by GC and ACA are responsible for suppression of lateral and rear pseudopods and signal relay, respectively.

1.1.2 The Receptor and Heterotrimeric G-protein

The external gradient information is transmitted to the cell interior by means of surface receptors (Fig. 1.2). The extracellular cAMP molecules bind to receptors on the plasma membrane that interact with heterotrimeric guanosine triphosphate binding proteins (G-proteins). Four genes encoding cAMP receptors (cARs) have been identified, of which cAR1 is essential for the cell development (Manahan *et al.,* 2004). The deduced amino acid sequences for cARs predict that they pass the membrane seven times, typical for G-protein coupled receptors (GPCRs) (Kim *et al.,* 1997; Xiao *et al.,* 1997). The heterotrimeric G-protein, located on the inner face of the plasma membrane, is a complex of three proteins, Gα, Gβ and Gγ. Upon binding of a ligand molecule, a GPCR is thought to undergo a conformational change leading to the activation of the G-protein (Bissantz 2003; Yeagle and Albert 2003). Gα, which is GDP-bound in its inactive state, exchanges the GDP for a GTP and dissociates from the Gβγ subunits. The Gα and Gβγ are then free to interact with downstream effectors and transduce the signal further (Clapham and Neer 1997; Sprang 1997; Morris and Malbon 1999; Janetopoulos *et al.,* 2001; Cabrera-Vera *et al.,* 2003). Throughout the signaling the Gβ and Gγ

subunits are associated in a tight complex. The formation of this complex is essential for the stability and proper functioning of both, β and γ subunits. The assembly of Gβγ is thought to occur in the cytosol where the Gγ subunit also undergoes a lipid modification. This lipid modification is responsible not only for the membrane localization of the Gβγ complex but also for its interaction with Gα (Schmidt and Neer 1991; Iniguez-Lluhi *et al.,* 1992; Higgins and Casey 1994; Wedegaertner *et al.,* 1995; Garcia-Higuera *et al.,* 1996; Higgins and Casey 1996).

Dictyostelium contains at least 11 α subunits of which mainly $G\alpha_2$ is thought to be associated with the cAMP receptor (Brzostowski *et al.,* 2002). There is however, only one G-protein β and one γ subunit and the Gβγ complex is essential for chemotaxis (Lilly *et al.,* 1993; Wu *et al.,* 1995; Jin *et al.,* 1998; Zhang *et al.,* 2001). In fact, it appears that the downstream signaling events are primarily mediated by Gβγ (Manahan *et al.,* 2004).

1.1.3 Downstream Effectors

Five main effectors that are regulated by the activation of cAR1 are phospholipase C (PLC), adenylyl cyclase A (ACA), guanylyl cyclase (GC), phosphoinositide 3-kinase (PI3K) and PI 3-phosphatase (PTEN). The PLC pathway is not essential for chemotaxis as cells lacking PLC or putative inositol (1,4,5)-phosphatase (IP_3) receptor do not show marked chemotaxis defects (Drayer *et al.,* 1994; Traynor *et al.,* 2000). Also ACA activation is not essential for chemotaxis as cells lacking ACA can respond to cAMP gradients. However, its localization at the posterior of a chemotaxing cell helps in relay of the signal over long range and *aca* null cells are unable to align in a head-to-tail fashion to form aggregation streams (Insall 2003; Kriebel *et al.,* 2003).

The other pathways, of GC, PI3K and PTEN are needed for efficient chemotaxis. Two GCs – soluble GC (sGC) and GCA have been identified in *Dictyostelium discoideum* (Roelofs *et al.,* 2001a; Roelofs *et al.,* 2001b; Roelofs and Van Haastert 2002). Cells lacking the two GCs generate no cGMP (guanosine 3′,5′-cyclic monophosphate), aggregate slowly and exhibit reduced chemotactic activity. The cGMP pathway is thought to be responsible for myosin filament formation at the rear of the cell and suppression of pseudopod formation at the lateral edges and back of the cell (Bosgraaf *et al.,* 2002). The PI3K and PTEN, on the other hand, appear to control the events at the leading edge of a chemotaxing cell (Chung and Firtel 2002; Iijima *et al.,* 2002). While G-protein mediated activation of PI3K increases local levels of phosphatidylinositol triphosphate, $PI(3,4,5)P_3$, at cell surface, PTEN is responsible for its degradation. In a chemotaxing cell, PI3K is focused at the leading edge whereas PTEN is restricted to the sides and rear of the cell resulting in increased $PI(3,4,5)P_3$ levels at the leading edge. Local levels of $PI(3,4,5)P_3$ at the inner cell membrane

regulate actin polymerization by regulating chemotactic events such as recruitment of pleckstrin homology (PH) domain containing proteins. PH domains are homologous regions of ~120 amino acids found in a number of proteins that are quite diverse in their cellular functions. They can form electrostatically polarized tertiary structures with a positively charged face that can interact with negatively charged membrane surfaces. PH domains are thought to be responsible for translocation of cytosolic PH domain containing proteins to the plasma membrane, where they can initiate further action (Bottomley *et al.,* 1998; Hirata *et al.,* 1998; Lemmon and Ferguson 2000). In *Dictyostelium*, PH domain containing proteins such as, cytosolic regulator of adenylyl cyclase (CRAC), protein kinase B (PKB) and PH domain containing protein A (PhdA), spatially localize downstream signaling events (Parent *et al.,* 1998; Parent 2004).

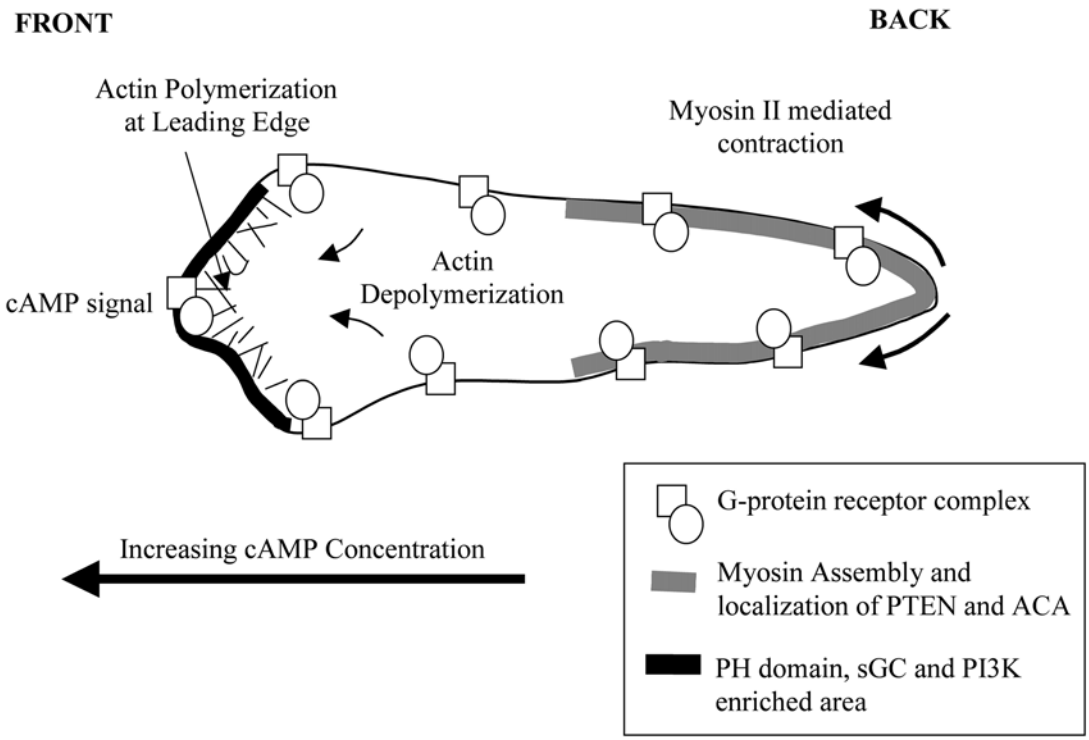

Figure 1.3: Cell Polarization. Cells chemotaxing in cAMP gradients display a defined front and back. Though the cAMP receptor cAR1 and the G-proteins are uniformly distributed around the cells, their downstream effectors display differential localization in the cell.

1.1.4 Chemotaxing cells are polarized

In cells moving in shallow cAMP gradients, cAR1 and G-proteins exhibit nearly uniform distribution on the cell surface (Xiao *et al.,* 1997; Jin *et al.,* 2000) (Fig. 1.3). However, their downstream effectors - PI3K, PTEN, F-actin, ACA, sGC and myosin II are highly localized (Kimmel and Parent 2003; Manahan *et al.,* 2004). Thus, chemotaxing cells are able to transduce and amplify weak extracellular signals into

highly organized steep intracellular gradients. How this is achieved is still poorly understood. Further investigations that can provide molecular level information on dynamics and interactions of the various regulatory proteins in moving cells are thus needed.

1.2 Fluorescence Fluctuation Spectroscopy

A technique of choice for obtaining quantitative information on dynamic events and molecular interactions in living cells is fluorescence fluctuation spectroscopy (FFS). It provides a sensitive, specific and non-invasive tool to probe dynamics of fluorescent species with high spatial and temporal resolution in living cells. The protein of interest can be tagged with a fluorescent molecule, e.g. an organic dye, and introduced in cells. Or more favorably, an intrinsically fluorescent protein such as the green fluorescent protein (GFP) can be genetically fused to the protein of interest, with the fluorescent fusion protein maintaining its normal function and localization (Tsien 1998). This fusion protein can be expressed in cells, making the use of invasive techniques such as microinjection and electroporation unnecessary. FFS makes use of tiny, spontaneous fluorescence intensity fluctuations caused by changes in emission characteristics of fluorescent molecules in thermodynamic equilibrium, to extract information about their physical parameters (Chen *et al.,* 1999a; Levin and Carson 2004; Vukojevic *et al.,* 2005) (Fig. 1.4). The fluctuations are monitored in a small (< 1 femtolitre) observation volume created in a confocal microscope by a tightly focused laser beam and a pinhole in the image plane. Since relative intensity fluctuations become stronger if the number of molecules in the observation volume is small, this technique works best with dilute (concentration ~ nano molar) solutions making it suitable for detection of proteins expressed at low levels in living cells. The intensity fluctuations monitored over time, as in fluorescence correlation spectroscopy (FCS) or a distribution of intensity fluctuation amplitudes, as in photon counting histogram (PCH) analysis or fluorescence intensity distribution analysis (FIDA) can provide a wealth of information about local concentrations, mobility coefficients and molecular interactions of fluorescent species in living cells (Chen *et al.,* 1999b; Kask *et al.,* 1999; Hess *et al.,* 2002).

1.2.1 Fluorescence Correlation Spectroscopy (FCS)

FCS can monitor any molecular process that gives rise to fluctuations in the intensity of a fluorescent species including translational diffusion, rotational diffusion, conformational changes and association and dissociation processes

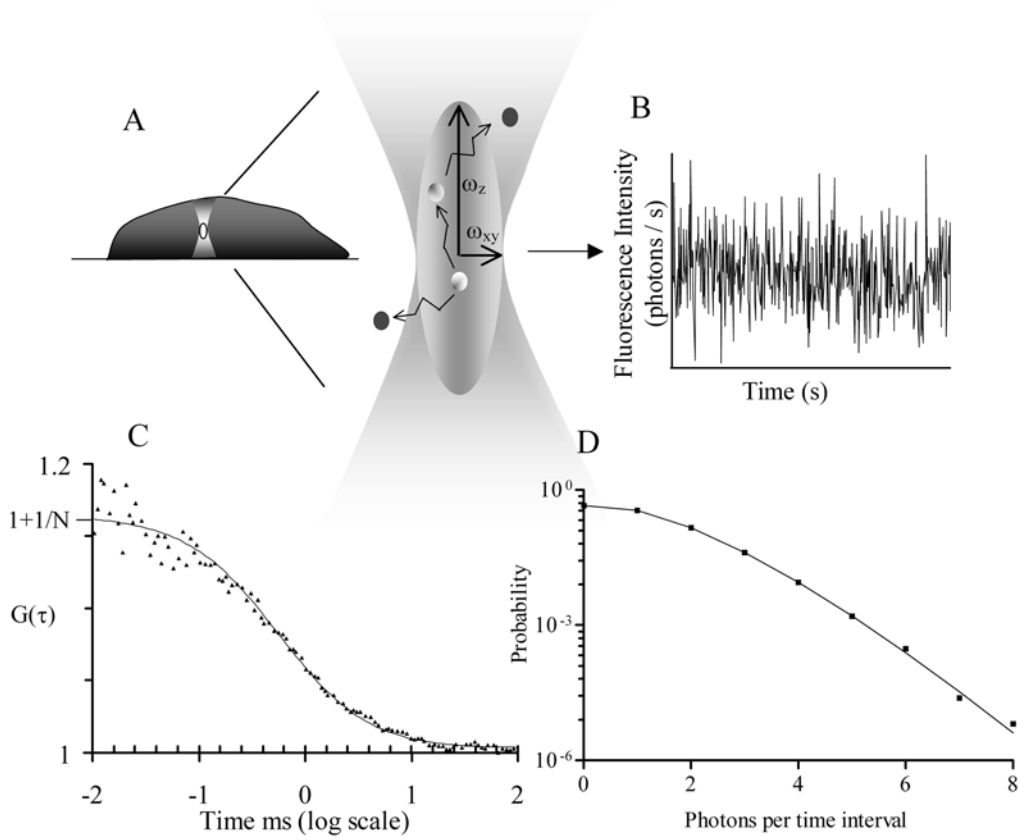

Figure 1.4: Fluorescence fluctuation spectroscopy. (A) Using a focused laser beam in a confocal setup a small observation volume is created in the sample (depicted here as a cell). This 3D Gaussian volume is described by an axial radius ω_z and equatorial radius ω_{xy}. Molecules moving into this volume get excited and give rise to burst of photons. (B) The fluctuations in the fluorescence intensity (or photon counts) as molecules move in and out of the observation volume are monitored. (C) The temporal intensity fluctuations can be autocorrelated to give rise to the autocorrelation curve, the decay of which contains information about kinetic events causing the fluctuation, such as diffusion of molecules. The amplitude of the curve extrapolated to time=0 is inversely proportional to the average number of molecules present in the observation volume. (D) The amplitude of the intensity fluctuations can be plotted as a probability distribution of detecting certain photons per time interval giving rise to the photon counting histogram (PCH). PCH analysis gives quantitative information about the molecular brightness and average concentration of fluorescent species.

(Hess *et al.,* 2002; Haustein and Schwille 2003). In recent years, FCS has been increasingly applied to living cells. The applications include the measurement of intracellular diffusion of biologically relevant molecules (Politz *et al.,* 1998; Schwille *et al.,* 1999), active protein transport (Köhler *et al.,* 2000), anomalous diffusion (Wachsmuth *et al.,* 2000; Weiss *et al.,* 2003; Weiss *et al.,* 2004), intracellular viscosity (Yoshida *et al.,* 2001) and ligand-receptor interactions (Hegener *et al.,* 2002; Briddon *et al.,* 2004; Hegener *et al.,* 2004).

FCS encompasses monitoring of the fluorescence emitted from a small observation volume as a function of time. The recorded emission signal, which is proportional to the number of fluorescent species present in the volume, fluctuates as molecules diffuse in

and out of the volume and as molecules transform to and from fluorescent states. The intensity fluctuations are temporally autocorrelated, resulting in the autocorrelation curve that carries information about the time scale of the dynamics and the average number of independent fluorescent species in the observation volume.

The normalized fluorescence fluctuation autocorrelation function $G(\tau)$ is defined as

$$G(\tau) = \frac{\langle F(t) \cdot F(t+\tau) \rangle}{\langle F(t) \rangle^2} = 1 + \frac{\langle \delta F(t) \cdot \delta F(t+\tau) \rangle}{\langle F(t) \rangle^2} \tag{1.1}$$

where, $F(t)$ is the fluorescence intensity at time t and $F(t + \tau)$ is the intensity after lag time τ. The angular brackets ($\langle\rangle$) indicate the quantities are averages. δF denotes the fluctuations from the average fluorescence intensity with $\delta F(t) = F(t) - \langle F(t) \rangle$. The fluorescence intensity fluctuations depend on various physical parameters, e.g., the overall fluorescence detection efficiency and spatial distribution of the excitation intensity.

When fluctuations arise only due to the free diffusion of fluorescent species e.g. proteins diffusing freely in the cytoplasm of a cell, the autocorrelation function can be described by Eq. 1.2 (Eigen and Rigler 1994; Brock *et al.,* 1998):

$$G(\tau) = 1 + \frac{1}{V_{3DG}\langle C \rangle} \sum_i \phi_i \frac{1}{\left(1 + \frac{\tau}{\tau_{d,i}}\right)\sqrt{1 + \left(\frac{\omega_{xy}}{\omega_z}\right)^2 \frac{\tau}{\tau_{d,i}}}}, where \phi_i = \frac{\varepsilon_i^2 Y_i}{\left(\sum_i \varepsilon_i Y_i\right)^2} \tag{1.2}$$

In Eq. 1.2, i denotes the number of independent fluorescent species with ε_i and Y_i being their molecular brightness and molar fraction, respectively. V_{3DG} is the 3D Gaussian shaped observation volume with equatorial radius ω_{xy}, and axial radius ω_z. The ratio ω_z/ω_{xy}, is also called the structural parameter and for an optimized system its value varies between 5 and 10. $\langle C \rangle$ is the average concentration of the fluorescent molecules. τ_d is the translational diffusion time describing the time a molecule stays in the observation volume V_{3DG} and is related to the translational diffusion coefficient D as:

$$\tau_d = \frac{\omega_{xy}^2}{4D} \tag{1.3}$$

The observation volume is given by Eq. 1.4 (Schwille *et al.,* 1997):

$$V_{3DG} = \pi^{3/2}\omega_{xy}^2\omega_z \tag{1.4}$$

Using fluorescent molecules with known diffusion coefficients, ω_{xy} and V_{3DG} can be calculated. These values can be used to calculate diffusion coefficients D from calculated τ_d using Eq. 1.3. The information about the average concentration C or average number N of fluorescent molecules present in the observation volume can be obtained from the amplitude of the correlation function (Eq. 1.5).

$$G(0) = 1 + \frac{1}{V_{3DG}\langle C\rangle} = 1 + \frac{1}{\langle N\rangle} \tag{1.5}$$

The diffusion coefficient for a spherical molecule, is inversely related to the viscosity of the solution η, according to the Stokes-Einstein's equation (Eq. 1.6)

$$D = \frac{kT}{6\pi\eta r_h} \tag{1.6}$$

where k is the Boltzmann constant, T is the temperature and r_h is the hydrodynamic radius of the solute. Thus, D values can also be used to estimate cellular viscosities or hydrodynamic radii of proteins.

When fluctuations arise not only from free diffusion of molecules in three dimensions, but also from diffusion restricted to two dimensions, e.g., in cells where a protein is also associated with the membrane, the autocorrelation function (Eq. 1.2) can be modified to include two dimensional diffusion of molecules at the membrane. In this case ω_z is much larger than the membrane thickness (Pramanik *et al.,* 2000).

$$G(\tau) = 1 + \frac{1}{\langle N\rangle}\left\{\frac{F_1}{\left(1+\frac{\tau}{\tau_{d,1}}\right)\sqrt{1+\left(\frac{\omega_{xy}}{\omega_z}\right)^2\frac{\tau}{\tau_{d,1}}}} + \frac{1-F_1}{\left(1+\frac{\tau}{\tau_{d,2}}\right)}\right\} \tag{1.7}$$

The second term in the parentheses denotes the fraction of molecules (1-F_1) diffusing in two dimensions with a diffusion time of $\tau_{d,2}$.

In heterogeneous intracellular environments, normal (Brownian) diffusion of a protein can be affected by the presence of barriers such as domains formed by the cytoskeleton (Luby-Phelps *et al.,* 1986) or by protein interaction with subcellular

structures giving rise to anomalous diffusion (Haustein and Schwille 2003; Weiss *et al.,* 2003). Presence of protein in small cellular compartments that can confine the observation volume (Gennerich and Schild 2000) or the process of active transport (Köhler *et al.,* 2000) will also affect normal diffusion. The autocorrelation function in such cases needs to be modified.

Though FCS offers many advantages for probing intracellular dynamics, it also suffers from a few limitations in living cells that must be taken into account. The presence of cellular autofluorescence, cell movement, light absorption by endogenous molecules, scattering from cell organelles or membranes and dye depletion due to photobleaching can potentially introduce artifacts in the autocorrelation curves (Brock and Jovin 2001). These factors will be discussed separately below.

Autofluorescence: Natural fluorescence of cells, caused by endogenous molecules such as flavins, flavoproteins, NAD(P)H and others (Aubin 1979; Benson *et al.,* 1979) can contribute to autocorrelation curves by either introducing a steady background of non-correlating species or an additional correlating component. A non-correlating background will lower the amplitude of the correlation curve leading to a higher apparent number of molecules in the observation volume (Brock *et al.,* 1998; Hink *et al.,* 2003); Eq. 1.8,

$$G_{total}(0) = 1 + \frac{\left(1 - \frac{F_{background}}{F_{total}}\right)^2}{N_{corr}} \tag{1.8}$$

where $F_{background}$ is the autofluorescence intensity, F_{total} is the total fluorescence intensity and N_{corr} is the corrected number of molecules, respectively. In case of correlating background, the autocorrelation function is modified to include the extra component, taking into account its molar fraction and relative molecular brightness according to Eq. 1.2. The autofluorescence of *Dictyostelium* cells has been studied in detail and is described in Chapter 2 of this thesis.

Cell Movement: Movement of a cell or subcellular structures during measurements can introduce drifts in intensity fluctuations leading to artifacts in the autocorrelation curve. Interference of such movement can be minimized by reducing the measurement time. Slow random fluctuations can be taken into account by adding an offset term in the autocorrelation curve (Brock *et al.,* 1998).

$$G_{corr}(\tau) = G(\tau) + offset \tag{1.9}$$

Light absorption and scattering: Light absorption by endogenous molecules or scattering by organelles and cell membranes, especially in thick samples can reduce the signal to noise ratio. A proper selection of fluorophore, excitation intensities and measurement period is thus required. However, since high excitation intensities or long measurement periods can lead to cell damage or death due to phototoxicity, a balance between high signal to noise ratio and low cellular damage needs to be maintained.

Dye depletion: Unlike *in vitro* experiments, for instance experiments in cuvettes where volumes are much larger, concentrations of fluorescent molecules in cells or subcellular compartments can reduce with time due to photobleaching at the focus. The change in the average number of molecules in the observation volume and the process of photobleaching during the measurement can introduce artifacts in the autocorrelation curve. Dye depletion can be minimized by making use of short measurement times and low excitation intensities.

1.2.2 Photon Counting Histogram (PCH) Analysis

PCH is a data analysis technique that makes use of the probability distribution of the fluctuation amplitudes to give quantitative description of the molecular brightness and concentration of fluorescent species present in a sample (Chen *et al.,* 1999b). This technique is complementary to FCS. While the time-dependent autocorrelation curve of FCS provides detailed information about kinetic processes such as translational diffusion causing fluorescence fluctuations, with the exception of $G(0)$, it lacks information about the amplitude distribution of intensities. Diffusion is relatively insensitive to changes in molecular weights since the diffusion coefficient of spherical particles scales as inverse cube root of molecular weight. Therefore, FCS cannot separate two species of similar masses, without *a priori* knowledge (Meseth *et al.,* 1999). PCH on the other hand, can retrieve information about molecular brightness of species independent of their diffusion times and can thus resolve a mixture of species of similar masses.

The PCH of an open observation volume, $\Pi(k;N,\varepsilon_t)$ describes the probability $p^{(N)}$ of detecting k photon counts per sampling time Δt_s for an open system with an average of N independent particles of a fluorescent species in the 3D Gaussian observation volume (V_{3DG}). The distribution of particles in the observation volume is given by the Poisson distribution $p(N)$.

$$\Pi(k;N,\varepsilon_t) \equiv \sum_{N=0}^{\infty} p^{(N)}(k;V_{3DG},\varepsilon_t)\cdot p(N) \tag{1.10}$$

$$\text{where, } p(N) = \frac{\langle N \rangle^N e^{-\langle N \rangle}}{N!} \tag{1.11}$$

The quantity ε_t describes the molecular brightness per sampling time. The chosen sampling times should be shorter than the intensity fluctuations. Since, the average number of photon counts detected $\langle k \rangle$ scales linearly with the sampling time, a quantity $\varepsilon = \varepsilon_t/\Delta t_s$ is defined, which is independent of the sampling time. The values of the molecular brightness ε, expressed in Hz/ molecule (≡ counts per second per molecule) from different experiments can thus be directly compared. The average number of photon counts received per second $\langle k \rangle$ is given by

$$\langle k \rangle = \varepsilon N \tag{1.12}$$

The PCH of a mixture of species with different molecular brightness' is given by the successive convolution of all single species photon counting histograms. For mixture of two species, *1* and *2*, the PCH is given as:

$$\Pi(k; N_1, N_2, \varepsilon_1, \varepsilon_2) = \Pi(k; N_1, \varepsilon_1) \otimes \Pi(k; N_2, \varepsilon_2) \tag{1.13}$$

PCH applications in living cells include characterization of eGFP in HeLa cells (Chen *et al.,* 2002), study of receptor oligomerization in COS-1 cells (Chen *et al.,* 2003) and investigation of protein oligomerization in cytoplasm of HeLa cells (Ruan *et al.,* 2002).

1.3 Thesis aim and outline

The aim of the study described in this thesis is to characterize the diffusion, localization and interactions of proteins involved in the chemotaxis mechanism of *Dictyostelium discoideum* using fluorescence fluctuation spectroscopy.

Before making use of any technique, the factors that may interfere or cause artifacts need to be known. With this aim, the autofluorescence of *Dictyostelium* cells was characterized in detail and the findings are described in **Chapter 2**. Also described in this chapter are the optimal experimental conditions for performing FFS in *Dictyostelium* cells. **Chapter 3** describes the diffusion of three GFP tagged pleckstrin homology domains, PH-CRAC, PH2 and PH10 in the cell cytoplasm and how it is affected upon initiation of chemotaxis. A comparison has been made with the diffusion of free eGFP in cells. Another important component of the chemotaxis mechanism in

Dictyostelium are the G-proteins. The diffusion and interaction of Gβ and Gγ subunits in cytoplasm and plasma membrane has been studied in **Chapter 4**. In **Chapter 5**, the effect of deletion of Phlp1, a protein that is thought to modulate Gβγ activity in *Dictyostelium*, on Gβ and Gγ dimerization is investigated. **Chapter 6** summarizes the findings in this thesis and discusses the use of FFS as a tool to probe protein dynamics in *Dictyostelium* cells.

2 Spectral Characterization of *Dictyostelium* Autofluorescence

Dictyostelium discoideum is used extensively as a model organism for the study of chemotaxis. In recent years, an increasing number of studies of *Dictyostelium* chemotaxis have made use of fluorescence-based techniques. One of the major factors that can interfere with the application of these techniques in cells is the cellular autofluorescence. In this study, the spectral properties of *Dictyostelium* autofluorescence have been characterized using fluorescence microscopy. Whole cell autofluorescence spectra obtained using spectral imaging microscopy show that *Dictyostelium* autofluorescence covers a wavelength range from ~ 500 – 650 nm with a maximum at ~ 510 nm and thus, potentially interferes with measurements of GFP fusion proteins with fluorescence microscopy techniques. Further characterization of the spatial distribution, intensity and brightness of the autofluorescence was performed with fluorescence confocal microscopy and fluorescence fluctuation spectroscopy (FFS). The autofluorescence in both chemotaxing and non-chemotaxing cells is localized in discrete areas. The high intensity seen in cells incubated in the growth medium HG5 reduces by around 50% when incubated in buffer, and can be further reduced by around 85% by photobleaching cells for 5-7s. The average intensity and spatial distribution of the autofluorescence do not change with long incubations in the buffer. The cellular autofluorescence has a 7 times lower molecular brightness than eGFP. The influence of autofluorescence in FFS measurements can be minimized by incubating cells in buffer during the measurements, prebleaching and making use of low excitation intensities. The results obtained in this study thus offer guidelines to the design of future fluorescence studies of *Dictyostelium*.

2.1 Introduction

Dictyostelium discoideum is used extensively as a model organism for the study of chemotaxis, the process of cell movement along a chemical gradient, because of its resemblance to mammalian cell movement. As a model system *Dictyostelium* offers many advantages, which include its genetic manageability and easy access for biochemical and biological studies. In recent years the chemotaxis mechanism of *Dictyostelium* has been increasingly probed using fluorescence based techniques. The phenomenon of fluorescence, by virtue of its multiple characteristics – intensity, brightness, lifetime, excitation-emission spectra, resonance energy transfer, to name a few, can be exploited to specifically study the behavior of one type of molecules in a medley of diverse molecules in the cell. The possibility of fusing the protein of interest to intrinsically fluorescent proteins, such as the green fluorescent protein (GFP), without loss of its normal function and localization (Tsien 1998), has made fluorescence based techniques a powerful tool available to biologists today to study various processes in living cells.

Fluorescence microscopic and spectroscopic techniques applied to study *Dictyostelium* chemotaxis include the use of confocal imaging to study localization and dynamics of cellular proteins e.g. G-proteins (Jin *et al.,* 2000; Blaauw *et al.,* 2003), PH-CRAC (pleckstrin homology domain of the cytosolic regulator of adenylyl cyclase) (Parent *et al.,* 1998), adenylyl cyclase A (ACA) (Kriebel *et al.,* 2003), guanylyl cyclase (GC) (Veltman *et al.,* 2005) actin cytoskeleton (Fischer *et al.,* 2004; Uchida and Yumura 2004); the use of fluorescence recovery after photobleaching (FRAP) to study cellular viscosities and diffusion of actin or actin binding proteins (Potma *et al.,* 2001; Bretschneider *et al.,* 2002) and the use of Förster resonance energy transfer (FRET) to detect interaction between G-protein subunits (Janetopoulos *et al.,* 2001; Xu *et al.,* 2005). In addition, fluorescence fluctuation spectroscopy (FFS) has been used to study the diffusion of GFP-tagged proteins in *Dictyostelium* cells (Ruchira *et al.,* 2004). FFS, comprising techniques such as fluorescence correlation spectroscopy (FCS) and photon counting histogram (PCH) analysis, makes use of tiny spontaneous fluorescence intensity fluctuations in a small volume (< 1 femtolitre) to extract information about their physical parameters (Hess *et al.,* 2002; Haustein and Schwille 2003; Levin and Carson 2004; Vukojevic *et al.,* 2005). Because of its high sensitivity, FFS can be used for detection at the single molecule level and can thus provide a means to study the behavior of biomolecules in cells at physiologically relevant concentrations.

Intrinsic cellular fluorescence is one of the major factors that can interfere with the application of fluorescence-based techniques in cells. Autofluorescence caused by

endogenous molecules such as flavins, flavoproteins and NAD(P)H (Aubin 1979; Benson *et al.,* 1979) can bias a measurement and reduce the signal to noise ratio. Thus knowledge of autofluorescence characteristics is essential to avoid or minimize its influence. In the present study we have characterized the spectral properties of *Dictyostelium* autofluorescence using fluorescence spectral imaging microscopy (FSPIM). The spatial distribution of autofluorescence and its intensity at different excitation wavelengths has been visualized using confocal laser scanning microscopy (CLSM). Fluorescence fluctuation spectroscopy was used to quantify molecular brightness and intensity in cells under different experimental conditions. The results obtained in this study offer guidelines to the design of future fluorescence studies of *Dictyostelium*.

2.2 Experimental Procedure

2.2.1 Sample preparation

Wild type *Dictyostelium discoideum* of strain AX3 were grown in HG5 medium that was composed of 14.3 g/l peptone; 7.15 g/l yeast extract; 0.54 g/l Na_2HPO_4; 0.49 g/l KH_2PO_4 and 10.0 g/l glucose. Cells were withdrawn from a confluent petriplate and were either directly used or washed twice in potassium phosphate buffer (pH 6.5, 17 mM) before use. For FSPIM measurements, cells were placed on a microscope slide (Menzel-Glaser) and allowed to settle after which a coverglass was gently placed on top. For confocal imaging and FFS measurements, cells were transferred to a 96-chambered glass bottom microplate (Whatman). Cells were starved by suspending vegetative cells at a density of 2.5 x 10^7 ml^{-1} in 500 µl potassium phosphate buffer in a 15 ml centrifuge tube (Sarstedt) for approximately five hours. After five hours small cell aggregates could be observed. FSPIM spectra were also obtained from 200 nM eGFP (F64L, S65T) dissolved in 50 mM Tris buffer (pH 8), and from 100 µM FMN (Sigma) dissolved in demineralised water.

2.2.2 Fluorescence Microscopy

Fluorescence Spectral Imaging Microscopy (FSPIM): The fluorescence spectra were obtained on a FSPIM setup comprising a Leica DMR epifluorescence microscope equipped with a 250IS imaging spectrograph (Chromex) coupled to a CH250 CCD camera (Photometrics, The Netherlands) (Hink *et al.,* 2003). A 100 W-mercury arc lamp provided the excitation light, which was filtered using a 435 DF 10 band pass filter (Omega) and a 470DRLP dichroic mirror (Omega). Fluorescence spectral images were acquired with the FSPIM setup using a Leica Plan Neofluar 40x oil immersion (N.A. 1.0) objective and a 475 long pass emission filter (Schott) using an integration time of

either 10 or 15 s. The emission spectra were recorded from 475 – 725 nm and corrected for background fluorescence and camera bias by subtracting an extracellular region from the same spectral image. The spectra for HG5, eGFP and FMN were corrected by subtracting a spectral image of water.

Confocal laser scanning microscopy: Confocal images of cells were obtained with a confocal laser-scanning microscope (ConfoCor 2 - LSM 510 combination setup, Carl-Zeiss, Germany), which is described in detail elsewhere (Hink *et al.,* 2003). Autofluorescence was excited with 458 and 488 nm wavelengths from an argon-ion laser and with 633 nm wavelength from a He-Ne laser, focused into the sample by a C-Apochromat 40x water-immersion objective with NA 1.2 (Zeiss). The excitation power during image acquisition was approximately 30 μW for the 458 nm laser line and 200 μW for the 488 and 633 nm laser line. The fluorescence passed through the main beam splitters HFT 458, 488 and 514/633 and was filtered using long pass filters 475, 505 and 650. Differential interference contrast (DIC) images were also acquired simultaneously. The acquired images were processed using Zeiss LSM Image Browser software package (V 3.2).

Fluorescence fluctuation spectroscopy (FFS): FCS and PCH measurements were performed with Zeiss-EVOTEC ConfoCor, as has been described previously (Ruchira *et al.,* 2004). Autofluorescent molecules were excited with a wavelength of 488 nm from an argon-ion laser, the power of which was attenuated with neutral density filters. For the quantification of autofluorescence of cells under different conditions and for PCH analysis, measurements were performed at a power of approximately 10 μW. Measurement duration in all cases was 10 s. In order to photobleach the autofluorescent molecules, cells were exposed to ~ 1mW laser power, for the times mentioned. For PCH analysis, between 3 x 10^5 and 1 x 10^6 photons were collected and the data were analyzed at a sampling frequency of 20 kHz. The autofluorescence characteristics, of vegetative cells incubated in buffer were measured at excitation intensities of 3, 10, 20, 70, 200 and 670 μW.

The FCS data were analyzed using the FCS data processor software package V 1.4 (Skakun *et al.,* 2005). The data were fit to a model describing the Brownian motion of molecules in three dimensions, given in Eq. 2.1.

$$G(\tau) = 1 + \frac{1}{N}\sum_i \phi_i \frac{1}{\left(1+\frac{\tau}{\tau_{d,i}}\right)\sqrt{1+\left(\frac{\omega_{xy}}{\omega_z}\right)^2 \frac{\tau}{\tau_{d,i}}}} + offset \qquad (2.1)$$

$$\text{where, } \phi_i = \frac{\varepsilon_i^2 Y_i}{\left(\sum_i \varepsilon_i Y_i\right)^2} \tag{2.2}$$

In Eq. 2.1, $G(\tau)$ is the autocorrelation function, N is the average number of molecules in the 3D Gaussian volume of radial radius ω_{xy} and axial radius ω_z. The molecules of species i have a diffusion time $\tau_{d,i}$, molecular brightness ε_i and molar fraction Y_i. If only one species is present ϕ_i becomes 1 (Eq. 2.2). The offset term in the equation accounts for slow drifts in the intensity fluctuation trace (in the time scales of seconds) due to which the autocorrelation function does not decay to 1 at infinitely long times (Brock *et al.,* 1999). τ_d is related to the translational diffusion coefficient D as:

$$\tau_d = \frac{\omega_{xy}^2}{4D} \tag{2.3}$$

The 3D Gaussian volume is given as (Schwille *et al.,* 1997):

$$V_{3DG} = \pi^{3/2} \omega_{xy}^2 \omega_z \tag{2.4}$$

The average concentration of the fluorescent species in the sample can be calculated using N and V_{3DG}.

$$C = \frac{N}{V_{3DG} A} \tag{2.5}$$

In Eq. 2.5, A is the Avogadro's number, which is 6.023 x 10^{23}. The instrument was calibrated with the dye rhodamine-110 (Molecular Probes) (D = 2.8 x 10^{-10} m^2/s), which gave a value of 10 for the ratio ω_z/ω_{xy}, also called the structural parameter, and τ_d = 55µs. V_{3DG} was calculated to be 0.85 femtolitre (fl). The D values for autofluorescent molecules could be subsequently calculated from the obtained τ_d and using Eq. 2.3.

The PCH data were fit assuming single species. The PCH function for an open detection volume describes the possibility of observing k photon counts per sampling time with N as the average number of molecules in the detection volume (Chen *et al.,* 1999b). The molecular brightness ε, expressed as kHz/molecule, is the ratio of the average number of photon counts $\langle k \rangle$ received per second to N (Eq. 2.6). ε is independent of the sampling frequency, as a result values from different experiments can be directly compared (Chen *et al.,* 1999b).

$$\varepsilon = \frac{\langle k \rangle}{N} \tag{2.6}$$

2.3 Results

2.3.1 Autofluorescence spectrum

Average autofluorescence spectra from wild-type *Dictyostelium* cells of strain AX3 were acquired using FSPIM (Fig. 2.1). The autofluorescence spectrum is broad and asymmetric with a peak at 510 nm and a slight shoulder around 565 nm. For comparison, emission spectra of eGFP, of the growth medium HG5 and of FMN, an enzymatic cofactor thought to be a constituent of cellular autofluorescence (Aubin 1979; Benson *et al.,* 1979), were obtained under similar experimental conditions (Fig. 2.1).

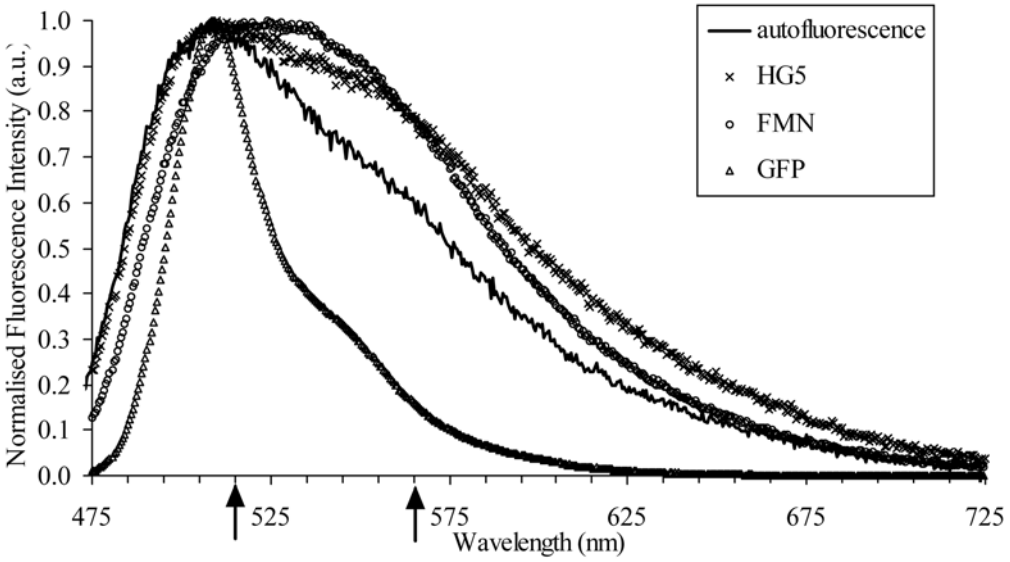

Figure 2.1: Autofluorescence spectrum. A comparison of the average *Dictyostelium* autofluorescence spectrum, calculated from 10 cells incubated in potassium phosphate buffer (17 mM, pH 6.5), to the spectra of HG5, eGFP in TRIS buffer (50 mM, pH 8) and flavin mononucleotide (FMN) in water. Excitation wavelength is 435 nm. The arrows on the x-axis denote the transmission range of the band-pass emission filter 515-565, used in the FFS measurements. The spectra are normalized to the maximum intensity.

The autofluorescence spectrum covers the entire region (475 – 625 nm) in which GFP also emits. The maximum in the autofluorescence spectrum is very close to the eGFP emission maximum (~ 508 nm), indicating that it can potentially interfere with measurements of GFP-fusion proteins. The HG5 medium, taken up by cells as they grow in it, is also fluorescent and displays a broad but characteristic spectrum. The spectrum, which is broader than the autofluorescence spectrum, also exhibits a peak

around 510 nm and a slight shoulder around 565 nm. The ratio of the shoulder to the emission maxima, however, is different from the autofluorescence spectrum. The growth medium, which consists of yeast extracts containing vitamin B_2 (riboflavin), has previously been suggested as the reason for *Dictyostelium* autofluorescence (http://dictybase.org/techniques/lowflomedium.htm). The free FMN spectrum was however, slightly red-shifted with a peak at 525 nm and no shoulder. Since the fluorescence of flavin nucleotides is sensitive to its environment, it is very likely that in the growth medium and in the cells, where the nucleotides may be present in association with proteins or peptides, the fluorescence spectrum is affected (Aubin 1979; Benson *et al.,* 1979; Visser *et al.,* 2001).

2.3.2 Visualizing autofluorescence with confocal microscopy

The whole cell FSPIM spectrum gives important information about the emission characteristics of the autofluorescent molecules. The spatial distribution of the autofluorescence at different excitation wavelengths was then visualized using confocal laser scanning microscopy. Fig. 2.2 shows the images acquired with excitation wavelengths of 458, 488 and 633 nm. The images show a patchy autofluorescence pattern that does not change when cells start aggregating. The images acquired at 633 nm excitation (Fig. 2.2C) show no detectable fluorescence signal indicating that the interference of autofluorescence can be minimized by the use of fluorophores that can be excited in this region. Cells incubated in the growth medium (Fig. 2.3A) exhibit higher autofluorescence than cells incubated in buffer (Fig. 2.3B), indicating that the fluorescent growth medium taken up by the cells, contributes to the autofluorescence. To investigate if the autofluorescence intensity decreased as cells exchanged the fluorescent medium for the non-fluorescent buffer, a series of images of cells incubated in buffer for various times was made. The autofluorescence intensity of cells incubated in buffer for 2 hours is similar to the intensity of cells incubated in buffer for 20 minutes (Fig. 2.3). Thus, it appears that the exchange of medium for buffer takes place within the first 20 minutes and thereafter the average autofluorescence intensity does not change perceptibly. This fast exchange rate is in keeping with previous studies on fluid uptake by *Dictyostelium* cells grown in liquid medium (Kayman and Clarke 1983; Aguado-Velasco and Bretscher 1999). AX3 cells have a fluid uptake rate of approximately 4 femtolitres (fl) $cell^{-1}min^{-1}$ (Kayman and Clarke 1983). Approximating the cell to a hemisphere of 5 μm radius, the cell volume is approximately 250 fl, which means that in 20 minutes a cell can exchange fluid equivalent to $1/3^{rd}$ of its total volume. Since autofluorescence appears to cover ~ 20 % of the cell volume (Fig. 2.2 and 2.3), this means that in 20 minutes the cells can effectively get rid of any fluorescence due to the growth medium.

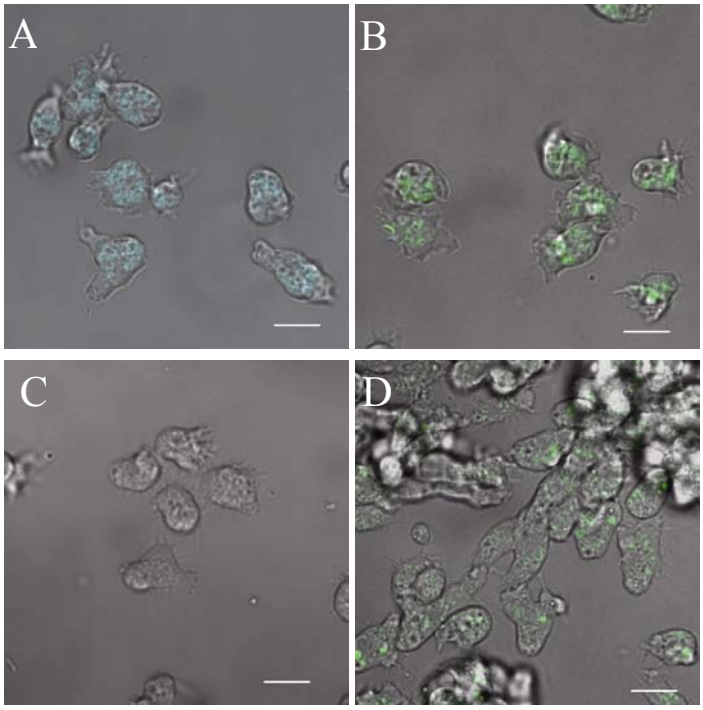

Figure 2.2: *Dictyostelium* autofluorescence imaged with fluorescence confocal laser scanning microscope. Vegetative AX3 cells incubated in buffer were excited at A) 458 nm B) 488 nm and C) 633 nm wavelength. Fluorescence was filtered using long pass filters 475, 505 and 650. Aggregating cells (D) were excited at 488 nm. Images shown are merge of differential interference contrast (DIC) and fluorescence image. Bar = 10 μm.

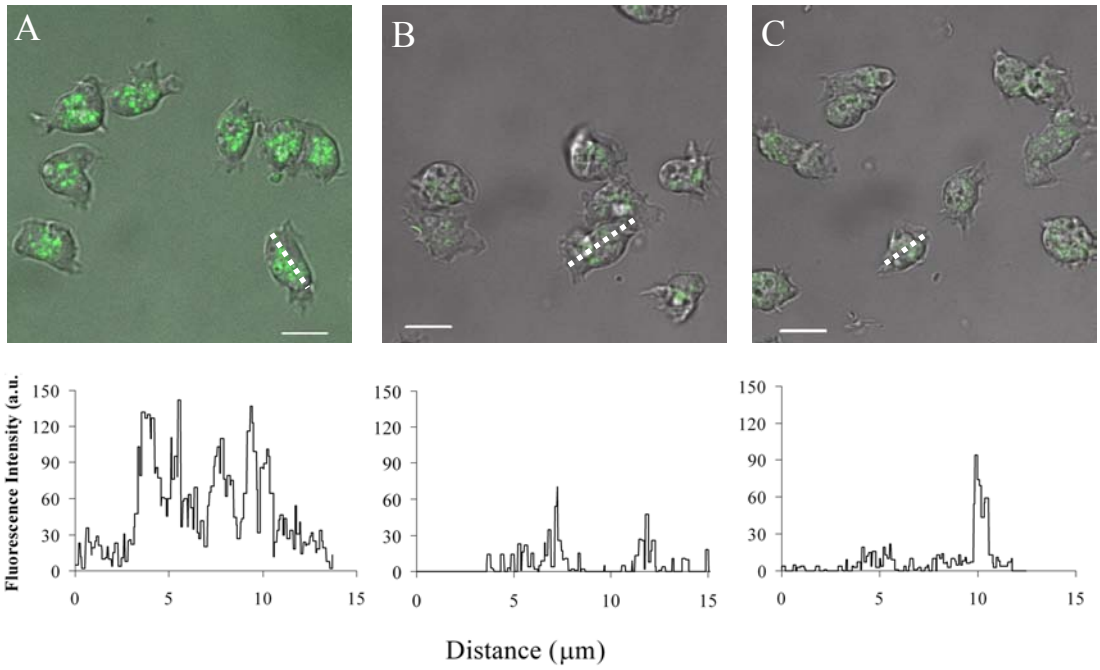

Figure 2.3: Autofluorescence images of AX3 cells incubated in HG5 medium or buffer for different periods. A) Cells in HG5 medium B) in buffer for 20 minutes and C) in buffer for 2 hours. The lower panels show the corresponding fluorescence intensity profiles taken along the white dotted line through a cell in each image. Excitation wavelength is 488 nm. Bar = 10 μm.

2.3.3 Fluorescence fluctuation spectroscopy of autofluorescent molecules

Further characterization of the autofluorescence intensity and molecular brightness was performed with FCS and PCH analysis. Autofluorescent molecules were excited with the 488 nm wavelength and fluctuation intensity traces and autocorrelation curves from cells under different experimental conditions were recorded. The autofluorescence intensity shows wide variation from cell to cell and the fluctuation intensity trace display large non-uniform fluctuations (Fig. 2.4). The average intensity obtained from a 10 s measurement in a cell was taken as the average autofluorescence intensity of that cell.

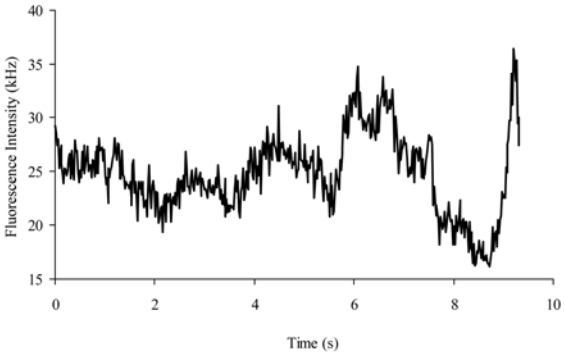

Figure 2.4: Autofluorescence intensity fluctuation. Representative curve of the fluorescence intensity trace obtained from a single measurement in an AX3 cell incubated in potassium phosphate buffer (pH 6.5, 17 mM) and excited with ~10 μW power of the 488 nm laser line.

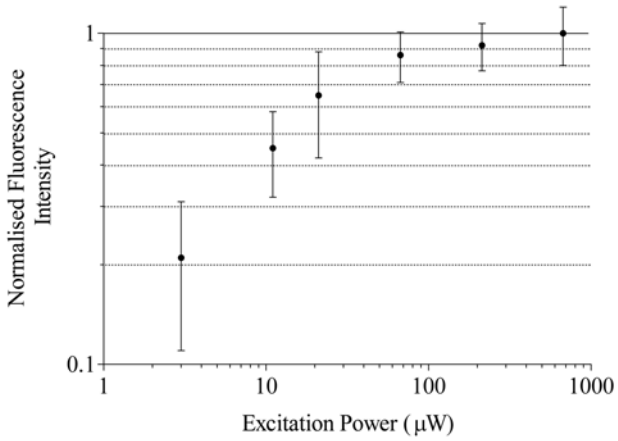

Figure 2.5: Average autofluorescence intensity depends on the excitation power. Plot shows the normalized intensities obtained from *Dictyostelium* AX3 cells incubated in buffer excited with varying powers of the 488 nm laser.

The autofluorescence dependence on laser power was first studied. AX3 cells incubated in buffer were excited with increasing power of the 488 nm laser line. With increasing laser powers the autofluorescence intensity initially increases linearly and then reaches saturation (Fig. 2.5). The autocorrelation curves recorded at the different laser powers are noisy, indicating low signal to noise ratios (Fig. 2.6). The curves were evaluated using Eq. 2.1. At excitation intensities of ~ 700 and 200 μW fast diffusion with average diffusion coefficient value of 220 ± 50 $\mu m^2/s$ (n=13) is observed. The diffusion appears slower, with an average diffusion coefficient value corresponding to 47 ± 23 $\mu m^2/s$ (n=11), when the excitation power is ~ 70 and 20 μW. Below excitation intensities of 20 μW, the curves became too noisy to be evaluated. The

apparently fast diffusion at higher intensities can be due to intense photobleaching or other fast photophysical effects e.g. triplet state dynamics and blinking, at these intensities (Widengren 2001).

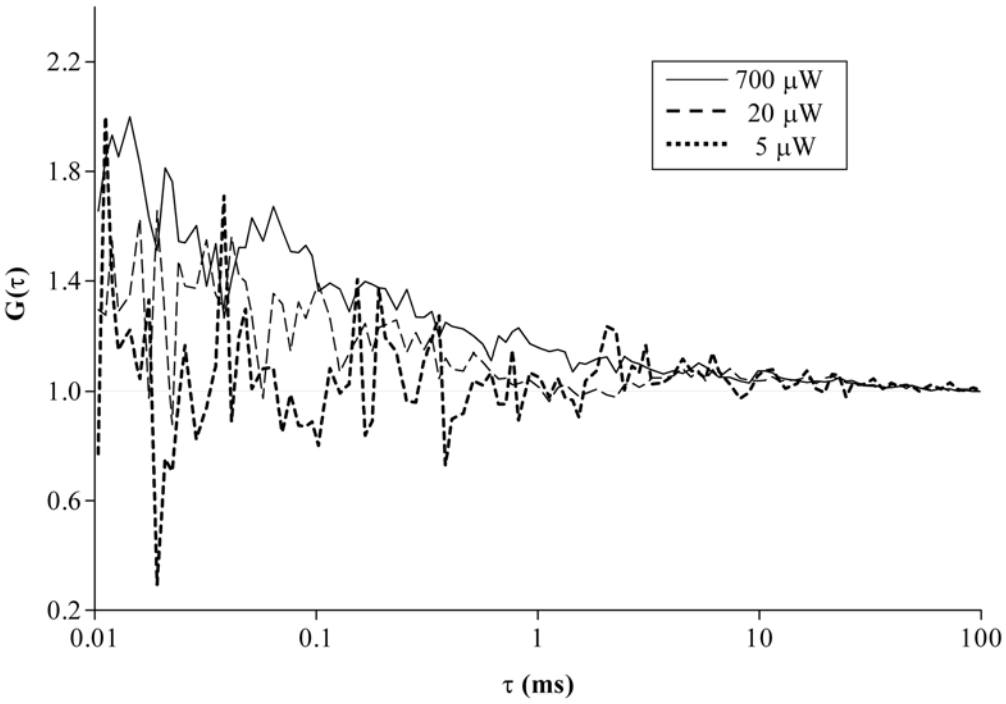

Figure 2.6: Normalized autocorrelation curves from *Dictyostelium* autofluorescence at different excitation intensities at 488 nm. Data were acquired for 10s from cells incubated in potassium phosphate buffer (pH 6.5, 17mM).

Since at excitation intensities below 20 µW the autofluorescence intensity fluctuations do not autocorrelate, it is more favorable to perform FCS measurements on GFP fusion proteins at these intensities. This would eliminate unwanted contribution of the autofluorescent species to the autocorrelation curve. The presence of non-correlating background does not affect the diffusion times obtained from FCS curves. However, it does lower the amplitude of the correlation curve leading to an apparently higher number of molecules in the detection volume (Brock *et al.,* 1998), which can be corrected for as described in Eq. 2.7

$$N_{corr} = N_{total}\left(1 - \frac{F_{background}}{F_{total}}\right)^2 \qquad (2.7)$$

where N_{corr} and N_{total} are the average corrected and uncorrected number of molecules in the detection volume, $F_{background}$ is the autofluorescence intensity and F_{total} is the total fluorescence intensity including background and GFP fluorescence. Tolerating a maximum error of 15% in determination of N_{corr}, the autofluorescence at excitation intensities below 20 μW can be ignored if F_{total} is at least 14 times higher than $F_{background}$.

Table 2.1: Autofluorescence intensities of *Dictyostelium* AX3 cells under different conditions. Average autofluorescence intensities and standard deviations obtained from 10 s measurements. Cells, incubated in either HG5 medium or potassium phosphate buffer (pH 6.5, 17 mM), were excited with 488 nm argon-ion laser line with power of ~10 μW.

Condition	I (kHz)	No. of cells
HG5 Medium	85 ± 30	40
Buffer ~ 15 min	44 ± 17	15
Buffer ~ 1 hour	37 ± 16	38
Buffer ~ 4 hours	41 ± 20	39
1-2s photobleaching (1mW)	16 ± 7	20
5-7 s photobleaching (1mW)	8 ± 3	20

Table 2.2: PCH analysis of *Dictyostelium* autofluorescence. Average values and standard deviations for brightness (ε), number of molecules in confocal detection volume (N), calculated average concentration (C) and fluorescence intensity (I) obtained for wild type AX3 cells incubated in potassium phosphate buffer (pH 6.5, 17mM), excited at 488 nm. The average concentration was calculated using Eq. 2.5. 3 x 10^5 – 1 x 10^6 photons were acquired at excitation intensity of ~ 10 μW. Data were analyzed at a sampling frequency of 20 kHz.

Condition	ε (kHz/molecule)	N	C (nM)	I (kHz)	No. of cells
No photobleaching	0.43 ± 0.3	89 ± 35	107 ± 42	33 ± 14	12
1-2s photobleaching (1mW)	0.33 ± 0.1	42 ± 17	41 ± 17	13 ± 8	17

The average autofluorescence intensities of cells excited at ~ 10 μW, under different experimental conditions, were next investigated (Table 2.1). Cells incubated in HG5 medium have the most intense autofluorescence signal (85 kHz), which reduces by 50% when the medium is replaced with buffer (44 kHz). In agreement with the confocal

imaging this value does not change further with time. The autofluorescence can be photobleached, by short exposure to the laser light. The autofluorescence of cells incubated in buffer reduces by 65% upon exposure to ~ 1 mW laser power for 1-2 s. Under similar experimental conditions free GFP expressed in *Dictyostelium* cell cytoplasm shows ~ 45% decrease in its fluorescence intensity (data not shown). The slower photobleaching rate of GFP compared to the autofluorescent molecules indicates that the signal to noise ratio in FFS measurements can be increased by photobleaching the autofluorescent molecules. Further reduction in autofluorescence intensity, up to 85% compared to initial values for cells incubated in buffer, can be obtained by exposing cells to the 1mW laser power for 5-7 s. During photobleaching, the microscope stage was moved so that the whole cell could be exposed to the high intensity beam. In this manner autofluorescent molecules throughout the cell can be photobleached and no recovery would be seen during a subsequent FFS measurement. The high laser intensity does not appear to harm the cells as they retain their irregular shape and continue to move. Thus, bleaching cells prior to FFS measurements on GFP fusion proteins can minimize the influence of autofluorescence.

The molecular brightness and concentration of autofluorescent molecules in cells incubated in buffer, with and without short photobleaching for 1-2 s was quantified using PCH analysis (Table 2.2). As expected, prebleaching does not affect the average molecular brightness of the autofluorescent molecules but the average concentration reduces by around 50%. Under similar experimental settings, the HG5 medium had a brightness value of 0.2 kHz, similar to what is observed in cells. But the concentration of the fluorescent species, of approximately 1 μM is much higher than in cells. An eGFP solution in TRIS buffer (pH 8) has approximately 7 times higher molecular brightness corresponding to a value of 2.57 ± 0.02 kHz. Since the relative contribution of different species to the autocorrelation curve is weighted by the square of the molecular brightness (Eq. 2.1 and 2.2), eGFP will contribute at least 50 times more to the autocorrelation curve, when the average number of eGFP molecules in the detection volume is equal to or higher than the autofluorescent molecules.

2.4 Discussion

Autofluorescence from cells is a major factor leading to reduced signal to noise ratios and artifacts in fluorescence microscopy measurements in cells. In this study, the spectral properties of *Dictyostelium discoideum* autofluorescence have been characterized using fluorescence microscopy. Whole cell autofluorescence spectra obtained using spectral imaging microscopy shows that *Dictyostelium* autofluorescence covers a wide wavelength range from ~ 500 – 650 nm. Cellular autofluorescence in this

wavelength range has been attributed to biomolecules such as flavin nucleotides, flavoproteins and NAD(P)H (Aubin 1979; Benson *et al.,* 1979). At the excitation wavelength (~435 nm) used in this study, NAD(P)H can not be excited. Hence, the detected autofluorescence results from flavin compounds. The spectrum of free FMN obtained under similar experimental conditions overlaps with the autofluorescence spectrum to a large extent, but is slightly red shifted. Also the spectrum of the growth medium HG5, which contains the vitamin riboflavin, shows nearly complete overlap with autofluorescence and FMN spectrum. The differences in the spectra of HG5, free FMN and autofluorescence can be attributed to the sensitivity of flavin fluorescence to its environment. Thus, factors such as pH, differences in viscosity and binding of FMN to proteins or peptides in both cells and the growth medium, would affect the spectrum (Aubin 1979; Benson *et al.,* 1979; Visser *et al.,* 2001).

The autofluorescence covers the entire eGFP emission range, and potentially interferes with fluorescence measurements of eGFP fusion proteins in cells. One way of minimizing interference of autofluorescence would be to fuse proteins of interest with other, more red-shifted fluorescent proteins e.g. mRFP or dTomato (Fischer *et al.,* 2004; Shaner *et al.,* 2004). Another way would be to reduce the autofluorescence signal such that its influence on the measurements reduces. To find means of achieving the latter, the autofluorescence characteristics were further studied using fluorescence confocal microscopy and fluctuation spectroscopy. The autofluorescence intensity can be reduced by around 50% by incubating the cells in buffer instead of the growth medium. The reduction is rapid, in agreement with reported fluid uptake rates by axenically grown AX3 cells. The residual autofluorescence, after the exchange of the growth medium with buffer, does not change with time suggesting that the remaining autofluorescent molecules are probably necessary for the cell functioning and can not be exchanged by the cell. However, this intensity of the autofluorescent molecules can be further reduced by another 85 % by photobleaching with high laser powers for short periods of time. As the high laser powers do not change the morphology and behavior of the cells and the autofluorescence reduces faster than the GFP fluorescence, prebleaching can be a convenient way of reducing autofluorescence interference. However, since bleaching would also reduce the signal from GFP, the time for which cells are exposed to high intensity should depend on the expression level of the GFP fusion proteins.

The extent of interference of autofluorescence in fluorescence fluctuation spectroscopy depends on the concentration and molecular brightness of the autofluorescent molecules compared to those of GFP or other fluorophore being used. In PCH analysis, the presence of autofluorescence can be taken into account using a model for two fluorescent species, with one species fixed to the autofluorescence parameters (Chen *et al.,* 2002). In autocorrelation curves autofluorescence can either

introduce a steady background of non-correlating species or an additional correlating component. The *Dictyostelium* autofluorescence did not show autocorrelation at excitation intensities lower than 20 μW. The presence of non-correlating background does not affect the diffusion times obtained from FCS curves but can influence the amplitude of the autocorrelation curve, which should be corrected. At excitation intensities above 20 μW the autofluorescence intensity fluctuations autocorrelate. However, the relatively high eGFP brightness, in cases where the average number of autofluorescent molecules in the detection volume is expected to be less than the average number of eGFP molecules, would make the autofluorescence contribution to the autocorrelation curve negligible.

To summarize, *Dictyostelium* autofluorescence displays a wide spectrum with a peak at ~ 510 nm and potentially interferes with measurements of GFP fusion proteins with fluorescence microscopy techniques. The autofluorescence is localized in discrete areas in the cell and the localization pattern and intensity does not change with long incubations in buffer. For FFS measurements the interference from autofluorescence can be minimized by incubating cells in buffer, prebleaching and making use of low excitation intensities.

3 Pleckstrin Homology Domain Diffusion in *Dictyostelium* Cytoplasm

The translocation of pleckstrin homology (PH) domain containing proteins from the cytoplasm to the plasma membrane plays an important role in the chemotaxis mechanism of *Dictyostelium* cells. The diffusion of three PH domain-green fluorescent protein (GFP) fusions, PH2-GFP, PH10-GFP and PH-CRAC (cytosolic regulator of adenylyl cyclase)-GFP in the cytoplasm of vegetative and chemotaxing *Dictyostelium* cells have been studied using fluorescence correlation spectroscopy (FCS) to gain a better understanding of the functioning of the domains and to assess the effect of initiation of chemotaxis on these domains in the cell. PH2-GFP is homogeneously distributed in vegetative as well as chemotaxing cells whereas PH10-GFP and PH-CRAC-GFP show translocation to the leading edge of the chemotaxing cell. The diffusion characteristics of PH2-GFP and PH-CRAC-GFP are very similar, however, PH10-GFP exhibits slower diffusion. Photon counting histogram (PCH) statistics show that this slow diffusion is not due to aggregation. Diffusion of the three PH domains is affected to similar extents by intracellular heterogeneities, in vegetative as well as chemotaxing cells. From the diffusion of free cytoplasmic GFP it is calculated that the viscosity in chemotaxing cells is 1.7 times lower than in vegetative cells. In chemotaxing cells, PH2-GFP shows increased mobility, whereas, the mobilities of PH10-GFP and PH-CRAC-GFP remain unchanged.

This chapter has been published as:
Ruchira, Mark A. Hink, Leonard Bosgraaf, Peter J.M. van Haastert and Antonie J.W.G. Visser "Pleckstrin Homology Domain Diffusion in *Dictyostelium* Cytoplasm Studied using Fluorescence Correlation Spectroscopy" *J. Biol. Chem*. 2004 (279) 10013-10019.

3.1 Introduction

The social amoeba *Dictyostelium discoideum* begins its life as single cells, feeding on bacteria. When the food supply is exhausted, starvation induces the single cells to aggregate and develop, to eventually form a multicellular organism. Aggregation of cells is governed by chemotaxis to cAMP. During chemotaxis cell movement is mediated by pseudopod formation that results from the activation of several second messenger pathways in response to the binding of cAMP to the receptor. It is thought that one crucial step leading to pseudopod formation is the activation of phosphatidylinositol-3 kinase (PI3K), which generates negatively charged phospholipids that act as binding sites for pleckstrin homology (PH) domains at the plasma membrane (Firtel and Chung 2000). PH domains are homologous regions of around 120 amino acids found in a number of proteins that are quite diverse in their cellular functions. Though the level of sequence similarity between different PH domains is quite low, the secondary structures of the domains are very similar. PH domains can form electro-statically polarized tertiary structure that can interact with negatively charged membrane surfaces. Apart from phospholipids, the βγ subunits of heterotrimeric G-proteins and protein kinase C have been proposed as common ligands for PH domains. PH domains are thought to be responsible for translocation of cytosolic PH domain containing proteins to the plasma membrane, where they can initiate further action (Bottomley *et al.,* 1998; Hirata *et al.,* 1998; Lemmon and Ferguson 2000). Chemotaxing *Dictyostelium* cells are polarized. It has been suggested that the directional response of the *Dictyostelium* cell comes from the selective recruitment of certain PH-domain containing proteins to the leading edge (Parent *et al.,* 1998; Firtel and Chung 2000). Although PH domains are known to play a very important role in the process of chemotaxis, very little is known about the dynamics of these domains in cells. Thus, we do not know if PH domains that have different functions in the cell would still show similar diffusion behavior, a property that depends on the structure, localization and intracellular interactions of the domain in the cell. Also, upon initiation of chemotaxis, it is not known how these diffusion characteristics would be affected. In polarized *Dictyostelium* cells, the formation of pseudopodia may lead to change in fluidity of cytoplasm or generation of force due to reorganization of the cytoskeleton. The changes in the intracellular environment upon polarization of the cell would affect the various intracellular species. A study by Potma *et al.,* 2001, has demonstrated that due to reduction of actin cytoskeleton in the non-cortical regions of polarized *Dictyostelium* cells, free GFP in these regions shows faster mobility than in vegetative cells. The altered environment in the cell should also affect the PH domains.

Quantifying the diffusion characteristics of the species of interest in vegetative cells and determining the changes in these characteristics upon polarization of the cell would thus provide information not only about the dynamics of different PH domains and possible interactions with other intracellular moieties, but also about the effect of cell polarization.

The technique of choice for obtaining quantitative information on dynamic events in living cells, in a non-invasive manner, is fluorescence correlation spectroscopy (FCS) (Hess *et al.,* 2002; Vukojevic *et al.,* 2005). FCS has been applied successfully to quantify the diffusion rates of cellular moieties (Brock *et al.,* 1999; Schwille *et al.,* 1999; Wachsmuth *et al.,* 2000; Dittrich *et al.,* 2001; Chen *et al.,* 2002). Along with FCS, a complementary technique, photon counting histogram (PCH) analysis can be used to provide additional information about the system, e.g. the aggregation state of the fluorescent species in the system on the basis of their brightness and independent of their diffusion times (Chen *et al.,* 1999b). In this paper, FCS has been applied to study diffusion characteristics of GFP fusions of PH domains in the cytoplasm of *Dictyostelium*. PCH analysis has been applied to determine the aggregation state of proteins in the cell.

For the study three PH domains were chosen, PH2, PH10 and PH domain of CRAC. PH2 is a domain of an unidentified protein in *Dictyostelium*, the gene of which has not been completely described (DDB0231560)[1]. The protein contains two PH-domains, one N-terminal and one C-terminal with a Rho-GAP (GTPase activating protein) domain in between. PH2 is the C-terminal PH domain. PH10 is a domain of a protein the gene of which has been cloned and is thought to be a novel Akt/PKB (protein kinase B) homologue (GenBank™/EBI accession number AF093877). PH-CRAC has been studied widely and is known to play a role in the directional response of a cell (Parent *et al.,* 1998). It transiently translocates to the leading edge of the chemotaxing cell. As an indicator of the intracellular environment we used free GFP, which is not likely to show non-specific interactions with intracellular moieties (Dittrich *et al.,* 2001), expressed in *Dictyostelium* cytoplasm. The goal of this study was thus, to determine the diffusion characteristics of PH2-GFP, PH10-GFP and PH-CRAC-GFP in *Dictyostelium* cytoplasm to gain a better understanding of the functioning of these domains in the cell and to assess the effect of initiation of chemotaxis on these domains.

[1] Available at dictybase.org

3.2 Experimental Procedure

3.2.1 Cells

Wild type *Dictyostelium discoideum* of strain AX3 were grown in HG5 medium (14.3 g/l pepton; 7.15 g/l yeast extract; 0.54 g/l Na_2HPO_4; 0.49 g/l KH_2PO_4 and 10.0 g/l glucose). For expressing free GFP in the cells, AX3 cells were transfected with the GFP S65T mutant gene that was cloned in the extrachromosomal expression vector for *Dictyostelium* MB74, which bears a neomycin resistance cassette. The open reading frame of the GFP gene was cloned behind a *Dictyostelium* actin 15 promoter and was succeeded by an actin 8 terminator. For the expression of the PH domains, the shuffle vector LB3Neo was created that contains an actin 15 promoter and a Kozak sequence (AAAAATG) succeeded by the S65T GFP gene that were cloned in the expression vector HK12Neo. LB3Neo also bears a neomycin resistance cassette and has a BglII site, a SpeI site and a 2H3 terminator behind the GFP gene. For PH10 the primers 5'-GCG CCA GAT CTA ATA ATA TGG CAG ATA AAC AAG-3' (BglII site underlined) and 5'-GCG CGA CTA GTC CAT TTA ATT GTT GAG TTA TAA TCT C-3' (SpeI site underlined) were used for a PCR reaction using genomic *Dictyostelium* DNA as a template. Likewise, PH2 was amplified using primers 5'-GCG GGG GAT CCG AAA TTG TTA AAC AAG GTT A-3' (BamHI site underlined) and 5'-GCG CCA CTA GTC CTT GTT GTG TTA TAC AAT TTG-3' (SpeI site underlined). PH2 and PH10 were cloned in the BglII and SpeI site of LB3Neo using the indicated restriction sites of the primers. The PH-CRAC-GFP construct WF38 was a kind gift of C.A. Parent and P.N. Devreotes. It is also an extrachromosomal *Dictyostelium* expression vector bearing nemoycin resistance. The transfected cells were grown in HG5 medium in the presence of 10 μg/ml of neomycin (Geneticin - G418 disulfate salt; Sigma). The molecular masses of free GFP, PH-CRAC-GFP, PH2-GFP and PH10-GFP fusion proteins are 27, 39, 40 and 39 kDa, respectively.

3.2.2 Sample preparation

200 μl or 40 μl of cell suspension was taken from a confluent petridish and added in either an 8-chambered coverglass (Lab-Tek, Nalge Nunc International Corp., Illinois, USA) or a 96-chambered glass bottom microplate (Whatman Inc., New Jersey, USA), respectively. Cells were allowed to settle down for 15 to 20 minutes. The medium was then removed and the cells were washed twice with phosphate buffer (17 mM, pH 6.5). Measurements were performed in cells incubated in buffer. For the measurements in polarized cells, the cells were incubated in the phosphate buffer for around five hours. After the incubation, the cells had elongated and had started aggregating.

3.2.3 Cell immobilization

Vegetative cells expressing free GFP were immobilized in 3% agarose (Gibco BRL; gelling temperature for 2% w/v 36 – 42^{0}C), a solution of which was added to the cells after removing the buffer completely. The agarose solidified in a couple of seconds reducing the mobility of cells significantly. Fig. 3.1 compares the movement of cells incubated in buffer with that of cells under agarose. The slow movement of cells under agarose indicates that the cells were alive.

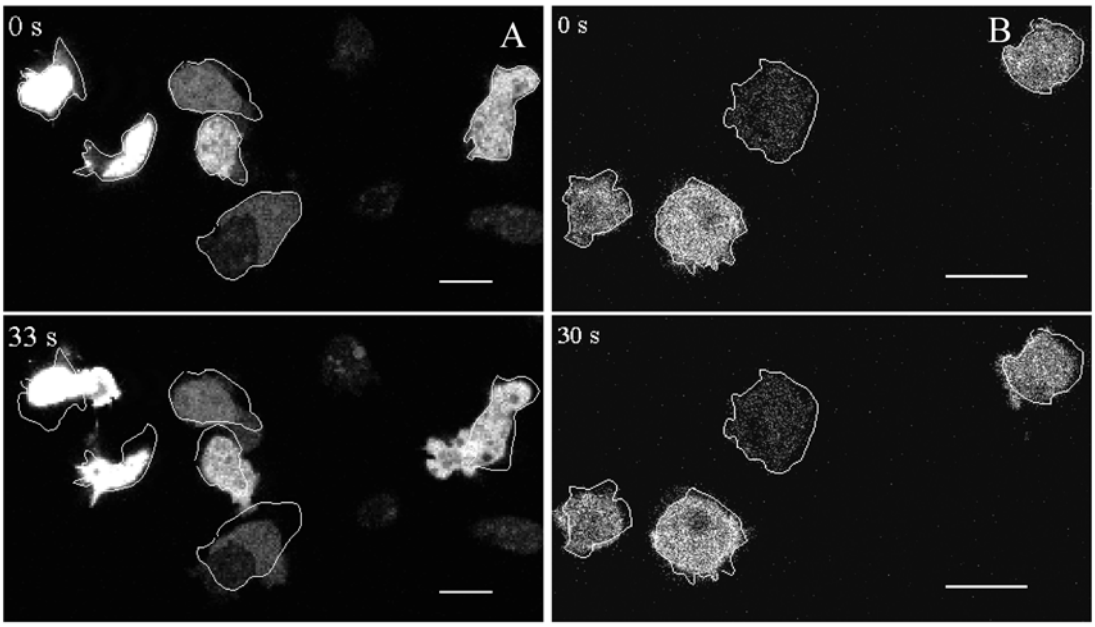

Figure 3.1: Cell immobilization. Confocal images of vegetative *Dictyostelium* cells A) incubated in buffer – at t = 0 s and t = 33 s and B) immobilized in 3% agarose – at t = 0 s and t = 30 s. The white outline shows the position of cells at t = 0. (Bar = 10 μm)

3.2.4 Instrumentation

FCS and PCH measurements were performed with Zeiss-EVOTEC ConfoCor, inverted confocal microscope. The details of the setup have been described previously (Hink *et al.,* 1999; Hink *et al.,* 2003). The microscope was equipped with a water immersive objective (C-Apochromat 40x, 1.2NA) and a 'fluorescein' filter set (Omega 505 dichroic, 540 DF 50 band pass filter) to separate the excitation and emission light. The sample was excited with a wavelength of 488 nm from the argon ion laser. The excitation intensity was attenuated with neutral density filters to approximately 10 μW. The pinhole, present for confocal detection, was set at 40 μm diameter. The autocorrelation curve was generated with a hardware correlator (ALV-5000E, ALV, Langen, Germany). For PCH, the signal was processed by a dual channel 32 bits, PCI photon counting card (ISS, USA) (Eid *et al.,* 2000).

Confocal images of the cells were obtained with a confocal laser scanning microscope (ConfoCor 2 - LSM 510 combination setup, Carl-Zeiss, Germany). GFP

was excited with the 488nm argon ion laser controlled by an acousto-optical tunable filter (AOTF). A dichroic beam splitter (HFT 488) separated the excitation from the emission. The GFP fluorescence was filtered through a BP 505-550 nm filter. The objective used was a 40x oil-immersion Plan-Neofluar with a numerical aperture of 1.3. The pinhole was set at 73 μm. Images were analyzed with the Zeiss LSM Image Browser software package.

3.2.5 FCS measurements

Around 100 to 150 autocorrelation traces were obtained for each cell strain. The measurements were made at 2 to 4 randomly chosen spots in the cytoplasm of 10 to 20 different cells of each cell strain. At each spot in the cell cytoplasm the measurements were repeated three or five times. Only cells that showed high expression and appeared healthy were chosen for the experiment. In cells expressing free GFP, PH-CRAC-GFP and PH2-GFP the expression level was too high for FCS measurements. In these cases the proteins were photobleached to acceptable fluorescence intensity levels before the measurement by exposing the cells to high intensity laser beam (~1 mW) for less than a second. Typically, for cells incubated in buffer, measurements of 10 s were performed in vegetative cells and 5 s in polarized cells. Measurements of 20 to 30 s were made in cells immobilized in agarose. Diffusion of GFP in phosphate buffer (17 mM, pH 8), containing 50% sucrose was also measured under similar experimental conditions as those employed for cellular measurements. Around 100 autocorrelation curves were collected for a measurement time of 10 s.

3.2.6 PCH measurements

The data were obtained from *Dictyostelium* cells expressing free GFP and PH10-GFP, incubated in phosphate buffer (17 mM, pH 6.5). Single measurements were made in 20 cells of each strain. Raw data were obtained in photon mode. 2 x 10^6 photons for cells with free GFP and 1 x 10^6 for cells expressing PH10-GFP were collected at a sampling frequency of 2 and 1 MHz respectively.

3.2.7 Data analysis

The autocorrelation traces were analyzed with FCS Data Processor version 1.3 (Skakun *et al.,* 2005).The analysis was performed using the global analysis approach, where five or six autocorrelation traces were fitted simultaneously, with their diffusion times τ_d, and triplet lifetimes T_{trip}, linked. The traces were fitted with a fixed value of the structural parameter *sp* that was obtained from calibration with a rhodamine-110 solution and varied between 8 and 12. The structural parameter is defined as the ratio of axial (ω_z) to radial (ω_{xy}) radii of the sample volume element. *N,* the average number of molecules, and F_{trip}, the fractional population of the triplet state were allowed to vary.

An offset term was added to take into account artifacts in the autocorrelation due to drift in average fluorescence intensity on time scales of > 1 s, possibly arising from cellular and intracellular movement (Brock *et al.,* 1999). The quality of the fit was judged by the reduced χ^2 criterion and by visual inspection of the residuals. Because all measurements were made in the cell cytoplasm, the autocorrelation function ($G(\tau)$) was fit to Eq. 3.1, which describes the three-dimensional Brownian motion of a single species.

$$G(\tau) = 1 + \frac{1}{N}\left(\left(1+\frac{\tau}{\tau_d}\right)\sqrt{1+\left(\frac{\omega_{xy}}{\omega_z}\right)^2\frac{\tau}{\tau_d}}\right)^{-1}\left(1+\frac{F_{trip}e^{-\tau/T_{trip}}}{1-F_{trip}}\right) \tag{3.1}$$

The translational diffusion coefficient D was calculated from the diffusion time τ_d using equation 3.2:

$$\tau_d = \frac{\omega_{xy}^2}{4D} \tag{3.2}$$

The intracellular viscosity was calculated according to the Stokes- Einstein's equation (Eq. 3.3),

$$D = \frac{kT}{6\pi\eta r_h} \tag{3.3}$$

where, k is the Boltzmann constant, T is the temperature, η is the viscosity of the solution and r_h is the hydrodynamic radius of the solute.

The raw data for photon counting histogram were acquired and analyzed using ISS – Alba FCS version 2.55 (ISS, USA) at a sampling frequency of 50 kHz and fit assuming single species. The PCH function for an open system describes the possibility of observing k photon counts per sampling time with N as the average number of molecules in the detection volume (Chen *et al.,* 1999b). The molecular brightness ε, expressed as kilohertz/molecule, is the ratio of the average number of photon counts ($\langle k \rangle$) received per second to N (Eq. 3.4).

$$\varepsilon = \frac{\langle k \rangle}{N} \tag{3.4}$$

ε is independent of the sampling frequency, and values from different experiments can be directly compared (Chen *et al.,* 1999b).

3.3 Results

3.3.1 Localization of PH domain-GFP fusions and free GFP in cells

Confocal images showing the localization of PH domain-GFP fusions and free GFP in vegetative *Dictyostelium* cells are shown in Fig. 3.2. PH2-GFP and free GFP are homogenously distributed in the cell whereas PH-CRAC-GFP and PH10-GFP transiently localize to parts of the membrane. Fig. 3.3 shows the translocation of PH10-GFP to a macropinosome in a vegetative cell. In polarized cells PH10-GFP translocates to the leading edge of the cell (Fig. 3.4). The distribution of free GFP and PH2-GFP in polarized cells remains similar to that in vegetative cells.

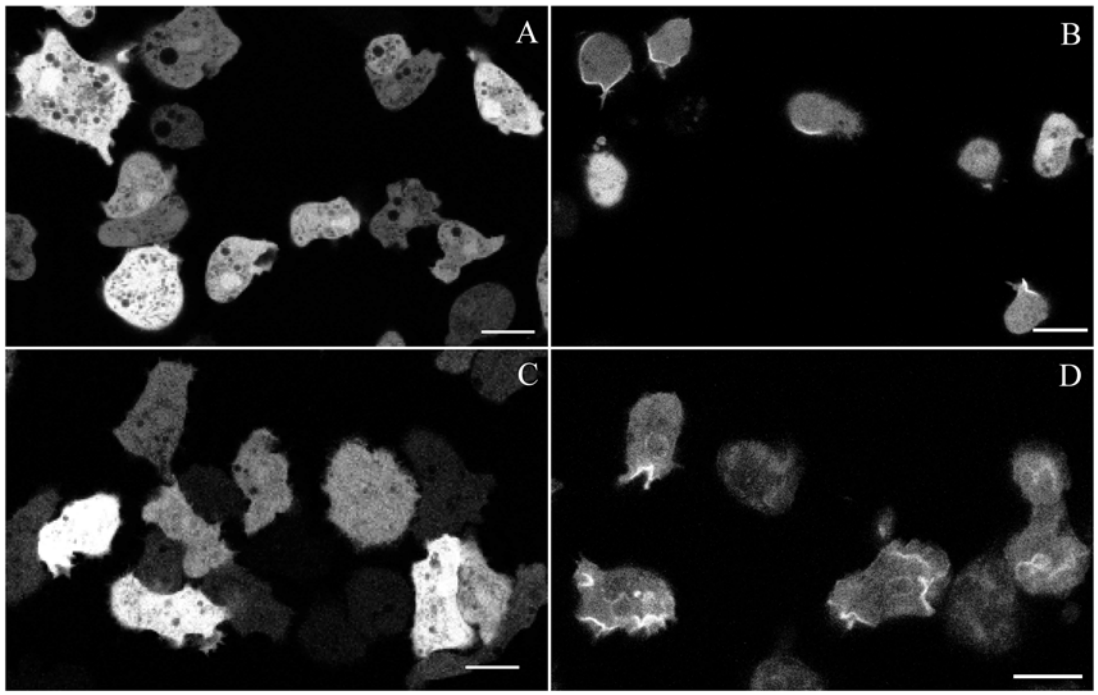

Figure 3.2: Vegetative *Dictyostelium* cells. Confocal images of cells expressing A) free GFP, B) PH-CRAC-GFP, C) PH2-GFP and D) PH10-GFP. Cells were incubated in potassium phosphate buffer (pH 6.5, 17 mM). (Bar = 10 μm)

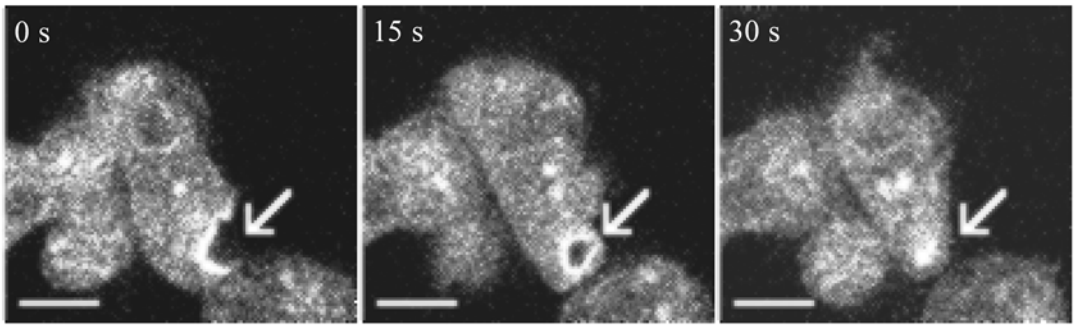

Figure 3.3: Translocation of PH10-GFP to macropinosomes in *Dictyostelium* cells. Images were taken at 10 s intervals. Cells were incubated in potassium phosphate buffer (pH 6.5, 17 mM). (Bar = 5μm)

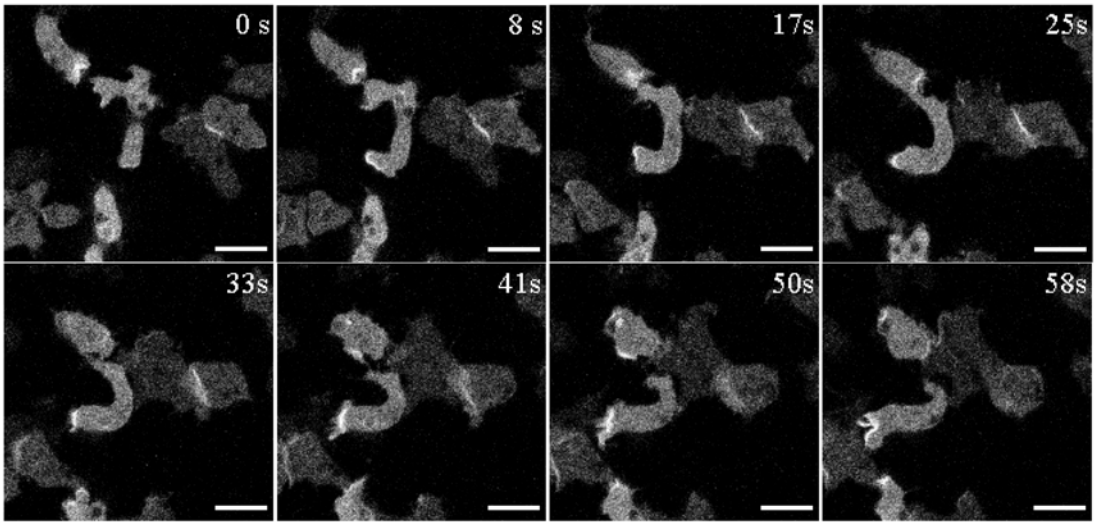

Figure 3.4: Translocation of PH10-GFP to the leading edge of polarized *Dictyostelium* cells. Cells were incubated in potassium phosphate buffer (17 mM, pH 6.5) for around 5 hours. (Bar = 10 μm)

3.3.2 Diffusion characteristics in vegetative cells

The distributions of diffusion coefficient values of free GFP and GFP fusions of PH domains in vegetative *Dictyostelium* cells incubated in buffer are plotted in Fig. 3.5B – E. For comparison with *in vitro* values, the distribution of diffusion coefficient values of GFP in potassium phosphate buffer (17 mM, pH 8) containing 50% sucrose, obtained under similar experimental conditions as used for the cellular measurements, is plotted in Fig. 3.5A. The diffusion coefficient distributions of PH-CRAC-GFP and PH2-GFP overlap with that of free GFP whereas that of PH10-GFP shows smaller diffusion coefficient values. The width of the distribution of diffusion coefficient values of GFP and the fusion proteins in cells is larger than of GFP in solution. An estimate of the width can also be obtained from the relative standard deviation (RSD) associated with each average value. The numerical average diffusion coefficients, standard deviations, confidence intervals and RSDs, as determined for each protein and for GFP *in vitro* are listed in Table 3.1. The RSD for free GFP and PH domain-GFP fusions are between 18 and 20% whereas that for free GFP *in vitro* is 5%. From the average diffusion coefficient obtained for free GFP in cells and buffer, the average intracellular viscosity in the vegetative cells is calculated to be 3.5 ± 0.7 cP (Eq. 3.3).

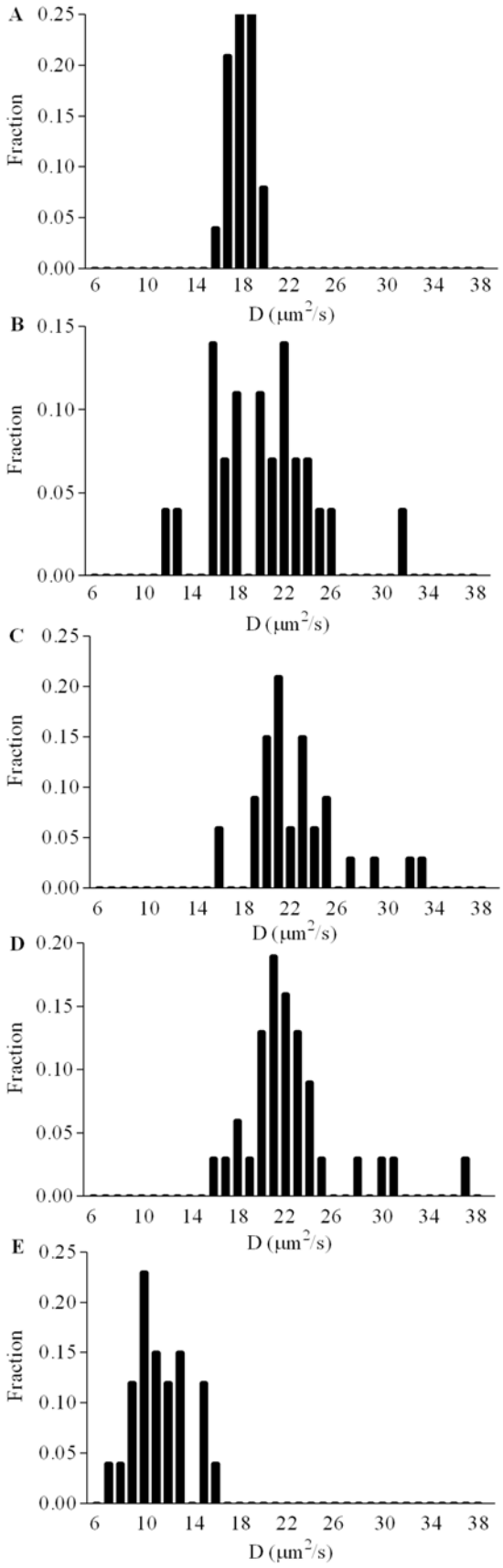

Figure 3.5: Distribution of diffusion coefficients *in vitro* and in vegetative cells. A) GFP in potassium phosphate buffer (17 mM, pH 8, containing 50% sucrose) B) free GFP, C) PH-CRAC-GFP, D) PH2-GFP and E) PH10-GFP in vegetative cells.

3.3.3 PH10-GFP is not aggregating

PCH measurements were performed to determine whether the slow diffusion of PH10-GFP could be caused by aggregation of the protein. PCH uses the intensity amplitude distributions to give a quantitative description of the molecular brightness values of the fluorescent species present in the sample. In the autocorrelation curve this amplitude information can only be obtained from the G(0). The molecular brightness of PH10-GFP in vegetative *Dictyostelium* cells was determined and compared to the molecular brightness of free GFP in the cells. The measurements gave an average molecular brightness of 3.7 ± 1.3 kHz per molecule for PH10-GFP and of 3.1 ± 0.9 kHz per molecule for free GFP. A representative histogram is shown in Fig. 3.6. The similar molecular brightness for the two proteins indicates that PH10-GFP is not aggregating.

Table 3.1: Diffusion of PH domain-GFP fusions and free GFP in cells and *in vitro*. Average diffusion coefficients, standard deviations, 95% confidence interval (CI) and relative standard deviations (RSD) as determined for free GFP and PH domain-GFP fusions in the cytoplasm of vegetative and polarized cells incubated in potassium phosphate buffer (pH 6.5, 17 mM), and for GFP in potassium phosphate buffer (17 mM, pH 8, containing 50% sucrose).

Sample	Vegetative			Polarized		
	D ($\mu m^2/s$)	CI	RSD (%)	D ($\mu m^2/s$)	CI	RSD (%)
Cells incubated in buffer						
Free GFP	20 ± 4	18-22	20	32 ± 6	29-35	19
PH-CRAC-GFP	22 ± 4	21-24	18	23 ± 4	21-25	17
PH2-GFP	22 ± 4	21-24	18	27 ± 6	24-29	22
PH10-GFP	11 ± 2	10-12	18	12 ± 2	11-13	17
Cells immobilized in 3% agarose						
Free GFP	24 ± 4	22-25	17	-	-	
In vitro						
GFP	18 ± 1	18-19	5			

3.3.4 Diffusion characteristics in polarized cells

The effect of polarization on the distributions of diffusion coefficients of PH domain-GFP fusions and free GFP is shown in Fig. 3.7. PH2-GFP and free GFP show faster diffusion in polarized cells, as indicated by the shift of the diffusion coefficient distribution of the two proteins to higher values with respect to the distribution in vegetative cells. That the differences in these distributions are significant is confirmed by the unpaired t-test ($p < 0.005$). The shift is more pronounced for free GFP than for PH2-GFP. The diffusion coefficient distributions of PH-CRAC-GFP and PH10-GFP, however, totally overlap with that obtained from vegetative cells. Unpaired t-test gives $p > 0.5$. The numerical average diffusion coefficient values are listed in Table 3.1. The relative standard deviation associated with each value is between 17 and 22%, similar to the results from vegetative cells. From the average diffusion coefficient obtained for free GFP in the polarized cells, the intracellular viscosity is calculated to be 2.1 ± 0.4 cP, approximately 1.7 times lower than in vegetative cells.

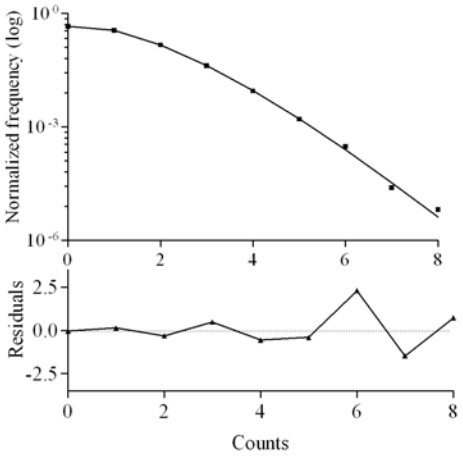

Figure 3.6: Photon counting histogram of PH10-GFP. Upper panel shows experimental data (squares) and the theoretical fit (line); lower panel shows the normalized residuals of the fit. Average brightness value for PH10-GFP is 3.7 ± 1.3 kHz/molecule.

3.3.5 Cellular movement and autofluorescence

Dictyostelium cells incubated in buffer move around continuously. The vegetative cells show random pseudopod formation and movement of the cells is slower than movement of polarized cells. A measurement time of 10 s for vegetative cells and 5 s for the polarized cells was chosen. This ensured that the cells did not move excessively during the measurement. Even during the chosen time, the fluorescence fluctuations did not remain steady around an average value, probably due to cellular or intracellular movement. A comparison of the intensity traces obtained from GFP diffusion in buffer containing 50% sucrose and GFP diffusion in cells is shown in Fig. 3.8. The autocorrelation curves obtained from cells could be fit well to the model describing 3D

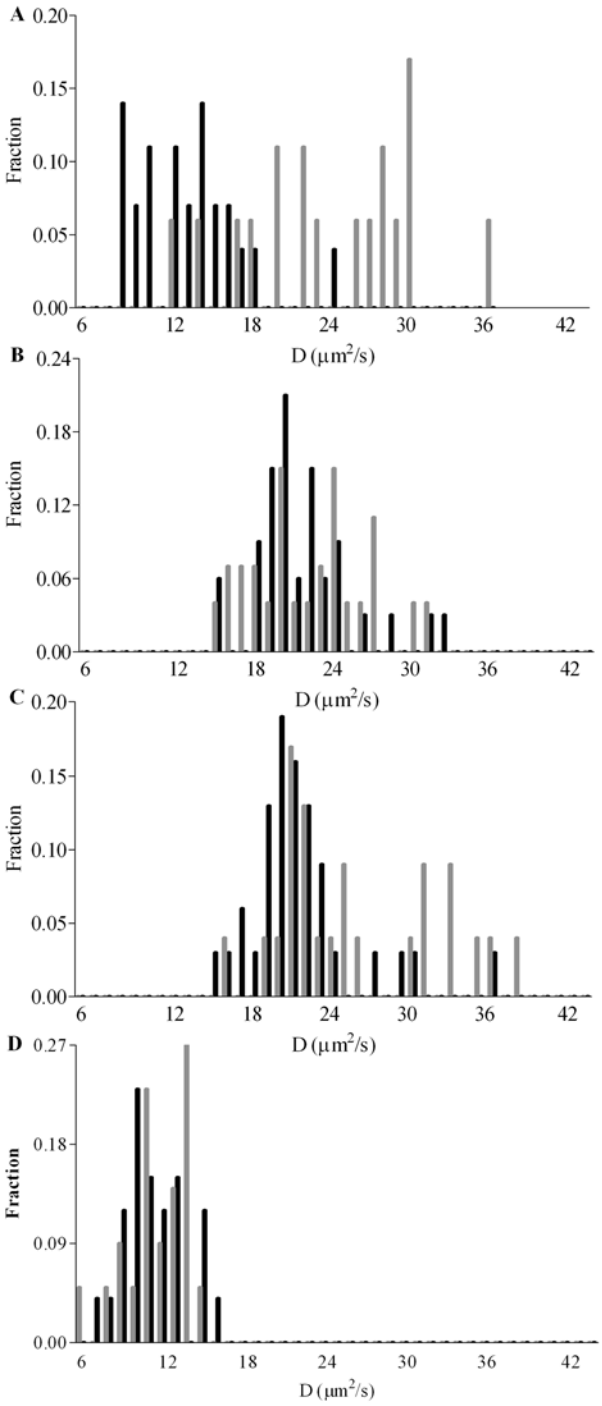

Figure 3.7: Effect of cell polarization on diffusion coefficient distributions of free GFP and PH domain-GFP fusions. A) Free GFP, B) PH-CRAC-GFP, C) PH2-GFP and D) PH10-GFP in vegetative (black bars) and polarized (grey bars) cells.

Brownian motion for a single species after an offset term had been added to it (Eq. 3.1). The offset term was needed to account for the slow intensity drifts. Fig. 3.9 shows a representative autocorrelation curve with the fit and the residuals of the fit.

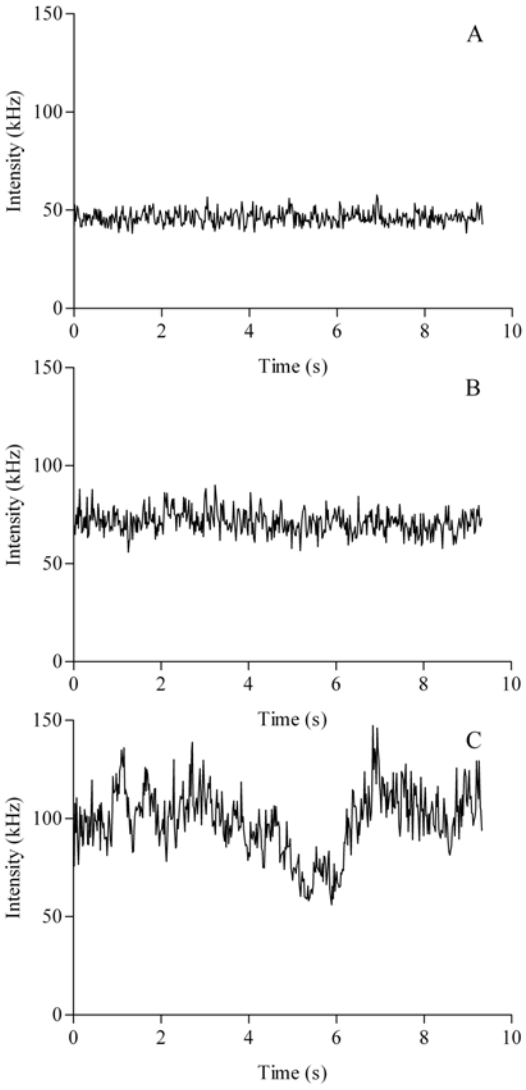

Figure 3.8: Fluorescence intensity traces. Uniform fluctuations obtained from A) GFP in potassium phosphate buffer containing 50% sucrose B) GFP in cell cytoplasm and non-uniform fluctuations from C) GFP in cell cytoplasm.

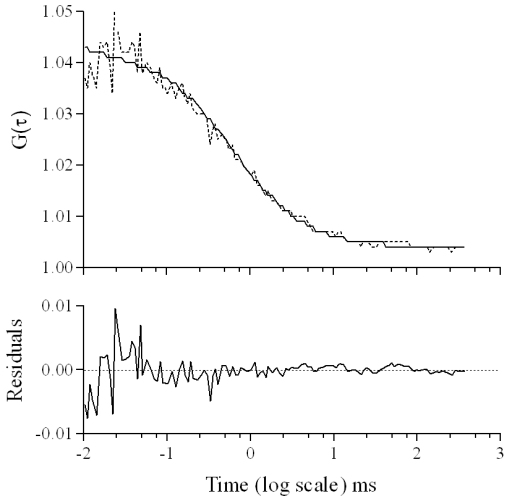

Figure 3.9: Representative autocorrelation curve. Autocorrelation curve from a 10 s measurement of PH2-GFP diffusion in the cytoplasm of vegetative cells. Experimental curve (⋯) and theoretical fit (—). Lower panel shows residuals of the fit.

To estimate the contribution of cell movement to the widening of the diffusion coefficient distributions obtained from measurements in the cells, autocorrelation traces were also obtained from free GFP expressing vegetative cells immobilized in agarose.

Longer measurement times of 20 to 30s were possible here. The numerical average diffusion coefficient for free GFP in the immobilized cells is 24 ± 4 $\mu m^2/s$, the standard deviation corresponding to 17% of the average diffusion coefficient value (Table 3.1). The RSD value is similar to that obtained for the various cell strains incubated in buffer indicating that the movement of the cells is not contributing significantly to the standard deviations associated with the measurements. Also in the case of immobilized cells, slow drifts in fluorescence intensity were seen, indicating intracellular movement.

The contribution of cellular autofluorescence was determined from measurements made in wild type *Dictyostelium* cells of strain AX3. The autofluorescence does not autocorrelate and hence, does not interfere with the measurement of diffusion times. It is thus ignored.

3.4 Discussion

The diffusion characteristics of PH2-GFP, PH10-GFP and PH-CRAC-GFP in the cytoplasm of vegetative and polarized *Dictyostelium* cells have been characterized to obtain a better understanding of the functioning of these domains in the cell and to study the effect of initiation of chemotaxis on these domains. The diffusion of the PH domain-GFP fusions was compared with the diffusion of free GFP in the cells. Free GFP is homogenously distributed in the *Dictyostelium* cytoplasm (Fig. 3.2A). Of the three PH domains studied, PH2-GFP is homogenously distributed in the cytoplasm in vegetative cells (Fig. 3.2 C) and does not show change in the localization upon cell polarization. This indicates that PH2 is not involved in membrane recruitment of the protein bearing it and plays a different role in the signaling pathway in *Dictyostelium*. Because it remains cytosolic in polarized cells, it is possible that PH2, like some other PH domains (Hirata *et al.,* 1998; Varnai *et al.,* 2002), binds to soluble inositol phosphates and perform functions such as negative regulation of signaling pathways by reducing the amount of free inositol phosphates available for other processes. PH10-GFP and PH-CRAC-GFP show transient translocation to macropinosomes in vegetative cells (Fig. 3.3) and to the leading edge of the polarized cell (Fig. 3.4) (Parent *et al.,* 1998). Thus, PH-CRAC and PH10 are involved in membrane binding in *Dictyostelium* whereas PH2 is not. However, the diffusion characteristics of PH2-GFP and PH-CRAC-GFP in vegetative cells are very similar. Their diffusion coefficient distributions also overlap with that of free GFP. This is expected as the molecular weight of GFP differs from that of the PH domain-GFP fusions only by a factor of 1.5. With FCS it is not possible to distinguish two species, in an identical environment, without *a priori* knowledge, until the molecular weights differ by a factor of four at least (Meseth *et al.,* 1999). Free GFP, which lacks non-specific interactions with cellular moieties (Dittrich *et al.,* 2001), is a good indicator of the intracellular environment. The similarity in the diffusion characteristics of PH2-GFP and PH-CRAC-GFP with that of free GFP indicates that the two PH domains are not interacting with any bulky intracellular moiety in the cytosol. It is surprising that the diffusion of PH10-GFP is slower than that of the other PH domains and free GFP. With PCH it has been shown that this slow diffusion is not due to aggregation of the protein. A possible reason for the slow diffusion of PH10-GFP could be that the domain is interacting with a bulky intracellular moiety, approximately 8

times its molecular weight since the diffusion is twice as slow as that of the other PH domains or that it is enclosed in high viscosity micro-regions formed by the cytoskeleton in the cytoplasm. (Luby-Phelps *et al.,* 1986), have demonstrated the presence of structural barriers in the form of filamentous meshwork of varying pore sizes in the cytoplasm.

The diffusion coefficients obtained from measurements at different positions in cells show wide distributions, compared to GFP *in vitro* (Fig. 3.5 and 3.7). The wide distributions illustrate the heterogeneity and dynamics of the intracellular environment. From the width of the distributions and RSD values for the PH domain-GFP fusions and free GFP in the cells (Table 3.1), it is clear that the intracellular heterogeneities affect all the species to a similar extent. Also the effect is similar in vegetative and polarized cells. However, the changes in the intracellular environment upon polarization of the cell affect free GFP and the three PH domain-GFP fusions differently. The diffusion of free GFP in the cell cytoplasm is faster in polarized cells than in vegetative cells, as indicated by the shift of the distribution of the diffusion coefficient values to higher values (Fig. 3.7). Diffusion coefficients obtained for free GFP in buffer and cells indicate that the intracellular viscosity in polarized cells is around 1.7 times lower than in vegetative cells. A 1.4 times decrease in the cytoplasmic viscosity in polarized *Dictyostelium* cells was observed in a previous study using FRAP (Potma *et al.,* 2001). Faster diffusion is also seen for PH2-GFP in polarized cells though, in this case the shift in distribution of diffusion coefficient values is less pronounced. Surprisingly, PH10-GFP and PH-CRAC-GFP show no change in their diffusion characteristics upon polarization of the cells. Thus, the lowering of viscosity has no detectable effect on PH10-GFP and PH-CRAC-GFP diffusion. This can be the case if the effect of change in viscosity on PH10 and PH-CRAC diffusion is cancelled by another event taking place in the polarized cells. At this stage it is not clear what that event might be.

The factors that could have interfered with FCS measurements are cellular autofluorescence and fluorophore depletion in the cell because of photodestruction at the focus (Brock and Jovin 2001). An additional factor in *Dictyostelium* is the movement of the cells. Below it is shown that these three factors do not interfere with our measurements. The autofluorescence from the cells does not correlate, and so does not contribute to the autocorrelation function derived from the diffusion of GFP and GFP fusion proteins. Thus, it does not interfere with the measurement of diffusion times and is ignored. The second factor i.e. the possibility of photodestruction in the excitation volume during the measurement is minimized by making short measurements (of 5 – 10 s) at low excitation intensities (< 10 μW). The expression levels of cells with free GFP, PH-CRAC-GFP and PH2-GFP are too high for FCS and so the fluorophore is bleached before the measurement. However, no fluorescence recovery or

photobleaching is observed during the measurement. This indicates that the average number of molecules in the detection volume remains constant. Consequently, the diffusion times are not affected by the bleaching procedure. The third factor that has to be taken into account is the high mobility of *Dictyostelium* cells. Cells incubated in buffer constantly form pseudopodia and move around. This makes it difficult to make repeated measurements in these cells. The measurement times chosen for the experiments (5 - 10 s) not only minimize the possibility of photodepletion but also ensure that the movement of the cells during the measurement is limited. Longer measurements of up to 30 s are possible in cells immobilized in agarose. For most of the measurements it is observed that the average fluorescence intensity does not remain steady around an average value but shows a slow drift (Fig. 3.8). This also holds true for cells immobilized in agarose. Similar drifts in average fluorescence intensity, obtained from the cytoplasm, have also been observed in other cells (Chen *et al.,* 2002). The slow drifts in intensity, on the time scale of seconds, are attributed to cellular and intracellular movements. The drifts are accounted for by adding an offset value to the autocorrelation curve.

In conclusion, three PH domains in *Dictyostelium* cells have been studied. Of the three domains, PH2 is homogenously distributed in vegetative and polarized cells whereas PH10 and PH-CRAC show transient translocation to the leading edge of the polarized cell. The diffusion characteristics of PH2 and PH-CRAC in vegetative cells are very similar but PH10 exhibits slower diffusion. All three PH domains are similarly affected by the intracellular heterogeneities. However, in polarized cells, where the viscosity is 1.7 times lower than in vegetative cells, only PH2 shows increased mobility. PH10 and PH-CRAC do not show any change.

4 Characterization of G-protein βγ Complex Diffusion in Chemotaxing *Dictyostelium* Cells

Heterotrimeric G-protein mediated signaling plays a crucial role in the chemotactic movement of *Dictyostelium* cells. In chemotaxing cells, the downstream effectors of G-proteins, but not the G-proteins themselves, show highly polarized spatial localization. The mechanism of internal signal amplification to achieve this polarized state is still unresolved. In this chapter, the diffusion of GFP fusions of Gβ and Gγ in *Dictyostelium* cells has been studied using fluorescence correlation spectroscopy (FCS). The aim was to investigate whether initiation of chemotaxis has an affect on the diffusion of the subunits and whether this could directly or indirectly influence the polarization of the cell. The results indicate that Gβ and Gγ are associated with each other, in both vegetative and chemotaxing cells. In cytoplasm of chemotaxing cells, the Gβγ complex shows increased mobility most likely due to rearrangements of the cytoskeleton. The diffusion of the subunits at the plasma membrane however, is not affected by initiation of chemotaxis. Interestingly, in chemotaxing cells stimulated with the chemoattractant cAMP, the diffusion of the Gβγ complex in the front region of the cell cytoplasm is significantly faster than in the mid or back of the cell. While this variable diffusion within a cell is itself, probably, a consequence of the polarization of the actin cytoskeleton, its presence implies that G-protein from the cytoplasmic pool is more easily available to the plasma membrane at the front of the cell, aiding the signaling in the front. It is proposed that this variable diffusion contributes to the amplification of the intracellular chemotactic response after an initial polarity has been established by other mechanisms.

4.1 Introduction

The heterotrimeric GTP-binding proteins (G-proteins), composed of α, β and γ subunits, play a central role in the specificity and temporal regulation of signaling processes (Sprang 1997; Cabrera-Vera *et al.,* 2003). For the social amoeba *Dictyostelium discoideum*, G-protein mediated signaling is crucial for development (Wu *et al.,* 1995; Zhang *et al.,* 2001; Manahan *et al.,* 2004). Single cells of *Dictyostelium* are able to chemotax and aggregate in response to cAMP gradients to develop into a multicellular organism through G-protein signaling. The cells can respond to as low as a 2% concentration difference between their front and back, when the mean concentration is only ~1 nM (Mato *et al.,* 1975). In response to the cAMP signal, G-proteins at the cytoplasmic side of the plasma membrane are activated via the receptor, leading to the dissociation of the Gα subunit from the Gβγ subunits (Janetopoulos *et al.,* 2001). The dissociated subunits can then modulate downstream effectors. During the activation of the G-protein a GDP molecule bound to the Gα subunit is exchanged for a GTP molecule. The Gβ and Gγ subunits remain associated with each other throughout (Clapham and Neer 1997; Hamm 1998; Schwindinger and Robishaw 2001). *Dictyostelium* cells chemotaxing in cAMP gradients extend pseudopods preferentially in the direction of rising cAMP concentrations and acquire an elongated, polarized morphology, with a defined anterior and posterior. In these cells many of the downstream effectors, PI3K (phosphoinositide 3-kinase), PTEN (PI 3-phosphatase), F-actin, ACA (adenylyl cyclase A), sGC (soluble guanylyl cyclase) and myosin II show highly polarised localization (Kimmel and Parent 2003; Postma *et al.,* 2004; Manahan *et al.,* 2004). However, the G-proteins themselves and also the cAMP receptor-cAR1 are uniformly distributed in the cells (Xiao *et al.,* 1997; Jin *et al.,* 2000). The mechanism of internal signal amplification by means of which chemotaxing cells are able to attain a highly polarized morphology is still unresolved.

The Gβ and Gγ subunits are functional when localized at the membrane (Zhang *et al.,* 2001; Blaauw *et al.,* 2003). However, the assembly and post-translational modifications of the Gβγ complex and also probably its interaction with Gα are thought to occur in the cytosol (Higgins and Casey 1994; Higgins and Casey 1996; Cabrera-Vera *et al.,* 2003). The formation of the Gβγ complex is essential for the stability of both, β and γ subunits and also for interaction with Gα subunit. The activation of signaling events in a cell largely depends on how fast regulatory molecules, such as the G-proteins, can diffuse through the cell to reach other molecules. It has been suggested that the ability of G-proteins to diffuse both in the cytosol and the membrane makes them ideal candidates for transmission of temporal information globally in a cell and

also for preserving and integrating spatial information locally (Postma *et al.,* 2004). Here, the diffusion of G-proteins in *Dictyostelium* cells is characterized and the effect of initiation of chemotaxis on this diffusion is studied.

GFP fusions of Gβ and Gγ have been expressed in *Dictyostelium* cells and their diffusion is studied using fluorescence correlation spectroscopy (FCS). The suitability of fluorescence fluctuation techniques as tool to study protein diffusion in *Dictyostelium* cells has been previously demonstrated (Ruchira *et al.,* 2004). Detailed information about the diffusion of the GFP tagged subunits is obtained from the cytoplasm of chemotaxing and non-chemotaxing cells. In addition, since the complex is functional at the membrane, the diffusion of the membrane bound protein is also studied.

4.2 Experimental procedure

4.2.1 Cells

Wild type *Dictyostelium* cells expressing GFP-Gβ, GFP-Gγ and free GFP were transfected and grown as described earlier (Blaauw *et al.,* 2003; Ruchira *et al.,* 2004). The double-labeled Gβγ cell line was prepared as follows: Cells expressing GFP-Gγ with the neomycin selection marker (Blaauw *et al.,* 2003) were transformed with plasmid GFP-Gβ/LB5Hyg that expresses GFP-Gβ using a hygromycin selection marker. GFP-Gβ/LB5Hyg was constructed by cloning the hygromycin resistance cassette from LB8 into the XbaI/BstXI sites of Gβ/LB5Neo (Blaauw *et al.,* 2003). The hygromycin resistance cassette (kind gift of J. Williams) is comprised of an actin 15 promoter followed by the HPH hygromycin resistance gene and the cabA terminator TAAATAAAATAAATAAATTGT.

4.2.2 Sample preparation

Cells from a confluent dish were washed twice with potassium phosphate buffer (17 mM, pH 6.5) and were either transferred to a 96-chambered glass bottom microplate (Whatman) for measurements in vegetative cells or suspended in 500 µl of the same buffer at a density of 2.5 x $10^7 ml^{-1}$ in a centrifuge tube (Sarstedt) for at least five hours, to allow the cells to starve, and then transferred to the microplate. During the measurement, cells were incubated in the same phosphate buffer. All measurements were performed at room temperature.

Chemotaxis Assay: Approximately 40 µl of suspension of starving cells was pipetted on a 24 x 50 mm cover-glass (Menzel-Glaser) and allowed to settle for 10-15 minutes. The cover-glass was then mounted on the microscope stage to which a microinjection module (Eppendorf Microinjector 5242 and Micromanipulator 5170) was coupled. A femtotip (Eppendorf) filled with 10 µM cAMP was positioned next to some starving

cells with the help of the microinjection module. Before starting measurements, the buffer around the cells was replaced by 300 µl of 1 µM latrunculin A (Molecular Probes) solution in phosphate buffer. Fresh latrunculin A dilutions in phosphate buffer were prepared from a 1 mM stock solution in DMSO, every time before use.

4.2.3 Instrumentation

FCS measurements were performed on ConforCor 2 – LSM 510 combination setup (Carl Zeiss, Germany) (Hink *et al.,* 2003). GFP was excited with the 488 nm line from an argon-ion laser (excitation intensity ~ 11 µW) focused into the sample with a water immersion C-Apochromat 40x objective lens N.A. 1.2 (Zeiss). After passing through the main beam splitters HFT 488/633 the fluorescence was filtered with a band pass 505-550. The pinhole for confocal detection was set at 70 µm. The microscope was controlled by Zeiss AIM 3.2 software. The position of the confocal observation volume within the cell cytoplasm or membrane was determined by imaging the cells immediately before and after the measurements. For imaging, GFP was excited using the 488 nm laser line and the emission was filtered with BP 505-550. The acquired images were processed using Zeiss LSM Image Browser software package (V 3.2).

Raw intensity fluctuation data consisting of up to 2 x 10^6 photons were collected from single measurements in 30 to 50 different cells of each strain. The data collection time ranged between 15 - 50 s. Since expression levels in all cell lines were too high for FCS, GFP was photobleached to acceptable fluorescence intensity levels by exposing the cells to a high intensity laser beam (~ 1 mW) for one second, prior to the measurements. The data were acquired at a sampling frequency of 1 MHz with a dual channel 32 bits, PCI photon counting card (ISS, USA). The data acquisition was controlled by Alba FCS 3.03 software (ISS, USA). Autocorrelation curves were generated and analyzed from the recorded data using FCS Data Processor version 1.4 (Skakun *et al.,* 2005)

4.2.4 Data analysis

The intensity fluctuation traces exhibited wide non-uniform fluctuations due to cellular movement (Ruchira *et al.,* 2004). To minimize the influence of the non-uniform fluctuations, autocorrelation curves were generated from intensity traces split into smaller parts, of 1 – 5 s, where the fluctuations were within ± 25% of the average intensity. The autocorrelation curves thus generated were analyzed globally (Skakun *et al.,* 2005). The curves were fit with either a model describing the diffusion of a single component in three dimensions (Eq. 4.1) or a model describing the diffusion of one component in three dimensions and a second component in two dimensions (Eq. 4.2). Representative autocorrelation curves and fits are shown in Fig. 4.1. The component

diffusing in three dimensions describes cytosolic diffusion while the component diffusing in two dimensions describes membrane diffusion. An offset term was added to take into account the artifacts in the autocorrelation curves caused due to the remaining, small intensity drifts in the average fluorescence intensity (Brock *et al.,* 1999; Ruchira *et al.,* 2004).

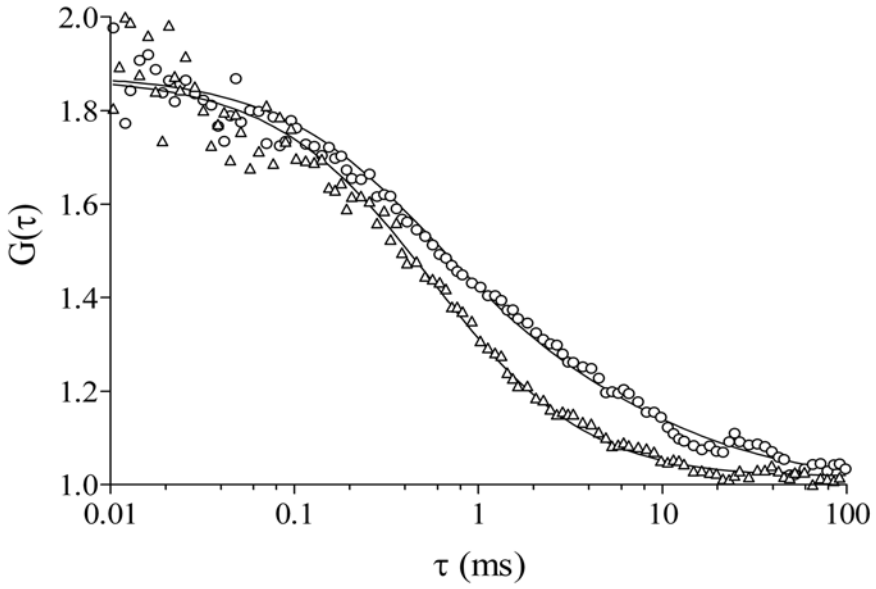

Figure 4.1: Representative autocorrelation curves obtained from GFP-Gβ diffusion in vegetative *Dictyostelium* cells. FCS traces were generated from raw intensity fluctuation data and represent either cytosolic diffusion (triangles) or cytosolic and membrane diffusion (circles). The traces are fit to Eq. 4.1 and Eq. 4.2, respectively (solid lines).

$$G(\tau) = 1 + \frac{1}{N}\left(\left(1+\frac{\tau}{\tau_{d1}}\right)\sqrt{1+\frac{\tau}{sp^2\tau_{d1}}}\right)^{-1} + offset \tag{4.1}$$

$$G(\tau) = 1 + \frac{1}{N}\left\{F_1\left(\left(1+\frac{\tau}{\tau_{d1}}\right)\sqrt{1+\frac{\tau}{sp^2\tau_{d1}}}\right)^{-1} + (1-F_1)\left(1+\frac{\tau}{\tau_{d2}}\right)^{-1}\right\} + offset \tag{4.2}$$

In equations 4.1 and 4.2, $G(\tau)$ is the autocorrelation function, N is the average number of molecules in the detection volume, τ_{d1} and τ_{d2} are the diffusion times of the cytosolic and membrane bound species, respectively, F_1 is the fraction of cytosolic species and sp is the structural parameter, which is the ratio of the axial radius ω_z to the equatorial radius ω_{xy} of the 3D Gaussian detection volume. The analysis was performed

with the diffusion times linked. In Eq. 4.2 τ_{d1} was fixed to the value obtained from fitting data from the same cell line to Eq. 4.1. The value of *sp* was fixed to 5, as was determined from calibration measurements of a rhodamine-110 solution. Confidence intervals for the linked diffusion times were calculated using the asymptotic error analysis (Straume *et al.,* 1991; Johnson and Flaunt 1992). The translational diffusion coefficient *D* was calculated from the diffusion time τ_d using Eq. 4.3,

$$D = \frac{\omega_{xy}^2}{4\tau_d} \tag{4.3}$$

where ω_{xy} is obtained from the calibration measurements. τ_d for rhodamine 110 in our setup varied between 14 – 19 μs. $D_{rhodamine110}$ was taken as 2.8 x 10^{-10} m^2/s (Magde *et al.,* 1974).

4.3 Results

4.3.1 Cytoplasmic Gβγ diffuses faster in chemotaxing cells

The effect of cell polarization on diffusion of Gβγ was studied by measuring the diffusion characteristics of Gβ and Gγ in three wild type *Dictyostelium* cell-lines, one expressing GFP-Gβ, the second expressing GFP-Gγ and a third expressing both GFP-Gβ and GFP-Gγ. Measurements were performed in vegetative cells and chemotaxing cells in early aggregation stage. The results are summarized in Table 4.1. The average diffusion coefficient of GFP-Gβ in vegetative cells is 9 $\mu m^2/s$, similar to the value of 10 $\mu m^2/s$ for GFP-Gγ in vegetative cells reported by us previously (Knol *et al.,* 2005). The similarity in the diffusion coefficients of the two subunits despite differences in their molecular weights, GFP-Gβ is 66 kDa and GFP-Gγ is 35 kDa, indicates that GFP-Gβ and GFP-Gγ are associated with each other. The expected mass of a GFP-Gβ.Gγ complex is approximately 73 kDa. Since diffusion coefficient is proportional to the inverse cube root of the molecular weight, the expected diffusion coefficient for the GFP-Gβ.Gγ complex can be estimated by comparing with the diffusion coefficient value of the free GFP (27 kDa) in cell cytoplasm (Table 4.1; (Ruchira *et al.,* 2004)). Such a comparison shows that the observed average diffusion coefficients of 9 and 10 $\mu m^2/s$ are slightly lower than expected for the complex. Thus, it is possible that the Gβγ complex in cell cytoplasm interacts with other proteins there. It has been suggested before that the cytoplasmic Gβγ is also associated with Gα (Janetopoulos *et al.,* 2001). However, it should be noted here that comparison of the diffusion coefficients of GFP and the complex of Gβγ holds only if both species are globular. In this case, while GFP

is nearly globular, a GFP-Gαβγ complex is rather elongated (Wall *et al.,* 1995; Lambright *et al.,* 1996; Ormö *et al.,* 1996), which can give rise to diffusion coefficient values which are slightly lower than expected.

In chemotaxing cells, as in vegetative cells, the average diffusion coefficient values of the GFP-Gβ and GFP-Gγ subunits (13 $\mu m^2/s$) are similar, suggesting that the two subunits remain associated with each other in these cells. However, these values are higher than those obtained in vegetative cells, demonstrating the effect of cell polarization on Gβγ diffusion (Fig. 4.2). This increase in the average diffusion coefficient of Gβγ is somewhat lower than observed for free GFP in *Dictyostelium* cells, which becomes approximately 1.6 times faster in polarized cells (Ruchira *et al.,* 2004). The retardation of Gβγ mobility in chemotaxing cells could be due to its interactions with intracellular moieties.

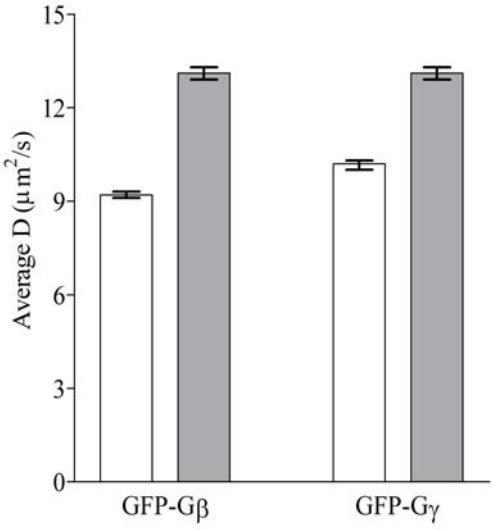

Figure 4.2: Effect of cell polarization on Gβγ diffusion. Comparison of diffusion characteristics of GFP-Gβ and GFP-Gγ in cytoplasm of vegetative (white bar) and chemotaxing (grey bars) cells. Histograms represent the average diffusion coefficient values obtained for the two subunits. Error bars represent the 95% confidence interval.

The average diffusion coefficients obtained from the cell line expressing both GFP-Gβ and GFP-Gγ simultaneously, were very similar to the ones observed for wild type cells expressing either GFP-Gβ or GFP-Gγ (Table 4.1). This is not surprising since the addition of a GFP would only change the mass of the complex from 73 kDa (GFP.Gβ.Gγ) to 100 kDa (GFP-Gβ.GFP-Gγ), a difference too small to be measured by FCS. The data was well described by a model assuming free diffusion of a single species in three dimensions, again pointing to the existence of GFP-Gβ and GFP-Gγ as a single species in the cells.

Table 4.1: Diffusion of GFP fusions of G-protein subunits in *Dictyostelium* cells. Average diffusion coefficients ($\mu m^2/s$) and 95 % confidence intervals (in brackets) as determined for GFP-G-protein βγ subunits in various cell lines and conditions. Measurements were made in 20 – 50 cells incubated in potassium phosphate buffer (pH 6.5, 17 mM). *n* indicates the number of FCS curves analyzed.

Cell line	Vegetative cells				Polarized cells			
	Cytoplasm	n	Membrane	n	Cytoplasm	n	Membrane	n
GFP-Gβ	9.2 (9.1-9.3)	108	0.5 (0.4-0.6)	81	13.1 (12.9-13.3)	137	0.5 (0.4-0.6)	22
GFP-Gγ	10.2[a] (10.1-10.4)	140	0.6 (0.5-0.9)	59	13.1 (12.9-13.3)	90		
GFP-Gβ.GFP-Gγ	8.9 (8.7-9.0)	122			11.1 (10.9 – 11.2)	79		
GFP-Gβ.GFP-Gγ + latrunculin A	10.9 (10.8-11.0)	114						
Free GFP	20.6 [b] (20.4-20.8)	79						
Free GFP + latrunculin A	25.4 (25.1-25.7)	68						

[a] Reference: (Knol *et al.,* 2005)
[b] Reference: (Ruchira *et al.,* 2004)

4.3.2 Gβγ diffusion at the membrane is unaffected by initiation of chemotaxis

Since G-protein signaling mainly takes place via membrane-anchored Gβγ subunits, the effect of cell polarization on the membrane diffusion of these subunits was investigated. Measurements performed in the cell lines expressing only GFP-Gβ or GFP-Gγ showed that also here the diffusion characteristics of the two subunits are very similar (Table 4.1). The data can be fit well to a model assuming the presence of two components, a cytosolic component diffusing in three dimensions and a membrane component diffusing in two dimensions (Eq. 4.1). However, unlike the faster diffusion observed for Gβγ in cytoplasm of chemotaxing cells, no change in the average diffusion coefficient compared to the diffusion in vegetative cells could be detected. The 95 % confidence intervals associated with the measurements from the membrane were relatively high (~40% as opposed to ~3% in cytoplasmic measurements), therefore, small changes in diffusion of Gβγ subunits at the membrane upon polarization of the cell cannot be ruled out.

4.3.3 Gβγ diffusion in chemotaxing cell cytoplasm is faster in the front

The diffusion of the G-protein subunits in the cytoplasm of chemotaxing cells was further characterized in the wild type cells expressing both GFP-Gβ and GFP-Gγ subunits. For this purpose, starving cells were stimulated with cAMP and then treated with 1 μM latrunculin A to stop cell movement. The latrunculin treatment, however, did not completely immobilize the cells although they adopted a more spherical form (Fig. 4.3). The movement of the cells in the direction of the femtotip containing the cAMP made it possible to distinguish the front face of the cells. Measurements were then performed in three different areas in the cell cytoplasm, designated as front, mid and back (Fig. 4.4A). The results are summarized in Fig. 4.4B. Interestingly, the diffusion of GFP-Gβ.GFP-Gγ in the front region of the cell is significantly faster than in the mid and the back regions of the cells. The average number of molecules obtained from the three regions was very similar, agreeing well with the confocal images that show uniform localization of G-protein subunits throughout a chemotaxing cell (Fig. 4.3). These results strongly indicate that G-protein signal is *dynamically* polarized though it is spatially uniform, in a chemotaxing cell.

In vegetative cells treated with latrunculin the average diffusion coefficient value is approximately 1.2 times higher than in untreated cells (Table 4.1). A similar increase in average diffusion coefficient value is also observed for free GFP, where the average diffusion coefficient value increases from 20.6 $\mu m^2/s$ (n=79) in untreated vegetative cells to 25.4 $\mu m^2/s$ (n=68) in latrunculin treated cells (Table 4.1), indicating a reduction in filamentous actin from the cell interior.

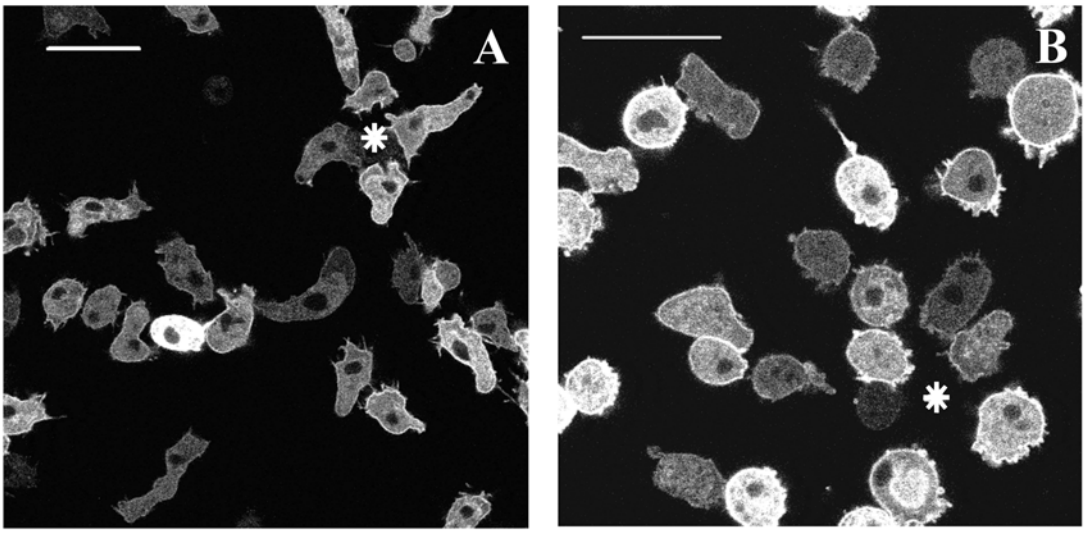

Figure 4.3: Chemotaxing GFP-Gβ.GFP-Gγ expressing cells stimulated with 10 μM cAMP. A) Cells incubated in buffer B) cells 45 minutes after addition of 1 μM latrunculin. Asterisk denotes position of the needle containing cAMP. Bar = 20 μm

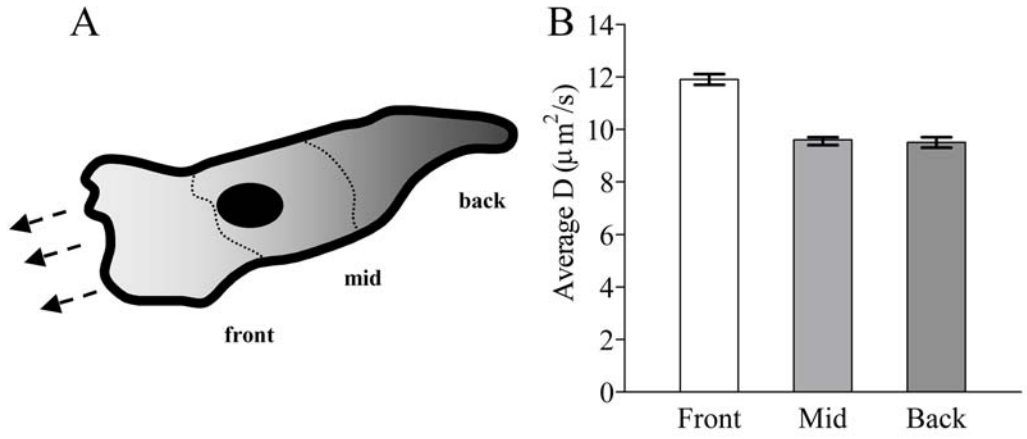

Figure 4.4: Diffusion of Gβγ in different regions of chemotaxing cells. A) Cartoon depicting the arbitrary division of a chemotaxing *Dictyostelium* cell in three regions: front, mid and back. The arrows indicate the direction of migration of the cell. FCS measurements were performed in the three regions of chemotaxing cells stimulated with cAMP. Average diffusion coefficient and 95% confidence intervals in the front, mid and back were 11.9 $\mu m^2/s$ (CI: 11.7-12.1); 9.6 $\mu m^2/s$ (CI: 9.4 -9.7); 9.5 $\mu m^2/s$ (CI: 9.3 – 9.7), respectively. This was calculated from 50 autocorrelation traces in the front, 39 in the mid and 41 traces in the back region of the cell. A repeat of the experiment gave very similar results. B) Average diffusion coefficients of GFP-Gβ.GFP-Gγ in different areas of chemotaxing cell. Bars indicate the 95% confidence interval of the mean.

4.4 Discussion

4.4.1 Gβγ in the cytosol of chemotaxing cells is dynamically polarized

Dictyostelium cells chemotaxing towards a cAMP source display a polarized morphology with the signaling components downstream of G-proteins localized either in the front or back of cells. However, G-proteins themselves are not spatially polarized. Here the diffusion characteristics of GFP tagged G-protein βγ subunits have been studied and it is found that Gβ and Gγ subunits form a complex with each other in both vegetative and chemotaxing cells and that this complex is 'dynamically polarized' in the cytoplasm of chemotaxing cells.

Presence of Gβ and Gγ as a Gβγ complex is indicated by the similarity in the diffusion characteristics of GFP tagged Gβ and Gγ subunits, despite their different molecular masses. The observed average diffusion coefficient of the complex is slightly lower than expected from comparison with the diffusion coefficient value of free GFP in the *Dictyostelium* cytoplasm, which can indicate that Gβγ might be interacting with other proteins in the cytosol. A likely candidate for interaction is Gα, as has been suggested previously (Janetopoulos *et al.,* 2001).

The diffusion of the Gβγ complex in the cytoplasm becomes faster when cells start chemotaxing. This could be caused by the dissociation of the Gβγ complex from its interaction partners in the cytoplasm, in response to the cAMP signal. Another factor

that can influence the mobility of the Gβγ complex in the cytoplasm is the rearrangements of the cytoskeleton. In chemotaxing cells, filamentous actin is localized preferentially in the cell cortex due to which the viscosity in the non-cortical areas decreases, resulting in a faster diffusion of proteins in this area (Yumura and Fukui 1998; Potma *et al.,* 2001; Bretschneider *et al.,* 2002). Free GFP expressed in *Dictyostelium* cells exhibits faster mobility in chemotaxing than in non-chemotaxing cells, pointing to changes in the intracellular environment occurring in response to the cAMP signal (Potma *et al.,* 2001; Ruchira *et al.,* 2004). Thus, the most likely explanation for the faster diffusion of Gβγ complex in chemotaxing cells is the reorganization of the cytoskeleton. However, the increase in the average diffusion coefficient of Gβγ in the cytoplasm of chemotaxing cells compared to that in vegetative cells is less than what has been previously observed for free GFP in *Dictyostelium* cells (Ruchira *et al.,* 2004) indicating that in chemotaxing cells also, the Gβγ complex may interact with other intracellular moieties that retard its mobility.

The diffusion characteristics of the membrane-anchored Gβγ, unlike that of the cytosolic protein do not change upon polarization of cells. It can be expected that initiation of chemotaxis might induce faster diffusion of membrane anchored G-proteins to aid rapid signaling. On the other hand, polymerization of actin and myosin at the cell cortex might reduce the G-protein mobility. The results however, do not indicate either of the possibilities. It must be pointed out here that the present data does not preclude small changes in the diffusion characteristics of the Gβγ at the membrane, which probably could not be detected.

A detailed characterization of Gβγ diffusion in different areas of a chemotaxing cell could be made in latrunculin treated cells, stimulated with cAMP. At the suboptimal latrunculin concentration (1 μM) used in this study, the amount of filamentous actin in a cell becomes limiting (Bretschneider *et al.,* 2002). In vegetative cells treated with latrunculin A, the average diffusion of Gβγ became faster suggesting reduction in filamentous actin. The latrunculin A treated cells however, retained their polarity and showed movement towards the cAMP source making it straightforward to identify the 'front' and 'back' of the cells. Clear differences in the diffusion characteristics in the different areas of the cell were observed with the diffusion in the front part of the cell being significantly faster. These differences, as in the case of polarized aggregating cells, are most likely caused due to rearrangement of the cytoskeleton. Also, in chemotaxing cells the cellular particles or organelles are depleted from the cell front. Their accumulation in the mid and back of the cell as well as myosin II polymerization in the cell posterior would contribute to increased viscosity and decreased protein mobility in those regions (Swanson and Lansing Taylor 1982; Wessels and Soll 1990;

Rubin and Ravid 2002). Lower viscosity and stiffness in the leading edge has also been observed for chemotaxing neutrophils (Yanai *et al.,* 1999; Yanai *et al.,* 2004). In a previous study it was found that free GFP diffusion in polarized aggregating cells in the front and back areas of the cells was similar and that it was faster than in the mid (Potma *et al.,* 2001). In aggregating cells however, the 'front' and 'back' of a chemotaxing cell are more difficult to distinguish as at any given time more than one aggregate is forming and the cell can thus receive and respond to signals from different directions. This could probably explain the difference from the present observation of faster diffusion only in the front part of the cell. The average diffusion coefficient values in the mid and back of cell are very similar to the average values obtained from vegetative cells, which could suggest that the viscosity in these areas is similar to the average viscosity in a vegetative cell. The differences in the diffusion coefficient values within a chemotaxing cell can be regarded as 'dynamic polarity' in chemotaxing cells.

4.4.2 Dynamic polarization: does it play a role in internal signal amplification?

The question that arises then is what could be the consequence of such a dynamic polarization? A straightforward reply can be that the dynamic polarization serves no purpose and is merely a consequence of the G-protein activation and the resulting intracellular changes. On the other hand, the phenomenon of diffusion plays a crucial role in intracellular signaling. Thus, differences in the diffusion characteristics of a protein in different regions of a cell can imply that relay of information to different areas in the cell occurs at different rates.

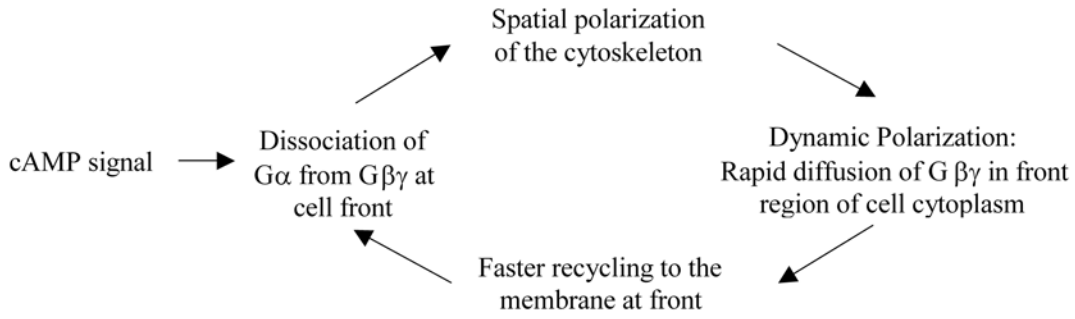

Figure 4.5: Amplification of chemotactic response by differential diffusion of Gβγ. The cAMP signal initiates a series of events, in which the dynamic polarization of the Gβγ is both the consequence and the cause of the spatial polarization of the cytoskeleton.

In the case of G-proteins, it is the membrane-anchored protein that is responsible for the relay of information from extracellular chemoattractant gradients to the cell interior. But this G-protein is supplied to the membrane from the cytoplasm where it is produced. Also, after activation of the G-protein complex it is likely that the free Gβγ

subunits are translocated back to the cytoplasm. Proteins such as phosducin, which modulate the G-protein activity, can bind to the free Gβγ and translocate the subunits away from the membrane, preventing its reassociation with Gα (Gaudet *et al.,* 1996; Bohm *et al.,* 1997; Loew *et al.,* 1998). Thus, an equilibrium exists between the cytoplasmic and membrane-anchored G-protein population. A faster diffusion of G-proteins in the front regions of the cell cytoplasm implies that there is an increased probability of cytoplasmic G-protein reaching the membrane at the front of the cell than at the back. Thus, the cytoplasmic pool of the G-protein is more easily available to the front part of the cell ensuring continuous G-protein signaling there. This would result in increased activation of signaling events in the front and ultimately a polarized localization of the cytoskeleton. However, the differential diffusion of the Gβγ in the cell itself is, most likely, a consequence of the spatial polarization of the cytoskeleton in response to the cAMP signal and accumulation of cellular organelles in the mid and back regions of the cells. Thus, it can be hypothesized that the activation of the G-proteins at the membrane in response to the cAMP signal induces an initial polarity in the cytoskeleton and causes the variable diffusion of the cytoplasmic G-protein. This in turn contributes to faster recycling of G-protein to the membrane at the front, thus, increasing G-protein signaling in the front and amplifying the signal internally (Fig. 4.5). Existence of an initial polarity in response to the cAMP signal has been suggested by a recent study, which shows that the fraction of G-proteins activated at the membrane in the front is higher than the back (Xu *et al.,* 2005). Also the kinetics of cAMP binding to the receptor at the front indicates a faster recycling of the receptor-G-protein complex (Ueda *et al.,* 2001). Hence, the cAMP signal initiates a series of events, in which the dynamic polarization of the Gβγ is both the consequence and the cause of the spatial polarization of the cytoskeleton. This cycle of events can contribute to the amplification of the intracellular gradient and to increased sensitivity of a cell in a chemoattractant gradient, after an initial polarity has been established by other mechanisms.

In conclusion, fluorescence correlation spectroscopy studies of Gβγ diffusion in *Dictyostelium* cells show that Gβ and Gγ are associated with each other in vegetative as well as chemotaxing cells. In chemotaxing cells the Gβγ complex exhibits a dynamic polarity. It is proposed that this dynamic polarity, which is both, the consequence and the cause of the spatial polarization of the cytoskeleton, contributes to the amplification of the intracellular chemotactic response of a cell.

5 The Phosducin-like Protein PhLP1 is Essential for Gβγ Dimer Formation in *Dictyostelium*

Phosducin proteins are thought to inhibit G protein-mediated signaling by sequestering Gβγ subunits. However, *Dictyostelium* cells lacking the phosducin-like protein PhLP1 display defective rather than enhanced G protein signaling. Fluorescence confocal microscopy imaging of cells expressing GFP-Gβ and GFP-Gγ shows that the Gβγ complex is not localized at the membrane in *phlp1*$^-$ cells, suggesting that either the Gβγ complex is not formed in these cells, or that the complex is not able to localize to the membrane. Biochemical experiments indicate that Gβ and Gγ are unstable in *phlp1*$^-$ cells and are not post-translationally modified, pointing to the absence of Gβγ complex in these cells. This is confirmed by the comparison of the diffusion characteristics of GFP-Gγ in wild type cells with that in *phlp1*$^-$ and *gβ*$^-$ cells. The diffusion of GFP-Gγ in *phlp1*$^-$ and *gβ*$^-$ cells is similar but significantly faster than in the wild type cells, suggesting that in the absence of PhLP1 Gγ does not associate with Gβ. Thus, PhLP1 plays a role in the Gβγ complex formation. It is proposed that PhLP1 may serve as a co-chaperone assisting the assembly of Gβ and Gγ into a functional Gβγ complex.

A modified form of this chapter will be published as:
Jaco Knol*, Ruchira Engel*, Mieke Blaauw, Antonie J.W.G. Visser and Peter J.M. van Haastert "The Phosducin-like Protein PhLP1 is Essential for Gβγ Dimer Formation in *Dictyostelium*" *Mol. Cell Biol.* (2005)
* Both authors contributed equally to the work

5.1 Introduction

Phosducin family proteins have been classically linked to G protein regulation. Both phosducin (Phd) and the related phosducin-like protein (PhLP) have been shown to bind Gβγ subunits (Lee *et al.,* 1987; Hawes *et al.,* 1994; Xu *et al.,* 1995; Schroder *et al.,* 1997; Thibault *et al.,* 1997; Savage *et al.,* 2000). In doing so, they are thought to function as a cellular 'sink' which sequesters free Gβγ subunits following their dissociation from receptor-activated G proteins (Bauer *et al.,* 1992; Lee *et al.,* 1992; Hekman *et al.,* 1994; Schroder and Lohse 1996; McLaughlin *et al.,* 2002). As G protein-coupled receptors only couple to Gαβγ trimers, the squelching of Gβγ attenuates transmembrane signaling. Thus, phosducin family proteins may adapt the cell's sensitivity to extracellular signals.

Recently three Phd-like protein genes have been identified in *Dictyostelium* (Blaauw *et al.,* 2003). Of these, PhLP1 is the most similar to mammalian Phd and PhLP. Surprisingly, G-protein signaling is completely defective rather than enhanced in *phlp1*$^-$ cells, which exhibit a phenotype, which is remarkably similar to that of *gβ* knockout cells. Fluorescence confocal microscopy imaging of cells expressing GFP-Gβ or GFP-Gγ fusion proteins indicate that Gβγ complexes are absent from the plasma membrane of *phlp1*$^-$ cells, providing a possible explanation for the abrogation of signal transduction (Blaauw *et al.,* 2003). These findings suggest that either Gβ and Gγ fail to assemble into a Gβγ complex in *phlp1*$^-$ cells or that the complex is not properly routed to the plasma membrane in these cells.

In this study, the Gβγ defect in *phlp1*$^-$ cells is further investigated. The steady state levels and posttranslational modifications of GFP tagged Gβ and Gγ subunits in *phlp1*$^-$ have been studied using biochemical means. Furthermore, to investigate if Gγ is present in a complex with Gβ in *phlp1*$^-$ cells the diffusion characteristics of GFP-Gγ have been quantified in the cytosol of wild type and *phlp1*$^-$ cells using fluorescence correlation spectroscopy (FCS).

Collectively, the biochemical and spectroscopic data strongly indicate that in *phlp1*$^-$ cells, Gβγ do not form a complex suggesting that the phosducin-like protein PhLP1 plays a role in Gβγ dimer formation. It is proposed that PhLP1 may function as a cytosolic co-chaperone for Gβγ assembly.

5.2 Experimental Procedure

5.2.1 Cell culture

All cell lines were grown in 9-cm dishes containing HG5 medium. The *Dictyostelium discoideum* AX3 strain was used as a wild-type control in all experiments. Transfectants expressing tagged Gβ or Gγ subunits were grown in HG5 medium containing 30 μg/ml G418 (GibcoBRL). The *gβ*$^-$ (LW6) and *phlp1*$^-$ knockout cell lines as well as cells expressing either GFP-Gβ or GFP-Gγ have been described previously (Lilly *et al.,* 1993; Wu *et al.,* 1995; Blaauw *et al.,* 2003).

5.2.2 Western blot analysis

Cells were either lysed directly by boiling in SDS-PAGE sample buffer, or by filter lysis and detergent solubilisation (see below). Lysates containing GFP-Gβ or GFP-Gγ were applied to standard 10 or 12% SDS-PAGE gels. Following electrophoresis, proteins were electroblotted onto PVDF membranes (Millipore), and the membranes were blocked for 2 h in 5% low-fat milk in TBST (20 mM Tris-HCl pH 7.4, 137 mM NaCl, 0.05% Tween-20). Subsequently, membranes were incubated overnight at 4 ^{0}C with polyclonal anti-GFP antibody ab6556 (Abcam) diluted 1:5000 in blocking buffer, washed several times with TBST, incubated for 1 h at room temperature with a peroxidase-coupled sheep-anti-rabbit antibody (Roche), washed several times with TBST and once with TBS without Tween-20, and developed with an ECL chemiluminescence kit (Roche).

5.2.3 Crude cell fractionation

Cells were harvested from confluent 9-cm dishes and washed twice with phosphate buffer (pH 6.5). Cell pellets were taken up in 150-300 μl ice-cold lysis buffer (50 mM Tris-HCl pH 7.5, 5 mM EDTA, 5 mM EGTA, 150 mM NaCl, 1 mM DTT, containing COMPLETE protease inhibitor cocktail (Roche)), and lysed through a 3-μm Nuclepore filter (Whatman). Lysates were centrifuged for 5 min in an Eppendorf centrifuge at 4 ^{o}C, and a sample of the supernatant was carefully removed while taking care not to take along any particulate matter. The pellets were washed, and then resuspended in an original volume of lysis buffer. Equal samples of supernatant (cytosolic) and pellet (particulate) fractions were used for western blot analysis.

5.2.4 Triton X-114 partitioning assay

Cells were prepared and lysed as described above. Subsequently, 100 μl lysate was diluted with 100 μl lysis buffer containing 2% Triton X-114, which had been precondensed thrice (Bordier 1981), and rotated for 40 min at 4 ^{o}C. Insoluble material was removed by spinning for 15 min at 4 ^{o}C in an Eppendorf centrifuge, and

supernatants were subjected to phase partitioning by incubation at 30 °C for 3 min and spinning for 5 min at room temperature. The upper, water phases were re-extracted with an equal volume of 2% Triton X-114, and the lower, detergent phases were re-extracted with 0.2% Triton X-114. Following partitioning at 30 °C, detergent phases were combined, and the volume was adjusted with lysis buffer to match the volume of the water phase samples. Equal samples of water and detergent phases were used for western blot analysis.

5.2.5 Fluorescence correlation spectroscopy

The diffusion measurements of GFP-tagged proteins in cells were performed on ConforCor 2 – LSM 510 combination setup (Carl Zeiss, Germany). The details of the setup have been described before (Hink *et al.,* 2003). In the experiments described here GFP was excited with the 488 nm line from an argon-ion laser, focused into the sample with a water immersion C-Apochromat 40x objective lens (Zeiss). The excitation intensity was ~ 11 μW. The excitation and emission light were separated by a dichroic beam splitter (HFT 488/633). The fluorescence was detected by an avalanche photodiode after being filtered through a BP 505-550 nm. The pinhole was set at 70 μm.

Cells from a confluent dish were transferred to a 96-chambered glass bottom microplate (Whatman Inc., New Jersey, USA) and washed twice with potassium phosphate buffer (17 mM, pH 6.5). Measurements were performed in cells incubated in buffer, at room temperature. Around 100 autocorrelation traces were obtained for each cell line from five measurements made at a randomly chosen spot in the cytoplasm of around 20 different cells. The expression levels in cells were too high for FCS measurements and so the GFP was photobleached to acceptable fluorescence intensity levels by exposing the cells to a high intensity laser beam (~ 1 mW) for a second. Measurement duration in all cell lines was 10 s.

The data were analyzed using the software FCS Data Processor (Skakun *et al.,* 2005). The autocorrelation traces were fitted with a model describing Brownian motion of a single species in three dimensions (Eq. 5.1) with an additional offset term to account for artifacts caused by drifts in average fluorescence on time scales of > 1 s arising from cellular and intracellular movement (Brock *et al.,* 1999).

$$G(\tau) = 1 + \frac{1}{N}\left(\left(1 + \frac{\tau}{\tau_d}\right)\sqrt{1 + \frac{\tau}{\tau_d sp^2}}\right)^{-1} + offset \qquad (5.1)$$

In equation 5.1, $G(\tau)$ is the autocorrelation function, N is the average number of molecules in the detection volume, τ_d is the average diffusion time of the molecules and

sp is the structural parameter. A global analysis approach was used to fit up to five traces simultaneously with the τ_d linked and a fixed value of *sp*. The value of *sp*, determined from calibration measurements with a rhodamine-110 solution, was around 5. The translational diffusion coefficient D was calculated from the diffusion time τ_d using Eq. 5.2,

$$D = \frac{\omega_{xy}^{\ 2}}{4\tau_d} \tag{5.2}$$

where ω_{xy} is the equatorial radius of the confocal volume element and is obtained from calibration measurements.

5.3 Results

5.3.1 GFP-Gβ and GFP-Gγ are expressed at reduced levels and do not associate with the plasma membrane in phlp1⁻ cells

To monitor the fate of Gβ and Gγ in intact cells, GFP-Gβ and GFP-Gγ fusion proteins were expressed in wild-type AX3 and in *phlp1⁻* cells (Blaauw *et al.,* 2003). Complexes of Gβ and Gγ tagged with GFP variants have been demonstrated to be fully functional in *Dictyostelium* amoebae (Jin *et al.,* 2000; Janetopoulos *et al.,* 2001). As a reference, *gβ⁻* cells that do not express Gβ and therefore lack normal Gβγ complexes were also employed (Lilly *et al.,* 1993; Wu *et al.,* 1995). Confocal fluorescence microscopy images show that while significant amounts of GFP-Gβ and GFP-Gγ are localized at the membrane in wild type cells, in *phlp1⁻* cells they are entirely cytosolic. GFP-Gγ localization in *phlp1⁻* cells is in fact very similar to its localization in g*β⁻* cells (Fig. 5.1); (Blaauw *et al.,* 2003). These observations are further confirmed with western blot analysis and crude cell fractionation studies.

Western blot analysis shows that correctly sized proteins are expressed in all cell lines (Fig. 5.2). However, the steady state level of GFP-Gβ and GFP-Gγ proteins is dramatically reduced (at least 20-fold) in *phlp1⁻* cells compared to wild-type cells. Such reduced protein levels were also observed for endogenously expressed Gβ using a Gβ–antibody (unpublished observations). The cellular level of GFP-Gγ in *gβ⁻* cells is also significantly lower than in control cells (at least 5-fold; Fig. 5.2). This indicates that Gγ subunits are less stable in the absence of Gβ. Such a mutual dependency of binding partners for stable expression has been previously documented for various protein

complexes, including Gβγ dimers (Schmidt and Neer 1991; Simonds *et al.,* 1991; Pronin and Gautam 1993; Hirschman *et al.,* 1997; Wang *et al.,* 1999).

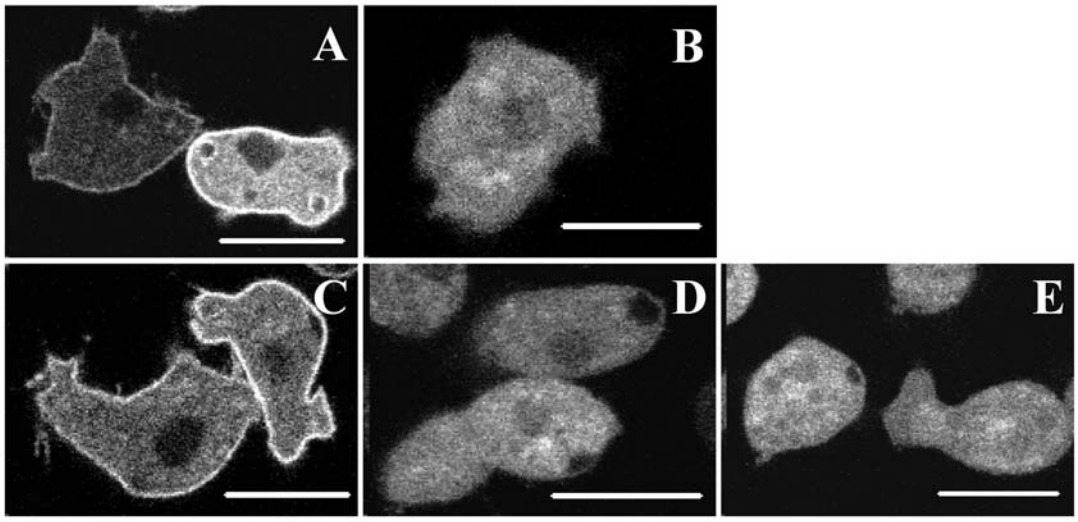

Figure 5.1: Fluorescence confocal images showing localization of GFP tagged G-protein subunits in *Dictyostelium* cells. GFP-Gβ in A) AX3 and B) *phlp1*$^-$ cells and GFP-Gγ in C) AX3, D) *phlp1*$^-$ and E) *gβ*$^-$ cells. Cells were incubated in potassium phosphate buffer (pH 6.5, 17 mM). Scale bar = 10 μm.

Crude cell fractionation of AX3 transfectants shows that GFP-Gβ and GFP-Gγ can be detected both in a cytosolic fraction and in a particulate fraction containing plasma membranes (Fig. 5.3). In striking contrast to the situation for wild-type cells, GFP-Gβ and GFP-Gγ cannot be detected in particulate fractions of *phlp1*$^-$ transfectants, although they are detected in cytosolic fractions. Again, in *gβ*$^-$ cells, GFP-Gβ can combine with endogenous Gγ and exhibit similar behavior as in wild-type cells, whereas GFP-Gγ does not reach the plasma membrane in default of a Gβ partner. Thus, in line with the confocal fluorescence images, these results provide possible reasons why G protein signaling is defective in cells lacking the PhLP1 protein. Either a Gβγ complex is formed, but not transported to its final destination, or the complex is not formed at all, with individual Gβ and Gγ subunits not being able to associate with the plasma membrane. In either case, this largely results in the demise of the non-functional protein.

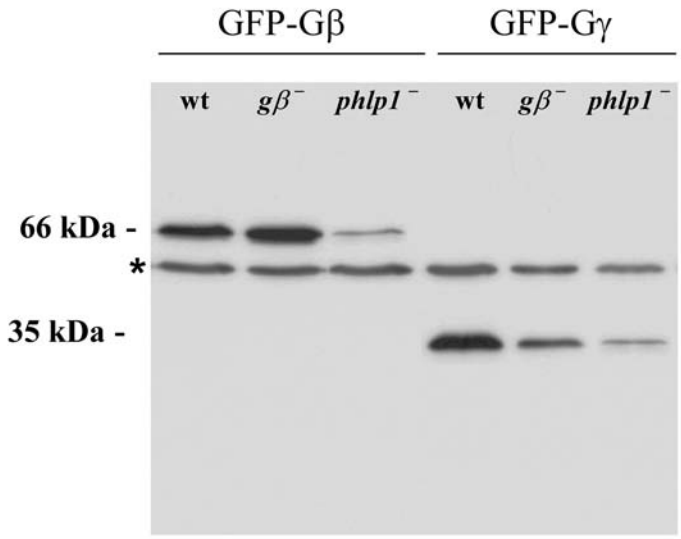

Figure 5.2: Steady state levels of GFP-Gβ and GFP-Gγ are reduced in *phlp1*⁻ cells. Wild-type AX3 (wt) and *gβ*⁻ and *phlp1*⁻ knockout cells were transfected with plasmids encoding GFP-Gβ or GFP-Gγ. Cell lysates were prepared and analyzed through western blot analysis with a GFP antibody. The molecular weights of GFP-Gβ and GFP-Gγ are indicated. The asterisk denotes a cross-reacting AX3 band that can serve as a loading control.

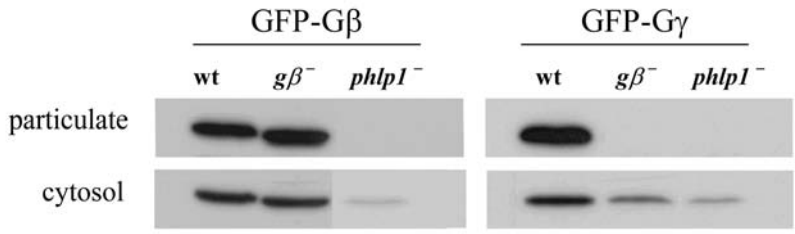

Figure 5.3: GFP-Gβ and GFP-Gγ are absent from plasma membranes in *phlp1*⁻ cells. Cells expressing GFP-Gβ or GFP-Gγ were subjected to crude fractionation by filter lysis and collection of particulate and cytosolic fractions after centrifugation in a microcentrifuge. Equal samples were used for western blot analysis with a GFP antibody as shown in Fig. 5.2.

5.3.2 GFP-Gγ in phlp1⁻ cells is not prenylated

To further define the stage at which the formation of functional Gβγ goes awry in *phlp1*⁻ cells, the post translational modification of Gγ subunits in *phlp1*⁻ cells was investigated with triton-X 114 partitioning. During normal Gβγ synthesis, a CAAX motif at the C-terminus of immature Gγ subunits is prenylated, followed by proteolytic removal of the last three residues (AAX) and carboxyl methylation of the now C-terminal prenyl-cysteine moiety (Higgins and Casey 1996; Zhang and Casey 1996). The attachment of a prenyl group is mandatory for stable membrane association of Gβγ subunits (Simonds *et al.,* 1991; Muntz *et al.,* 1992).

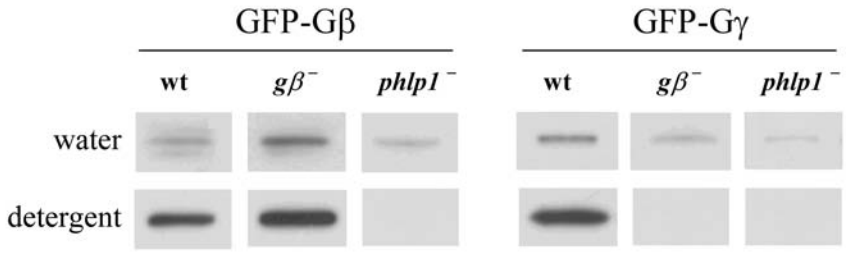

Figure 5.4: Triton X-114 partitioning suggests absence of lipid modification on GFP-Gγ in *phlp1*⁻ cells. Triton X-114-containing extracts were prepared from cells expressing GFP-Gβ or GFP-Gγ and subjected to phase partitioning at 30 ^{0}C. Water phases and detergent phases were separated and re-extracted, and then equal samples were used for western blot analysis with a GFP antibody as shown in Fig. 5.2.

In the triton-X 114 partitioning assay, substantial amounts of both GFP-Gβ and GFP-Gγ expressed in AX3 cells could be drawn into the detergent phase after partitioning (Fig. 5. 4). This indicates that GFP-Gγ is lipid-modified in wild-type cells and that GFP-Gβ must be associated with Gγ, since Gβ itself has no hydrophobic modifications. When expressed in *gβ*⁻ cells, GFP-Gβ also partitions into the detergent phase indicating its association with Gγ. However, GFP-Gγ expressed in *gβ*⁻ cells could only be detected in the water phase. This indicates that Gγ is not (efficiently) modified unless it is present in Gβγ heterodimers. Such a finding corroborates suggestions in the literature that it is the Gβγ complex which serves as a substrate for the prenylation machinery (Higgins and Casey 1996).

Significantly, GFP-Gβ and GFP-Gγ expressed in *phlp1*⁻ cells could only be detected in the water phase after extraction and partitioning. Thus, Gγ remains unmodified in *phlp1*⁻ cells, and fails to draw Gβ into the detergent phase. A lack of lipid attachment in *phlp1*⁻ cells might be explained by defective modification of an otherwise properly formed Gβγ complex, or, more likely, by the failure of Gβ and Gγ to form a complex in the first place.

5.3.3 Similar diffusion of GFP-Gγ in phlp1⁻ and gβ⁻ cells suggests absence of Gβγ complexes in phlp1⁻ cells

The biochemical experiments indicate that Gβ and Gγ subunits do not form a complex in cells lacking PhLP1. However, the experiments were complicated by the dramatically reduced steady state levels of GFP-Gβ and GFP-Gγ in *phlp1*⁻ cells. To overcome this problem, and to substantiate the *in vitro* findings in an *in vivo* environment, fluorescence correlation spectroscopy (FCS) was used. With FCS diffusion of proteins expressed at low concentrations in living cells can be monitored

(Hess *et al.,* 2002; Medina and Schwille 2002; Kim and Schwille 2003). The diffusion characteristics of a protein provide valuable clues about its aggregation state or intracellular interactions. Thus, the cytoplasmic diffusion coefficients obtained from FCS measurements can be used to discriminate free subunits from Gβγ complexes in different cell lines.

The 7 kDa Gγ is much smaller than the 40 kDa Gβ and thus, diffusion characteristics of GFP-Gγ would be more strongly affected than that of GFP-Gβ when Gβ and Gγ no longer form a complex. Therefore, we chose to analyze the diffusion of GFP-Gγ in the cytoplasm of wild type and mutant cell lines (Fig. 5.5 and Table 5.1).

The experimental data fit well to a model describing the diffusion of a single population of fluorescing molecules in three dimensions. Fig. 5.5 shows that the diffusion coefficient distribution for GFP-Gγ in *phlp*1$^-$ cells is shifted to higher values compared to that in wild-type AX3 cells. The slow diffusion of GFP-Gγ in wild type cells indicates that it is predominantly present as a complex in wild-type cells, but not in *phlp1*$^-$ cells.

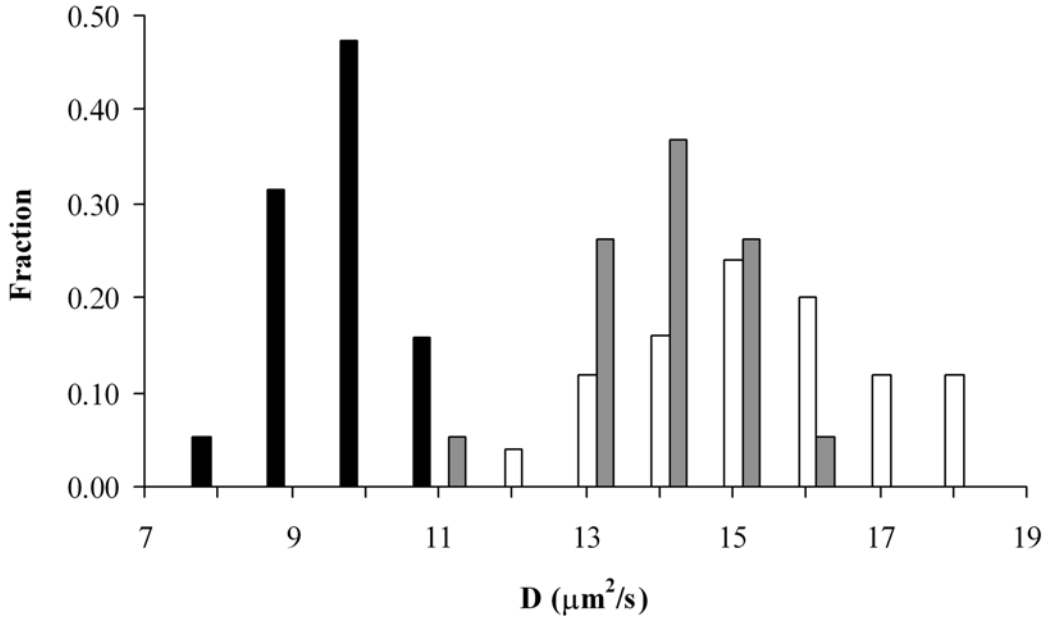

Figure 5.5: GFP-Gγ exhibits monomer-type diffusion characteristics in *phlp1*$^-$ cells. Comparison of the diffusion coefficient distribution of GFP-Gγ in wild-type AX3 (black bars), *phlp1*$^-$ (white bars) and *gβ*$^-$ (grey bars) cells. The diffusion coefficient distribution of GFP-Gγ proteins was determined in the cytosol of different cell lines using fluorescence correlation spectroscopy. Bars indicate the fraction of the total number of observations in which a specific diffusion coefficient (D) was found.

Table 5.1: Diffusion of GFP-Gγ in wild-type and mutant cell lines. Average diffusion coefficients (D) and standard deviation values were determined for GFP-Gγ in the cytoplasm of wild-type and mutant *Dictyostelium* cells incubated in 17 mM potassium phosphate buffer (pH 6.5); n = 20.

Cell line	D ($\mu m^2/s$)
AX3	10 ± 1
phlp1⁻	15 ± 2
Gγ	14 ± 1

To determine if the diffusion of GFP-Gγ in *phlp1⁻* cells was indeed the diffusion of free GFP-Gγ monomers, the diffusion of GFP-Gγ in *gβ⁻* cells was measured. As can also be seen in Fig. 5.5 the diffusion coefficient distribution for GFP-Gγ expressed in *gβ⁻* cells strongly overlaps with that obtained for *phlp1⁻* cells, clearly indicating that GFP-Gγ in *phlp1⁻* cells is free. The average diffusion coefficient of GFP-Gγ molecules in *gβ⁻* cells is very similar to the value obtained for GFP-Gγ in *phlp1⁻* cells (14 and 15 $\mu m^2/s$, respectively). These values are slightly smaller than the value of 20 $\mu m^2/s$ obtained for freely diffusing GFP monomers in *Dictyostelium* cells (Ruchira *et al.,* 2004). Since GFP-Gγ and GFP are similar in size (35 and 27 kDa, respectively), their diffusion coefficients are also expected to be similar. However, GFP is approximately globular (Ormö *et al.,* 1996) whereas Gγ in a Gβγ dimer has a rod-like structure (Sondek *et al.,* 1996) and though it is not known how the structure changes when Gγ is not associated with Gβ, it is likely that it is (partially) unfolded (Sondek *et al.,* 1996). The difference in shapes of GFP and GFP-Gγ can thus be the reason for the discrepancy seen between their diffusion coefficients. Taken together, the FCS data strongly suggest that, in cells that are devoid of PhLP1, GFP-Gγ molecules are present as free monomers. It is therefore concluded that Gβγ complexes, if present at all, form a very small minority in *phlp1⁻* cells.

5.4 Discussion

5.4.1 Absence of Gβγ dimers in cells lacking phosducin-like protein PhLP1

Dictyostelium amoebae lacking the phosducin-like protein PhLP1 exhibit a phenotype which is strikingly similar to the phenotype observed upon Gβ gene disruption (Blaauw *et al.,* 2003). Findings from this study suggest that the *gβ⁻*-like phenotype of *phlp1⁻* cells is due to defective Gβγ dimer formation.

Biochemical experiments show that the steady state protein levels of Gβ and Gγ in *phlp1*$^-$ cells are dramatically reduced. This is in accordance with the hypothesis that Gβγ complex formation is required for stable expression of either partner (Schmidt and Neer 1991; Simonds *et al.,* 1991; Pronin and Gautam 1993; Hirschman *et al.,* 1997; Wang *et al.,* 1999). In *phlp1*$^-$ cells the post-translational lipid attachment to GFP-Gγ is not detected, which is also in keeping with a lack of Gβγ dimer formation. It has been suggested that Gβγ assembly precedes cytosolic prenylation of the C-terminal CAAX motif of Gγ (Higgins and Casey 1996). Indeed, when GFP-Gγ is overexpressed in *gβ*$^-$ cells that cannot form Gβγ complexes, the protein is unstable and is not lipid-modified in triton X-114 partitioning assays.

The absence of Gβγ dimer formation is also strongly suggested by *in vivo* FCS experiments, which show that the diffusion of GFP-Gγ in *phlp1*$^-$ cells is similar to that in *gβ*$^-$ cells, whereas it is significantly slower in wild-type AX3 cells. The average diffusion coefficient values can be explained assuming the presence of free GFP-Gγ monomers in *phlp1*$^-$ and *gβ*$^-$ cells, and of GFP-Gβγ complexes in AX3 cells. Therefore, the FCS results indicate that Gβ and Gγ are indeed apart in cells which miss PhLP1.

Taken together, the above data strongly suggest that without the PhLP1 protein, Gβγ dimer formation is defunct in *Dictyostelium* cells. However, the formation of small amounts of Gβγ dimers in *phlp1*$^-$ cells cannot be completely ruled out. Maybe such traces of Gβγ can still provide some modulation of (a subset of) effectors, but in the assays reported previously no Gβγ function was detected (Blaauw *et al.,* 2003).

5.4.2 PhLP1: a co-chaperone for Gβγ dimer formation?

Whereas the Gγ subunit is a relatively small and flexible peptide lacking tertiary structure (Schmidt and Neer 1991; Dues *et al.,* 2001), the Gβ subunit exhibits complex folding. Gβ is a member of the WD repeat protein family and contains WD repeats that form a seven-membered β-propellor structure (Murzin 1992; Garcia-Higuera *et al.,* 1996; Smith *et al.,* 1999; Neer and Smith 2000). The repetitive and highly integrated structure of Gβ may not allow its folding and/or assembly to occur spontaneously (Clapham and Neer 1997).

The structural difference between Gβ and Gγ is also reflected in their ease of production. While Gγ can be produced in any expression system, Gβ production is more demanding (Schmidt and Neer 1991; Higgins and Casey 1994; Mende *et al.,* 1995; Garcia-Higuera *et al.,* 1996; Garcia-Higuera *et al.,* 1998). Thus, the Gβ subunit may require molecular chaperones (Frydman 2001; Hartl and Hayer-Hartl 2002) for its incorporation into functional a Gβγ complex.

A likely candidate as a molecular chaperone is the group II chaperonin CCT (Chaperonin Containing TCP-1) also known as TRiC (Leroux and Hartl 2000; Valpuesta *et al.,* 2002). CCT has been shown to interact with a large proportion of yeast proteins harboring seven WD repeats, including the yeast Gβ subunit STE4, and is thought to aid in their folding (Valpuesta *et al.,* 2002; Siegers *et al.,* 2003). It has also been implicated in the assembly of multimeric proteins (Feldman *et al.,* 1999; Gutsche *et al.,* 1999; Hansen *et al.,* 2002; Valpuesta *et al.,* 2002). Thus, CCT, aided by co-chaperones, may assist both folding and assembly of multimeric proteins, including WD repeat proteins such as Gβ.

The picture that emerges from the studies on *Dictyostelium phlp1*$^-$ cells is that Gβγ complex formation is abolished in the absence of PhLP1. It is unlikely that PhLP1 deficiency leads to a loss of function of the CCT machinery, as the latter is absolutely required for actin and tubulin folding and its absence is lethal in yeast (Ursic and Culbertson 1991; Li *et al.,* 1994). Rather, it is possible that PhLP1 plays a role as a cofactor co-operating with CCT in the formation of native Gβγ heterodimers. Interestingly, mammalian PhLP, but not Phd, has been shown to co-immunoprecipitate CCT subunits (McLaughlin *et al.,* 2002).

Recent studies conducted contemporarily to the present work, provide substantial support for the hypothesis that PhLP is a molecular chaperone for Gβγ assembly (Martin-Benito *et al.,* 2004; Lukov *et al.,* 2005; Humrich *et al.,* 2005). The structure of the complex between CCT and PhLP reveals PhLP binding at the apical top of CCT, above the folding activity. This leads to the hypothesis that PhLP delivers its binding partner (possibly Gβγ) to the CCT complex for folding (Martin-Benito *et al.,* 2004). Consistent with this hypothesis is the observation that RNAi inhibition of the CCT subunit TCP-1α leads to a strong reduction of the level of Gβγ subunits (Humrich *et al.,* 2005). Very recently, Lukov *et al.,* 2005 have shown that reduced expression of PhLP by RNAi results in inhibition of Gβγ expression and G-protein signaling, similar to PhLP-null cells in *Dictyostelium* (Blaauw *et al.,* 2003) and *C. parasitica* (Kasahara *et al.,* 2000). Furthermore, they demonstrate that the inhibition of G-protein signaling is due to an inability of nascent Gβγ to form dimers, as is also demonstrated in the present work. They provide a model in which PhLP binds to Gβ and stabilizes the nascent Gβ polypeptide until Gγ will associate and PhLP will dissociate to catalyze another round of assembly. Phosphorylation of PhLP at Ser18-20 enhances binding to CCT and is essential for Gβγ folding (Lukov *et al.,* 2005). However, the role of CCT remains unclear, since a PhLP mutant with reduced CCT binding (PhLP133-135A) is fully capable of Gβγ folding (Lukov *et al.,* 2005).

Clues to the co-chaperoning role of phosducin-like proteins can be obtained from the structure of Phd (phosducin)-Gβγ complex. Phd interacts with blades 6 and 7 of native Gβγ, and can induce conformational changes in that region while transporting Gβγ away from the membrane (Gaudet *et al.,* 1996; Loew *et al.,* 1998). During Gβ biosynthesis, the blade 7, which is made up of β-strands from the N-terminal and C-terminal WD repeats of Gβ, must be formed by bringing together the two ends and thus, closing the ring of the Gβ propeller (Clapham and Neer 1997). It has been observed that *in vitro* translated, assembly-competent Gβ has a larger Stokes radius than native Gβγ complexes pointing to its open structure (Schmidt and Neer 1991; Schmidt *et al.,* 1992; Higgins and Casey 1994). Molecules such as PhLP may facilitate ring closure of the Gβ propeller while Gβ and Gγ assemble. In the absence of PhLP1, a proportion of the CCT population might even get stuck with assembly-competent Gβ. Indeed, the fact that *phlp1*$^-$ cells grow significantly slower than both wild-type and *gβ*$^-$ cells (Blaauw *et al.,* 2003) could indicate that the cellular chaperone machinery is to some extent obstructed in the absence of PhLP1.

In conclusion, biochemical and spectroscopic data strongly suggest that cells lacking the phosducin-like protein PhLP1 are not able to form native Gβγ dimers. It is proposed that this is related to an essential co-chaperone function of PhLP1 during Gβγ assembly.

5.5 Acknowledgements

Dr. Peter Devreotes is acknowledged for providing the *gβ*$^-$ cell line LW6.

6 Summarizing Discussion

Cellular chemotaxis is a complex process that requires the coordination and interaction of various cellular signaling networks composed of a variety of regulatory molecules. To understand the process of chemotaxis, it is essential to know how, when and where these regulatory molecules get activated and interact. A substantial amount of our present knowledge of the chemotaxis process has come from the organism *Dictyostelium discoideum*, the chemotaxis mechanism of which is closely related to that of mammalian cells. As more and more of the regulatory molecules and interconnecting pathways have been discovered, our understanding of the chemotaxis mechanism has improved. However, many key links are still missing. To find these links it is essential to *look* into chemotaxing cells and obtain detailed information about the localization and dynamics of the regulatory molecules involved in the signaling processes. A technique for obtaining quantitative information on dynamic events and molecular interactions in living cells is fluorescence fluctuation spectroscopy (FFS). It provides a sensitive, specific and non-invasive tool to probe dynamics of fluorescent species with high spatial and temporal resolution in living cells. The aim of the research described in this thesis is to obtain information about the diffusion, localization and interaction of various regulatory molecules involved in the chemotaxis mechanism of *Dictyostelium* cells using FFS.

6.1 FFS in *Dictyostelium* cells

To perform high quality FFS measurements in living *Dictyostelium* cells, the optimal measurement conditions in these cells were first investigated. Factors such as autofluorescence, cell movement and light scattering or light absorption by endogenous molecules and intracellular moieties can reduce the signal to noise ratio and introduce artifacts in cellular FFS measurements. Thus, measurement conditions should be such that there is minimal interference of these factors. *Dictyostelium* autofluorescence is localized in discrete areas in both chemotaxing and non-chemotaxing cells and covers a wavelength range from ~ 500 – 650 nm with a maximum at ~ 510 nm. The autofluorescence thus, potentially interferes with measurements of GFP fusion proteins using fluorescence microscopy techniques. The extent of interference of autofluorescence in FFS depends on the molecular brightness and concentration of the autofluorescent molecules compared to those of GFP or other fluorophore being used.

In PCH analysis, the presence of autofluorescence can be taken into account using a model for two fluorescent species, with one species fixed to the autofluorescence parameters. In FCS curves autofluorescence can contribute by either introducing an additional correlating component or a steady background of non-correlating species. At excitation powers above 20 μW the autofluorescence intensity fluctuations autocorrelate. However, because of the relatively high GFP molecular brightness, the autofluorescence contribution to the autocorrelation curves is negligible when the average number of autofluorescent molecules in the detection volume is less than the average number of GFP molecules. At laser powers lower than 20 μW the *Dictyostelium* autofluorescence does not autocorrelate. However, even at these low powers, the autofluorescence intensity of cells incubated in the growth medium HG5 is high. Incubating the cells in buffer for 15 minutes reduces the autofluorescence intensity by around 50%. The autofluorescence can be further reduced by another 85% by photobleaching with high laser powers for short periods (3-7 s) of time. As the high laser powers do not affect the morphology and behavior of the cells, prebleaching can be a convenient way of reducing autofluorescence interference.

Dictyostelium cells also exhibit continuous movement giving rise to slow non-uniform intensity fluctuations around the average intensity value in FFS measurements. The effect of the cell movement can be minimized by acquiring data for short times of 5 –10 s. This also helps in minimizing cellular photodamage during measurements. Thus, the most optimal conditions for performing FFS measurements in *Dictyostelium* cells are excitation intensities below 20 μW, short measurement times and the use of prebleaching. Since autofluorescence intensity reduces at longer excitation wavelengths, in future FFS studies in *Dictyostelium* cells, the use of the newly developed red-shifted fluorophores e.g. dTomato (Shaner *et al.,* 2004) can be tested.

6.2 Cytoplasmic viscosity in *Dictyostelium* cells

The intracellular environment is crowded and heterogeneous. Diffusion of proteins in the cell cytoplasm is influenced not only by the high concentration of macromolecules but also the presence of organelles. In addition, the presence of the cytoskeletal network, which gives the cell its shape and provides it with the ability to move, also contributes to increasing the cytoplasmic viscosity and acts as a physical barrier to free movement of molecules. The cytoskeleton is dynamic and changes spatially as well as temporally (Luby-Phelps 2000). FFS study of free GFP (S65T) diffusion in *Dictyostelium* cells shows that the viscosity in vegetative cells is approximately 3.5 times higher than in water. To allow cells to move in a chemotactic gradient the cytoskeleton undergoes rapid rearrangements. In chemotaxing cells, filamentous actin is

predominantly localized at the cell cortex. The average cellular viscosity in non-cortical areas in these cells is reduced to approximately 2.2 times that of water. The changes in the intracellular environment would influence the mobility of proteins there and could thus have consequences for intracellular communication.

6.3 PH domain diffusion in cell cytoplasm

The translocation of PH domain-containing proteins from the cytoplasm to the plasma membrane is thought to play an important role in the chemotaxis mechanism of *Dictyostelium* cells (Parent *et al.,* 1998). In this thesis, the diffusion characteristics of three PH domains have been studied: PH2, which belongs to a protein that has not yet been identified, PH10, which is thought to belong to a novel PKB (protein kinase B) homolog and PH-CRAC (cytosolic regulator of adenylyl cyclase). While PH2-GFP shows a homogeneous distribution in vegetative as well as chemotaxing cells, PH10-GFP and PH-CRAC-GFP transiently translocate to the leading edge of chemotaxing cells. Of these three domains, the diffusion of PH10-GFP is slower than expected. With PCH, it is confirmed that this slow diffusion is not caused due to the aggregation of the protein. Thus, it is possible that the PH domain interacts with a bulky intracellular moiety or is trapped in a micro-region formed by the cytoskeleton. Surprisingly, of the three PH domains, only PH2-GFP shows slightly increased mobility in chemotaxing cells compared to vegetative cells whereas the mobilities of PH10-GFP and PH-CRAC-GFP remain unchanged. Hence, the lower viscosity in the non-cortical areas of the chemotaxing cells compared to vegetative cells does not affect the PH10-GFP and PH-CRAC-GFP diffusion. This can be the case if the effect of change in viscosity on PH10 and PH-CRAC diffusion is cancelled by another event taking place in the polarized cells. At present, it is not clear what that event might be.

6.4 Increased mobility of Gβγ in cytoplasm of chemotaxing cells

The heterotrimeric G-proteins, composed of Gα, Gβ and Gγ are crucial for the chemotactic signaling (Manahan *et al.,* 2004). Receptor-mediated activation of the G-protein, at the inner face of the plasma membrane, leads to the dissociation of the Gα subunit from the Gβγ subunits, which can then modulate downstream effectors. The Gβ and Gγ subunits, which remain associated with each other throughout, are localized both in the cytosol and the membrane. While the membrane localization is essential for the functioning of the complex, it is in the cytosol that the assembly and posttranslational modifications of Gβγ, and also probably its interaction with Gα, are thought to occur. FFS measurements of GFP-tagged Gβ and Gγ subunits indicate that the two subunits are

present in a complex with each other, in both vegetative and chemotaxing cells. In chemotaxing cells, unlike PH10 and PH-CRAC, they show an increase in their mobility in the cytoplasm. However, this change is less than observed for free GFP. This suggests that in chemotaxing cells, the Gβγ subunits are probably interacting with other proteins or intracellular moieties. In response to the cAMP signal the diffusion of the subunits at the membrane can also be affected. While the subunits can diffuse faster to aid rapid signaling during chemotaxis, their diffusion can also be retarded due to polymerization of actin or myosin at the cell cortex. However, it is observed that the diffusion of the subunits in the plasma membrane is not affected by initiation of chemotaxis.

6.5 Gβγ subunits diffuse faster in the front region of chemotaxing cells

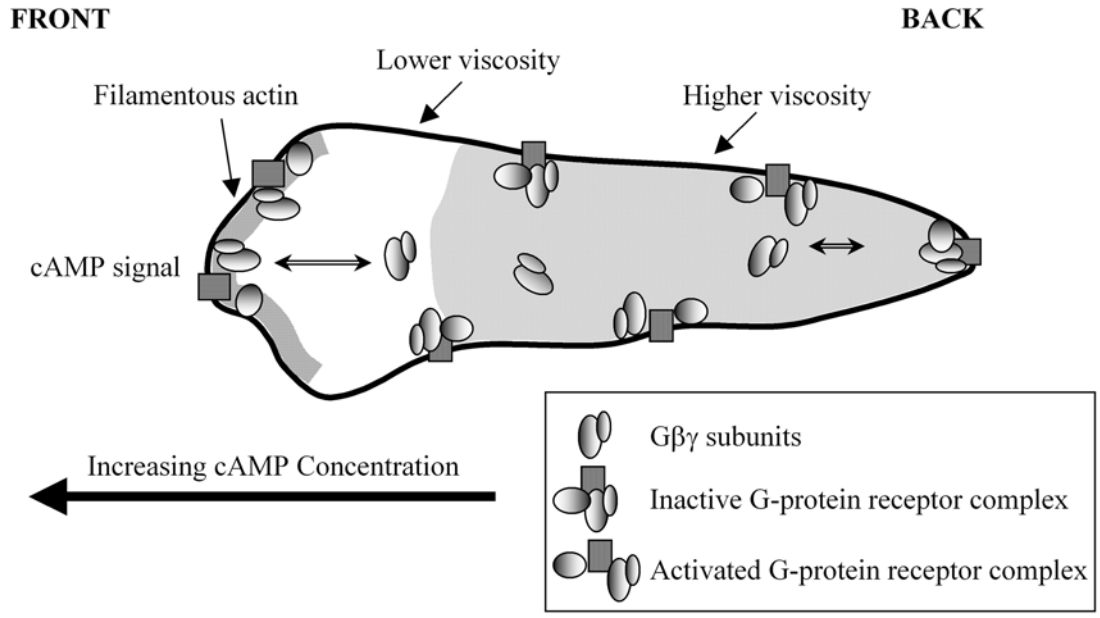

Figure 6.1: Amplification of signal by variable diffusion of Gβγ. The diffusion of Gβγ in the front region of the cytoplasm is faster than in the rest of the cell probably due to a polarized cytoskeleton and accumulation of the organelles in the mid and back of a chemotaxing cell. Thus G-proteins from the cytoplasmic pool are more readily available to the membrane at the front of the cell than the back, aiding the signaling in the front. After an initial polarity has been established, this variable diffusion can contribute to the amplification of the chemotactic response.

In chemotaxing cells many of the downstream effectors of Gβγ show highly polarized localization. However, the Gβγ themselves, as well as the cAMP receptor cAR1, are uniformly localized. One of the missing links in the unraveling of the chemotaxis mechanism is how the cells amplify weak extracellular gradients into steep intracellular ones, when the spatial distribution of the G-proteins and receptors is not polarized. Interestingly, the FFS study of the GFP tagged Gβγ subunits shows that

though the localization of the subunits in the cell is uniform, the diffusion of these subunits is not (Fig. 6.1). In the front region of the cell cytoplasm, the subunits show faster diffusion than in the mid or back of the cell. While this variable diffusion within a chemotaxing cell is itself, most likely, a consequence of the polarization of the cytoskeleton and accumulation of the organelles in the mid and back regions of the cell, its presence implies that G-protein from the cytoplasmic pool is more easily available to the plasma membrane at the cell's leading edge, aiding the signaling in the front. Thereby this variable diffusion can contribute to the amplification of the intracellular chemotactic response after an initial polarity has been established by other mechanisms.

6.6 PhLP1 is essential for Gβγ complex formation

The activity of the G-protein is modulated by phosducin like proteins (PhLP). PhLPs are thought to bind to free Gβγ and thus inhibit G-protein mediated signaling. Surprisingly, in *Dictyostelium* cells lacking the protein PhLP1, the G-protein mediated signaling is defective rather than enhanced. Fluorescence confocal microscopy of cells expressing GFP-Gβ and GFP-Gγ shows that the Gβγ complex is not localized at the membrane in *phlp1*$^-$ cells, suggesting that either the Gβγ complex is not formed in these cells, or that it is not able to be recruited to the membrane. Biochemical experiments indicate that Gβ and Gγ are unstable in *phlp1*$^-$ cells and are not post-translationally modified, pointing to the absence of Gβγ complex in these cells. This is confirmed by the comparison of the diffusion characteristics of GFP-Gγ in wild type cells with that in *phlp1*$^-$ and *gβ*$^-$ cells. The diffusion of GFP-Gγ in *phlp1*$^-$ and *gβ*$^-$ cells is similar but significantly faster than in the wild type cells, suggesting that in the absence of PhLP1 Gγ does not associate with Gβ. Thus, PhLP1 plays a role in the Gβγ complex formation (Fig. 6.2). It is proposed that PhLP1 may serve as a co-chaperone assisting the assembly of Gβ and Gγ into a functional Gβγ complex.

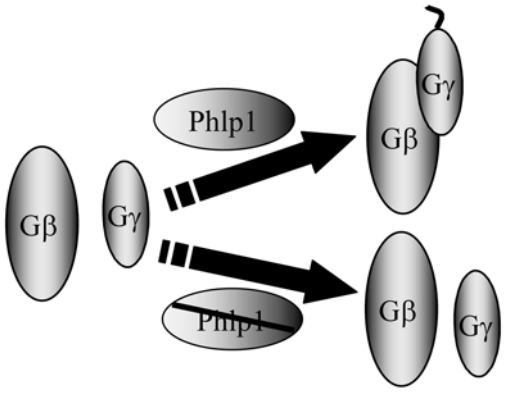

Figure 6.2: PhLP1 is essential for Gβγ dimer formation. In cells lacking PhLP1, Gγ does not have a lipid anchor and Gβ and Gγ are not associated with each other.

6.7 Concluding remarks and outlook

The activation of signaling events is to a large extent dependent on how fast regulatory molecules can diffuse through the cell and therefore, knowing the diffusion characteristics of the molecules involved gives important information about how fast intracellular events can occur in response to extracellular signals. The studies described in this thesis demonstrate that FCS can be successfully applied to characterize in detail the diffusion of regulatory molecules involved in the chemotaxis of *Dictyostelium* cells. This characterization provides a detailed picture of the dynamic events shaping the chemotactic response.

In addition, by characterizing the diffusion properties, molecular brightness and concentration of regulatory molecules in cells, FCS and PCH provide valuable information about the aggregation states and interactions of these molecules. In combination with fluorescence confocal microscopy details about the localization of various molecules can be obtained. All this information is essential in unraveling the connections between various signaling modules involved in the chemotaxis mechanism.

The FFS techniques applied in this thesis provide a wealth of information about molecular events in cells. Thus, while the study on PH domains provides valuable clues in predicting possible functions and interactions of the domains, the functions of which have not yet been characterized, the study of the role of PhLP1 in Gβγ dimerization confirms the *in vitro* observations in an *in vivo* environment. The power of the techniques used here can be further increased by simple modifications or combination with other techniques. E.g. instead of one color FCS, dual color FCS or fluorescence cross-correlation spectroscopy (FCCS) can be used to study specific interactions between different molecules and their dynamics in cells (Schwille *et al.,* 1997; Haustein and Schwille 2003). In this method the simultaneous diffusion of two molecules labeled with different dyes is monitored. This can be a useful technique e.g. for tracking the interaction of PH10 with a potential interaction partner or for further characterization of PhLP1 interaction with the Gβγ complex *in vivo*. Another variation, called image correlation spectroscopy (ICS) can be used to obtain information about slow diffusing species in cells (Petersen *et al.,* 1993; Wiseman and Petersen 1999). Here the pixel-to-pixel fluorescence fluctuations in images acquired with confocal laser scanning microscopy are autocorrelated. Slow diffusing molecules such as the receptor cAR1 can be studied with this technique. FCS can also be combined with total internal reflection illumination (TIR-FCS), which reduces the detection volume and thus, the contribution of background fluorescence (Starr and Thompson 2001; Haustein and Schwille 2003). This technique can be used to selectively study events close to the surface e.g., diffusion

of receptors at the substrate-attached surface, ligand-receptor association-dissociation kinetics or cytoskeleton dynamics.

Chemotaxis is a complicated process. In search for the missing links in the understanding of this process, FFS techniques can prove to be immensely valuable and powerful tools.

Samenvattende Discussie

Cellulaire chemotaxis is een complex proces waarbij de coördinatie en interactie van verscheidene cellulaire signaleringsnetwerken, bestaande uit een verscheidenheid aan regulerende moleculen, noodzakelijk is. Om het proces van chemotaxis te begrijpen is het essentieel om te weten hoe, waar en wanneer deze regulerende moleculen worden geactiveerd en op elkaar inwerken. Een aanzienlijk deel van onze huidige kennis van het proces van chemotaxis komt van het organisme *Dictyostelium discoideum*, dat een mechanisme van chemotaxis heeft dat sterk lijkt op dat van zoogdiercellen. Naarmate er meer regulerende moleculen en schakels in het netwerk worden ontdekt, verbetert ons begrip van het mechanisme van chemotaxis. Desondanks ontbreken er nog veel belangrijke schakels. Om deze schakels te ontdekken, is het noodzakelijk om in chemotactische cellen te kunnen *kijken* om zodoende gedetailleerde informatie te krijgen over de lokatie en de dynamiek van de regulerende moleculen die betrokken zijn bij signaleringsprocessen. Een techniek om kwantitatieve informatie over dynamische processen en interacties tussen moleculen in levende cellen te verkrijgen is fluorescentie fluctuatie spectroscopie (FFS). Dit is een gevoelige, specifieke en niet-invasieve techniek om de beweging van fluorescente moleculen in een levende cel vast te leggen met een hoge plaats- en tijdresolutie. Het doel van het onderzoek dat beschreven is in dit proefschrift is het verkijgen van informatie over de diffusie, lokatie en interactie van verscheidene regulerende moleculen die betrokken zijn bij het mechanisme van chemotaxis van *Dictyostelium*cellen met behulp van FFS.

FFS in *Dictyostelium*cellen

Om FFS metingen van hoge kwaliteit in levende *Dictyostelium*cellen te kunnen uitvoeren, zijn eerst de optimale meetcondities voor deze cellen onderzocht. Factoren zoals autofluorescentie, beweging van de cellen en lichtverstrooiing of lichtabsorptie door endogene moleculen en intracellulaire structuren kunnen de signaal-ruisverhouding verminderen en kunnen artefacten introduceren in cellulaire FFS metingen. De meetcondities moeten dus zodanig zijn dat er minimale verstoring is van deze factoren. De autofluorescentie van *Dictyostelium* is geconcentreerd in bepaalde gebieden in zowel chemotactische als niet-chemotactische cellen, en bestrijkt een golflengtegebied van ~ 500 – 650 nm met een maximum bij ~ 510 nm. Autofluorescentie zou dus storend kunnen zijn bij metingen van GFP fusie-eiwitten met behulp van

fluorescentiemicroscopie technieken. De mate van storing van autofluorescentie in FFS hangt af van de *molecular brightness* en de concentratie van de autofluorescente moleculen vergeleken met die van GFP of andere gebruikte fluoroforen.

Bij PCH analyse kan rekening worden gehouden met de aanwezigheid van autofluorescentie door een model te gebruiken voor twee fluorescente eenheden, waarbij er één wordt gerelateerd aan de autofluorescentie parameters. In FCS curven kan autofluorescentie zorgen voor een extra correlerende component of een constante achtergrond van niet-correlerende signalen. Bij excitatievermogens hoger dan 20 μW treedt er correlatie op van variaties in de autofluorescentie intensiteiten. Echter, door de relatief hoge *molecular brightness* van GFP is de contributie van autofluorescentie aan de autocorrelatie curven verwaarloosbaar als het gemiddelde aantal autofluorescente molecule in het detectievolume kleiner is dan het gemiddelde aantal GFP-moleculen. Bij excitatievermogens lager dan 20 μW correleert de autofluorescentie van *Dictyostelium* niet. Toch is zelfs bij deze lage excitatievermogens de intensiteit van de autofluorescentie van cellen geïncubeerd in het groeimedium HG5 nog hoog. Door cellen gedurende 15 minuten te incuberen in buffer gaat de autofluorescentie intensiteit omlaag met 50%. De autofluorescentie kan verder worden verminderd met 85% door *photobleaching* bij hoge laservermogens gedurende korte tijden (3-7 s). Omdat de hoge laservermogens de morfologie en het gedrag van de cellen niet beïnvloeden, kan *prebleaching* een geschikte manier zijn om de storing van autofluorescentie te verminderen.

De continue beweging van *Dictyostelium*cellen leidt tot langzame, niet-uniforme intensiteitsfluctuaties rond de gemiddelde intensiteit in FFS metingen. Het effect van de beweging van de cel kan worden geminimaliseerd door de data gedurende korte perioden van 5-10 s op te nemen. Dit helpt ook bij het minimaliseren van cellulaire beschadigingen door het laserlicht gedurende metingen. Derhalve zijn de meest optimale meetcondities voor FFS metingen in *Dictyostelium*cellen een excitatievermogen lager dan 20 μW, korte meettijden, en het gebruik van *prebleaching*. Omdat de autofluorescentie-intensiteit vermindert bij hogere excitatiegolflengten, kan bij toekomstige FFS studies het gebruik van recentelijk ontwikkelde *red-shifted* fluoroforen, zoals dTomato, (Shaner *et al.,* 2004) worden getest.

Viscositeit van het cytoplasma in *Dictyostelium*cellen

De intracellulaire massa van een cel is compact en heterogeen. De diffusie van eiwitten in het cytoplasma van de cel wordt niet alleen beïnvloedt door de hoge concentratie macromoleculen, maar ook door de aanwezigheid van organellen. Bovendien draagt ook de aanwezigheid van het cytoskelet, dat de cel zijn vorm geeft en

dat noodzakelijk is voor voortbeweging, bij aan de toename van de viscositeit van het cytoplasma. Dit cytoskelet is ook een fysieke barrière voor de vrije beweging van moleculen. Het cytoskelet is dynamisch en ondergaat veranderingen, zowel in de tijd als in ruimtelijke zin (Luby-Phelps 2000). De bestudering van de diffusie van vrij GFP (S65T) in *Dictyostelium*cellen met FFS toont aan dat de viscositeit in vegetatieve cellen ongeveer 3.5 maal hoger is dan in water. Om de voortbeweging van cellen in een chemotaxis veroorzakende gradiënt mogelijk te maken ondergaat het cytoskelet snelle ruimtelijke veranderingen. In chemotactische cellen bevindt zich het filamenteuze actine voornamelijk in de cortex van de cel. De gemiddelde cellulaire viscositeit in de niet-cortex gebieden van deze cellen is lager, met een waarde van ongeveer 2.2 maal die van water. De veranderingen in het intracellulaire milieu zouden de bewegingen van eiwitmoleculen kunnen beïnvloeden, en zouden dus consequenties kunnen hebben voor intracellulaire communicatie.

PH-domein diffusie in het cytoplasma van de cel

De translocatie van PH-domein-bevattende eiwitten van het cytoplasma naar het plasmamembraan speelt naar verwachting een belangrijke rol in het mechanisme van chemotaxis van *Dictyostelium*cellen (Parent *et al.,* 1998). In dit proefschrift worden de diffusiekarakteristieken van drie PH-domeinen bestudeerd: PH2, dat behoort bij een eiwit dat nog niet is geïdentificeerd, PH10, dat naar verwachting behoort bij een nieuw eiwit dat homoloog is aan PKB (proteïne kinase B), en PH-CRAC (cytosolische regulator van adenylyl cyclase). Terwijl PH2-GFP homogeen verdeeld is in zowel vegetatieve als chemotactische cellen, bevinden PH10-GFP en PH-CRAC-GFP zich aan de voorkant van chemotactische cellen. Van deze drie domeinen heeft PH10-GFP een langzamere diffusie dan verwacht. Met behulp van PCH is bevestigd dat deze langzame diffusie niet wordt veroorzaakt door aggregatie van het eiwit. Het is dus mogelijk dat het PH-domein interactie heeft met een grote intracellulaire eenheid of wordt vastgehouden in een klein compartiment in het cytoskelet. Van de drie PH domeinen vertoont PH2-GFP een verrassende, licht verhoogde mobiliteit in chemotactische cellen vergeleken met vegetatieve cellen, terwijl de mobiliteit van PH10-GFP en van PH-CRAC-GFP ongewijzigd is. De lagere viscositeit in de niet-cortex gebieden van de chemotactische cellen, vergeleken met die van vegetatieve cellen, heeft dus geen invloed op de diffusie van PH10-GFP en PH-CRAC-GFP. Dit kan het geval zijn als het effect van de verandering in de viscositeit op de diffusie van PH10-GFP en PH-CRAC-GFP wordt tenietgedaan door een ander proces dat plaatsvindt in de gepolariseerde cel. Op dit moment is het niet duidelijk wat dit proces zou kunnen zijn.

Verhoogde mobiliteit van Gβγ in het cytoplasma van chemotactische cellen

The heterotrimere G-eiwitten, bestaande uit Gα, Gβ en Gγ, zijn cruciaal voor signaaloverdrachtsprocessen bij chemotaxis (Manahan *et al.,* 2004). De receptor-gekoppelde activering van het G-eiwit, aan de binnenzijde van het plasmamembraan, zorgt ervoor dat het Gα subunit dissocieert van het Gβγ subunit, dat vervolgens *downstream* gelegen componenten kan moduleren. De Gβ en Gγ subunits, die continu een eenheid vormen, bevinden zich zowel in het cytoplasma als in het membraan. Hoewel aanwezigheid in het membraan essentieel is voor het functioneren van het complex, wordt verondersteld dat de assemblage en de posttranslationele modificaties van Gβγ, en waarschijnlijk ook de interactie met Gα, plaatsvinden in het cytoplasma. FFS metingen van GFP-gelabelde Gβ- en Gγ subunits duiden erop dat de twee subunits zich in een complex bevinden, zowel in vegetatieve als in chemotactische cellen. In chemotactische cellen vertonen zij, in tegenstelling tot PH10 and PH-CRAC, een toename in mobiliteit in het cytoplasma. Echter, deze verandering is minder dan die waargenomen voor vrij GFP. Dit suggereert dat de Gβγ subunits in chemotactische cellen waarschijnlijk een wisselwerking vertonen met andere eiwitten of met intracellulaire eenheden. De diffusie van de subunits in het membraan kan ook worden beïnvloed door een cAMP signaal. Hoewel de subunits een hogere diffusie kunnen hebben ter ondersteuning van snelle signaalverwerking tijdens chemotaxis, kan hun diffusie ook worden vertraagd als gevolg van polymerizatie van actine of myosine in de cortex van de cel. Niettemin is waargenomen dat diffusie van de subunits in het plasmamembraan niet wordt beïnvloed door initiatie van chemotaxis.

Gβγ subunits hebben een snellere diffusie aan de voorkant van chemotactische cellen

In chemotactische cellen vertonen veel van de *downstream* Gβγ componenten een sterk gepolariseerde localisatie. Gβγ evenwel, net als de cAMP receptor cAR1, zijn uniform verdeeld. Eén van de ontbrekende schakels van het mechanisme van chemotaxis is de manier waarop cellen een zwakke extracellulaire gradiënt versterken tot een steile intracellulaire gradiënt, wanneer de ruimtelijke verdeling van de G-eiwitten en receptoren niet gepolariseerd is. De bestudering met FFS van GFP-gelabelde Gβγ subunits toont verrassenderwijs aan dat, hoewel de verdeling van de subunits in de cell uniform is, de diffusie van deze subunits dat niet is (Fig. 1). In het cytoplasma aan de voorkant van de cel vertonen de subunits snellere diffusie dan in het midden of aan de achterkant van de cel. Hoewel deze variabele diffusie binnen een chemotactische cel zelf waarschijnlijk een gevolg is van de polarisatie van het cytoskelet en ophoping van organellen in het midden en aan de achterkant van de cel, impliceert de aanwezigheid

van variabele diffusie dat G-eiwit uit het cytoplasma makkelijker beschikbaar is voor het plasmamembraan aan de voorkant van de cel, daarbij bijdragend aan signaalverwerking aan de voorkant. Bovendien zal deze variabele diffusie bijdragen aan de versterking van de intracellulaire chemotactische respons nadat een initiële polariteit op een ander manier tot stand is gekomen.

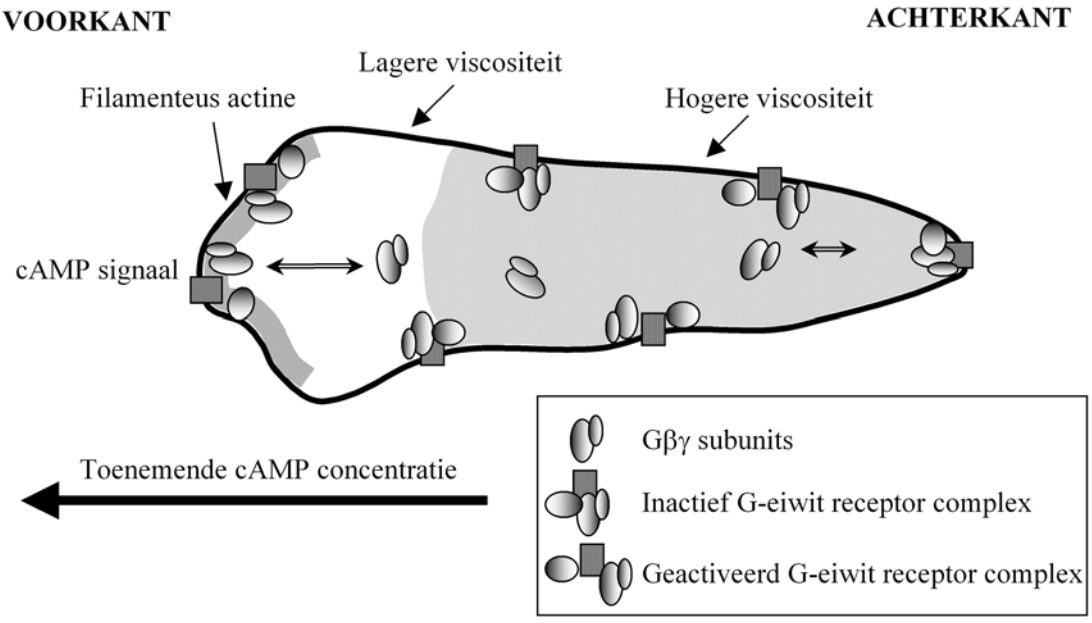

Figuur 1: Signaalversterking door variabele diffusie van Gβγ. De diffusie van Gβγ in de voorkant van de cel is sneller dan in de rest van de cel, waarschijnlijk veroorzaakt door een gepolarizeerd cytoskelet en door ophoping van organellen in het midden en aan de achterkant van de chemotactische cel. Het gevolg is dat G-eiwitten in het cytoplasma makkelijker beschikbaar zijn voor het membraan aan de voorkant van de cel dan aan de achterkant, en zodoende helpen zij bij de signaalverwerking aan de voorkant van de cel. Nadat een initiële polariteit is ontstaan, kan deze variabele diffusie bijdragen aan versterking van de chemotactische respons.

PhLP1 is essentieel voor vorming van het Gβγ complex

De activiteit van het G-eiwit wordt gemoduleerd door phosducine-achtige eiwitten (PhLP). PhLPs binden waarschijnlijk aan vrij Gβγ en remmen zodoende de door G-eiwitten gereguleerde signaalverwerking. In *Dictyostelium*cellen zonder PhLP1 eiwit, is de door G-eiwitten gereguleerde signaalverwerking verrassenderwijs niet verslechterd, maar juist verbeterd. Confocale fluorescentie microscopie van cellen die GFP-Gβ en GFP-Gγ tot expressie brengen, toont aan dat het Gβγ complex niet aanwezig is in het membraan in *phlp1*$^-$ cellen, wat erop duidt dat het Gβγ complex niet wordt gevormd in deze cellen of dat het complex niet in staat is om het membraan te bereiken. Biochemische experimenten tonen aan dat Gβ en Gγ instabiel zijn in *phlp1*$^-$ cellen en bovendien niet posttranslationeel gemodificeerd zijn, wat duidt op de afwezigheid van het Gβγ complex in deze cellen. Dit wordt bevestigd door vergelijking van de

diffusiekarakteristieken van GFP-Gγ in wild-type cellen met die in *phlp1*$^-$ en *gβ*$^-$ cellen. De diffusie van GFP-Gγ in *phlp1*$^-$ en *gβ*$^-$ cellen is vergelijkbaar, maar significant sneller dan in wild-type cellen, wat erop duidt dat in de afwezigheid van PhLP1 het Gγ niet bindt aan het Gβ. PhLP1 speelt dus een rol bij de vorming van het Gβγ complex (Fig. 2). PhLP1 zou kunnen fungeren als een co-chaperone die helpt bij de assemblage van Gβ en Gγ tot een functioneel Gβγ complex.

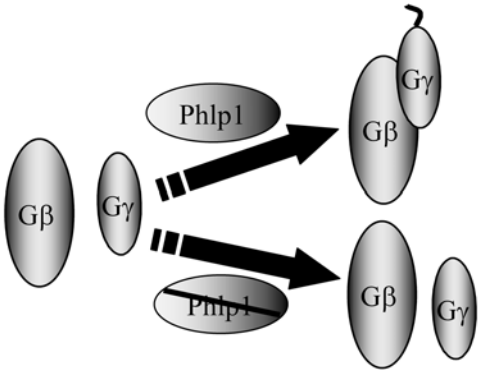

Figuur 2: PhLP1 is essentieel voor de dimeervorming van Gβγ. In cellen zonder PhLP1, heeft Gγ geen lipide-anker en zijn Gβ en Gγ niet met elkaar verbonden.

Conclusies en perspectieven

De activering van signaleringsstappen hangt voor een groot deel af van de diffusiesnelheid waarmee regulerende moleculen door een cel bewegen, en daarom geeft kennis van de diffusiekaraktersitieken van de betrokken moleculen belangrijke informatie over de snelheid van intracellulaire gebeurtenissen in reactie op extracellulaire signalen. Het onderzoek dat in dit proefschrift is beschreven toont aan dat FCS succesvol kan worden toegepast om in detail de diffusie van regulerende moleculen die betrokken zijn bij chemotaxis van *Dictyostelium*cellen te bestuderen. Deze karakterisatie geeft een gedetailleerd beeld van de dynamische gebeurtenissen die de chemotactische respons vormgeven.

De karakterisatie van de diffusie-eigenschappen, de *molecular brightness*, en de concentratie van regulerende moleculen in de cel met behulp van FCS en PCH geeft bovendien waardevolle informatie over de aggregatietoestand en de interacties van deze moleculen. In combinatie met confocale fluorescentie microscopie kunnen details omtrent de locatie van de verschillende moleculen worden verkregen. Deze informatie is essentieel bij het ophelderen van de schakels tussen de verscheidene signaleringsmodules die betrokken zijn bij het mechanisme van chemotaxis.

De FFS technieken die in dit proefschrift worden toegepast verschaffen een schat aan informatie over moleculaire gebeurtenissen in de cel. Waar het onderzoek aan PH-domeinen waardevolle aanwijzingen oplevert betreffende het voorspellen van mogelijke

functies en interacties van de domeinen, hoewel deze functies nog niet zijn gekarakteriseerd, bevestigt het onderzoek naar de rol van PhLP1 in Gβγ dimerizatie de *in vitro* bevindingen in een *in vivo* omgeving. De kracht van deze technieken kan verder worden uitgebreid door eenvoudige modificaties of combinaties met andere technieken. In plaats van *one color* FCS kan bijvoorbeeld *dual color* FCS of fluorescentie cross-correlatie spectroscopy (FCCS) worden gebruikt, om specifieke interacties tussen verschillende moleculen in cellen te bestuderen (Schwille *et al.,* 1997; Haustein and Schwille 2003). Bij deze laatstgenoemde methode wordt de simultane diffusie van twee moleculen die zijn gelabeld met twee verschillende fluoroforen gevolgd. Dit zou een nuttige techniek kunnen zijn voor bijvoorbeeld het volgen van de interactie van PH10 met een potentiële interactie-partner of voor de verdere karakterisatie van de interactie van PhLP1 met het Gβγ complex *in vivo*. Een andere variant, genaamd image correlatie spectroscopie (ICS), kan worden gebruikt voor het verkrijgen van informatie over moleculen met een langzame diffusie in cellen (Petersen *et al.,* 1993; Wiseman and Petersen 1999). Hierbij worden fluorescentiefluctuaties ge-autocorreleerd die per beeldpunt worden vastgelegd met behulp van confocale laser scanning microscopie. Moleculen met een langzame diffusie, zoals de receptor cAR1, kunnen met deze techniek worden bestudeerd. FCS kan ook worden gecombineerd met totale interne reflectie verlichting (TIR-FCS), waardoor het detectievolume wordt gereduceerd en dus de bijdrage van de achtergrondfluorescentie vermindert (Starr and Thompson 2001; Haustein and Schwille 2003). Deze techniek kan worden gebruikt om selectief processen te bestuderen die vlakbij het oppervlak plaatsvinden, bijvoorbeeld de diffusie van receptoren aan de onderzijde van de cel, ligand-receptor associatie-dissociatie kinetiek, of de dynamiek van het cytoskelet.

Chemotaxis is een complex process. In de zoektocht naar de ontbrekende schakels voor het begrijpen van dit proces blijken FFS technieken enorm waardevolle en krachtige hulpmiddelen te zijn.

Bibliography

Aguado-Velasco C, Bretscher MS. (1999). Circulation of the plasma membrane in *Dictyostelium*. *Mol. Biol. Cell* 10: 4419-4427.

Aubin J. (1979). Autofluorescence of viable cultured mammalian cells. *J. Histochem. Cytochem.* 27: 36-43.

Balkwill F. (2004). Cancer and the chemokine network. *Nat. Rev. Cancer* 4: 540-550.

Bauer PH, Muller S, Puzicha M, Pippig S, Obermaier B, Helmreich EJ, Lohse MJ. (1992). Phosducin is a protein kinase A-regulated G-protein regulator. *Nature* 358: 73-76.

Benson R, Meyer R, Zaruba M, McKhann G. (1979). Cellular autofluorescence - is it due to flavins? *J. Histochem. Cytochem.* 27: 44-48.

Bissantz C. (2003). Conformational changes of G protein-coupled receptors during their activation by agonist binding. *J. Recept. Signal Transduct. Res.* 23: 123-153.

Blaauw M, Knol JC, Kortholt A, Roelofs J, Ruchira, Postma M, Visser AJWG, Van Haastert PJM. (2003). Phosducin-like proteins in *Dictyostelium discoideum*: implications for the phosducin family of proteins. *EMBO J.* 22: 5047-5057.

Bohm A, Gaudet R, Sigler PB. (1997). Structural aspects of heterotrimeric G-protein signaling. *Curr. Opin. Biotechnol.* 8: 480-487.

Bordier C. (1981). Phase separation of integral membrane proteins in Triton X-114 solution. *J. Biol. Chem.* 256: 1604-1607.

Bosgraaf L, Russcher H, Smith JL, Wessels D, Soll DR, Van Haastert PJM. (2002). A novel cGMP signalling pathway mediating myosin phosphorylation and chemotaxis in *Dictyostelium*. *EMBO J.* 21: 4560-4570.

Bottomley MJ, Salim K, Panayotou G. (1998). Phospholipid-binding protein domains. *Biochim. Biophys. Acta* 1436: 165-183.

Bretschneider T, Jonkman J, Kohler J, Medalia O, Barisic K, Weber I, Stelzer EH, Baumeister W, Gerisch G. (2002). Dynamic organization of the actin system in the motile cells of *Dictyostelium*. *J. Muscle Res. Cell Motil.* 23: 639-649.

Briddon SJ, Middleton RJ, Cordeaux Y, Flavin FM, Weinstein JA, George MW, Kellam B, Hill SJ. (2004). Quantitative analysis of the formation and diffusion of A1-adenosine receptor-antagonist complexes in single living cells. *Proc. Natl. Acad. Sci. U. S. A.* 101: 4673-4678.

Brock R, Hink MA, Jovin TM. (1998). Fluorescence correlation microscopy of cells in the presence of autofluorescence. *Biophys. J.* 75: 2547-2557.

Brock R, Jovin TM. (2001). Fluorescence correlation microscopy (FCM): fluorescence correlation spectroscopy (FCS) in cell biology. In: Rigler R, Elson ES, editors.

Fluorescence Correlation Spectroscopy: Theory and Applications. Berlin Heidelberg: Springer-Verlag. p 132-161.

Brock R, Vamosi G, Vereb G, Jovin TM. (1999). Rapid characterization of green fluorescent protein fusion proteins on the molecular and cellular level by fluorescence correlation microscopy. *Proc. Natl. Acad. Sci. U. S. A.* 96: 10123-10128.

Brzostowski JA, Johnson C, Kimmel AR. (2002). Gα-mediated inhibition of developmental signal response. *Curr. Biol.* 12: 1199-1208.

Buehr M. (1997). The primordial germ cells of mammals: some current perspectives. *Exp. Cell Res.* 232: 194-207.

Cabrera-Vera TM, Vanhauwe J, Thomas TO, Medkova M, Preininger A, Mazzoni MR, Hamm HE. (2003). Insights into G-protein structure, function, and regulation. *Endocr. Rev.* 24: 765-781.

Chen Y, Müller JD, Berland KM, Gratton E. (1999a). Fluorescence fluctuation spectroscopy. *Methods* 19: 234-252.

Chen Y, Müller JD, Ruan Q, Gratton E. (2002). Molecular brightness characterization of eGFP in vivo by fluorescence fluctuation spectroscopy. *Biophys. J.* 82: 133-144.

Chen Y, Müller JD, So PT, Gratton E. (1999b). The photon counting histogram in fluorescence fluctuation spectroscopy. *Biophys. J.* 77: 553-567.

Chen Y, Wei L-N, Müller JD. (2003). Probing protein oligomerization in living cells with fluorescence fluctuation spectroscopy. *Proc. Natl. Acad. Sci. U. S. A.* 100: 15492-15497.

Chung CY, Firtel RA. (2002). Signaling pathways at the leading edge of chemotaxing cells. *J. Muscle Res. Cell Motil.* 23: 773-779.

Clapham DE, Neer EJ. (1997). G protein βγ subunits. *Annu. Rev. Pharmacol. Toxicol.* 37: 167-203.

Dittrich P, Malvezzi Campeggi F, Jahnz M, Schwille P. (2001). Accessing molecular dynamics in cells by fluorescence correlation spectroscopy. *Biol. Chem.* 382: 491-494.

Drayer AL, Van der Kaay J, Mayr GW, Van Haastert PJM. (1994). Role of phospholipase C in *Dictyostelium*: formation of inositol 1,4,5- trisphosphate and normal development in cells lacking phospholipase C activity. *EMBO J.* 13: 1601-1609.

Dues G, Muller S, Johnsson N. (2001). Detection of a conformational change in Gγ upon binding Gβ in living cells. *FEBS Lett.* 505: 75-80.

Eid JS, Müller JD, Gratton E. (2000). Data acquisition card for fluctuation correlation spectroscopy allowing full access to the detected photon sequence. *Rev. Sci. Instrum.* 71: 361-368.

Eigen M, Rigler R. (1994). Sorting single molecules: application to diagnostics and evolutionary biotechnology. *Proc. Natl. Acad. Sci. U. S. A.* 91: 5740-5747.

Feldman DE, Thulasiraman V, Ferreyra RG, Frydman J. (1999). Formation of the VHL-elongin BC tumor suppressor complex is mediated by the chaperonin TRiC. *Mol. Cell* 4: 1051-1061.

Firtel RA, Chung CY. (2000). The molecular genetics of chemotaxis: sensing and responding to chemoattractant gradients. *BioEssays* 22: 603-615.

Fischer M, Haase I, Simmeth E, Gerisch G, Muller-Taubenberger A. (2004). A brilliant monomeric red fluorescent protein to visualize cytoskeleton dynamics in *Dictyostelium*. *FEBS Lett.* 577: 227-232.

Frydman J. (2001). Folding of newly translated proteins in vivo: the role of molecular chaperones. *Annu. Rev. Biochem.* 70: 603-647.

Garcia-Higuera I, Fenoglio J, Li Y, Lewis C, Panchenko MP, Reiner O, Smith TF, Neer EJ. (1996). Folding of proteins with WD-repeats: comparison of six members of the WD-repeat superfamily to the G protein β subunit. *Biochemistry* 35: 13985-13994.

Garcia-Higuera I, Gaitatzes C, Smith TF, Neer EJ. (1998). Folding a WD repeat propeller: Role of highly conserved aspartic acid residues in the G protein β subunit and Sec13. *J. Biol. Chem.* 273: 9041-9049.

Gaudet R, Bohm A, Sigler PB. (1996). Crystal structure at 2.4 Å resolution of the complex of transducin βγ and its regulator, phosducin. *Cell* 87: 577-588.

Gennerich A, Schild D. (2000). Fluorescence correlation spectroscopy in small cytosolic compartments depends critically on the diffusion model used. *Biophys. J.* 79: 3294-3306.

Gutsche I, Essen LO, Baumeister W. (1999). Group II chaperonins: new TRiC(k)s and turns of a protein folding machine. *J. Mol. Biol.* 293: 295-312.

Hamm HE. (1998). The many faces of G-protein signaling. *J. Biol. Chem.* 273: 669-672.

Hansen WJ, Ohh M, Moslehi J, Kondo K, Kaelin WG, Welch WJ. (2002). Diverse effects of mutations in exon II of the von Hippel-Lindau (VHL) tumor suppressor gene on the interaction of pVHL with the cytosolic chaperonin and pVHL-dependent ubiquitin ligase activity. *Mol. Cell. Biol.* 22: 1947-1960.

Hartl FU, Hayer-Hartl M. (2002). Molecular chaperones in the cytosol: from nascent chain to folded protein. *Science* 295: 1852-1858.

Haustein E, Schwille P. (2003). Ultrasensitive investigations of biological systems by fluorescence correlation spectroscopy. *Methods* 29: 153-166.

Hawes BE, Touhara K, Kurose H, Lefkowitz RJ, Inglese J. (1994). Determination of the Gβγ-binding domain of phosducin. A regulatable modulator of Gβγ signaling. *J. Biol. Chem.* 269: 29825-29830.

Hegener O, Jordan R, Haberlein H. (2002). Benzodiazepine binding studies on living cells: application of small ligands for fluorescence correlation spectroscopy. *Biol. Chem.* 383: 1801-1807.

Hegener O, Prenner L, Runkel F, Baader SL, Kappler J, Haberlein H. (2004). Dynamics of β2-adrenergic receptor-ligand complexes on living cells. *Biochemistry* 43: 6190-6199.

Hekman M, Bauer PH, Sohlemann P, Lohse MJ. (1994). Phosducin inhibits receptor phosphorylation by the β-adrenergic receptor kinase in a PKA-regulated manner. *FEBS Lett.* 343: 120-124.

Hess ST, Huang S, Heikal AA, Webb WW. (2002). Biological and chemical applications of fluorescence correlation spectroscopy: a review. *Biochemistry* 41: 697-705.

Higgins J, Casey P. (1994). In vitro processing of recombinant G protein γ subunits. Requirements for assembly of an active βγ complex. *J. Biol. Chem.* 269: 9067-9073.

Higgins JB, Casey PJ. (1996). The role of prenylation in G-protein assembly and function. *Cellular Signalling* 8: 433-437.

Hink MA, Borst JW, Visser AJ. (2003). Fluorescence correlation spectroscopy of GFP fusion proteins in living plant cells. *Methods Enzymol.* 361: 93-112.

Hink MA, van Hoek A, Visser AJWG. (1999). Dynamics of phospholipid molecules in micelles: Characterization with fluorescence correlation spectroscopy and time-resolved fluorescence anisotropy. *Langmuir* 15: 992-997.

Hirata M, Kanematsu T, Takeuchi H, Yagisawa H. (1998). Pleckstrin homology domain as an inositol compound binding module. *Jpn. J. Pharmacol.* 76: 255-263.

Hirschman JE, De Zutter GS, Simonds WF, Jenness DD. (1997). The Gβγ complex of the yeast pheromone response pathway. Subcellular fractionation and protein-protein interactions. *J. Biol. Chem.* 272: 240-248.

Humrich J, Bermel C, Bunemann M, Harmark L, Frost R, Quitterer U, Lohse MJ. (2005). Phosducin-like protein regulates G-protein βγ folding by interaction with tailless complex polypeptide-1α: dephosphorylation or splicing of PhLP turns the switch toward regulation of Gβγ folding. *J. Biol. Chem.* 280: 20042-20050.

Iijima M, Huang YE, Devreotes P. (2002). Temporal and spatial regulation of chemotaxis. *Dev. Cell* 3: 469-478.

Iniguez-Lluhi J, Simon M, Robishaw J, Gilman A. (1992). G protein βγ subunits synthesized in Sf9 cells. Functional characterization and the significance of prenylation of γ. *J. Biol. Chem.* 267: 23409-23417.

Insall R. (2003). *Dictyostelium* chemotaxis: fascism through the back door? *Curr. Biol.* 13: R353-354.

Janetopoulos C, Jin T, Devreotes PN. (2001). Receptor-mediated activation of heterotrimeric G-proteins in living cells. *Science* 291: 2408-2411.

Jin T, Amzel M, Devreotes PN, Wu L. (1998). Selection of Gβ subunits with point mutations that fail to activate specific signaling pathways in vivo: dissecting cellular responses mediated by a heterotrimeric G protein in *Dictyostelium discoideum*. *Mol. Biol. Cell* 9: 2949-2961.

Jin T, Zhang N, Long Y, Parent CA, Devreotes PN. (2000). Localization of the G protein βγ complex in living cells during chemotaxis. *Science* 287: 1034-1036.

Johnson ML, Flaunt LM. (1992). Parameter estimation by least-squares methods. *Methods Enzymol.* 210: 1-37.

Kasahara S, Wang P, Nuss DL. (2000). Identification of bdm-1, a gene involved in G protein beta-subunit function and alpha-subunit accumulation. *Proc. Natl. Acad. Sci. U. S. A.* 97: 412-417.

Kask P, Palo K, Ullmann D, Gall K. (1999). Fluorescence-intensity distribution analysis and its application in biomolecular detection technology. *Proc. Natl. Acad. Sci. U. S. A.* 96: 13756-13761.

Kayman S, Clarke M. (1983). Relationship between axenic growth of *Dictyostelium discoideum* strains and their track morphology on substrates coated with gold particles. *J. Cell Biol.* 97: 1001-1010.

Kim JY, Caterina MJ, Milne JL, Lin KC, Borleis JA, Devreotes PN. (1997). Random mutagenesis of the cAMP chemoattractant receptor, cAR1, of *Dictyostelium*. Mutant classes that cause discrete shifts in agonist affinity and lock the receptor in a novel activational intermediate. *J. Biol. Chem.* 272: 2060-2068.

Kim SA, Schwille P. (2003). Intracellular applications of fluorescence correlation spectroscopy: prospects for neuroscience. *Curr. Opin. Neurobiol.* 13: 583-590.

Kimmel AR, Parent CA. (2003). The signal to move: *D. discoideum* go orienteering. *Science* 300: 1525-1527.

Knol JC, Engel R, Blaauw M, Visser AJWG, Van Haastert PJM. (2005). The phosducin-like protein PhLP1 is essential for Gβγ dimer formation in *Dictyostelium*. *Mol. Cell. Biol.* In press.

Köhler RH, Schwille P, Webb WW, Hanson MR. (2000). Active protein transport through plastid tubules: velocity quantified by fluorescence correlation spectroscopy. *J. Cell Sci.* 113: 3921-3930.

Kriebel PW, Barr VA, Parent CA. (2003). Adenylyl cyclase localization regulates streaming during chemotaxis. *Cell* 112: 549-560.

Lambright DG, Sondek J, Bohm A, Skiba NP, Hamm HE, Sigler PB. (1996). The 2.0 Å crystal structure of a heterotrimeric G protein. *Nature* 379: 311-319.

Lee RH, Lieberman BS, Lolley RN. (1987). A novel complex from bovine visual cells of a 33,000-dalton phosphoprotein with β- and γ-transducin: purification and subunit structure. *Biochemistry* 26: 3983-3990.

Lee RH, Ting TD, Lieberman BS, Tobias DE, Lolley RN, Ho YK. (1992). Regulation of retinal cGMP cascade by phosducin in bovine rod photoreceptor cells. Interaction of phosducin and transducin. *J. Biol. Chem.* 267: 25104-25112.

Lemmon MA, Ferguson KM. (2000). Signal-dependent membrane targeting by pleckstrin homology (PH) domains. *Biochem. J.* 350: 1-18.

Leroux MR, Hartl FU. (2000). Protein folding: versatility of the cytosolic chaperonin TRiC/CCT. *Curr. Biol.* 10: R260-264.

Levin MK, Carson JH. (2004). Fluorescence correlation spectroscopy and quantitative cell biology. *Differentiation* 72: 1-10.

Li WZ, Lin P, Frydman J, Boal TR, Cardillo TS, Richard LM, Toth D, Lichtman MA, Hartl FU, Sherman F *et al.,*. (1994). Tcp20, a subunit of the eukaryotic TRiC chaperonin from humans and yeast. *J. Biol. Chem.* 269: 18616-18622.

Lilly P, Wu L, Welker D, Devreotes P. (1993). A G-protein β-subunit is essential for *Dictyostelium* development. *Genes Dev.* 7: 986-995.

Loew A, Ho Y-K, Blundell T, Bax B. (1998). Phosducin induces a structural change in transducin βγ. *Structure* 6: 1007-1019.

Luby-Phelps K. (2000). Cytoarchitecture and physical properties of cytoplasm: volume, viscosity, diffusion, intracellular surface area. *Int. Rev. Cytol.* 192: 189-221.

Luby-Phelps K, Taylor DL, Lanni F. (1986). Probing the structure of cytoplasm. *J. Cell Biol.* 102: 2015-2022.

Lukov GL, Hu T, McLaughlin JN, Hamm HE, Willardson BM. (2005). Phosducin-like protein acts as a molecular chaperone for G protein βγ dimer assembly. *EMBO J.* 24: 1965-1975.

Magde D, Elson EL, Webb WW. (1974). Fluorescence correlation spectroscopy. II. An experimental realization. *Biopolymers* 13: 29-61.

Manahan CL, Iglesias PA, Long Y, Devreotes PN. (2004). Chemoattractant signaling in *Dictyostelium discoideum*. *Annu. Rev. Cell. Dev. Biol.* 20: 223-253.

Martin P, Parkhurst SM. (2004). Parallels between tissue repair and embryo morphogenesis. *Development* 131: 3021-3034.

Martin-Benito J, Bertrand S, Hu T, Ludtke PJ, McLaughlin JN, Willardson BM, Carrascosa JL, Valpuesta JM. (2004). Structure of the complex between the cytosolic chaperonin CCT and phosducin-like protein. *Proc. Natl. Acad. Sci. U. S. A.* 101: 17410-17415.

Mato JM, Losada A, Nanjundiah V, Konijn TM. (1975). Signal input for a chemotactic response in the cellular slime mold *Dictyostelium discoideum*. *Proc. Natl. Acad. Sci. U. S. A.* 72: 4991-4993.

McLaughlin JN, Thulin CD, Bray SM, Martin MM, Elton TS, Willardson BM. (2002). Regulation of angiotensin II-induced G protein signaling by phosducin-like protein. *J. Biol. Chem.* 277: 34885-34895.

Medina MA, Schwille P. (2002). Fluorescence correlation spectroscopy for the detection and study of single molecules in biology. *BioEssays* 24: 758-764.

Mende U, Schmidt CJ, Yi F, Spring DJ, Neer EJ. (1995). The G protein γ subunit. Requirements for dimerization with β subunits. *J. Biol. Chem.* 270: 15892-15898.

Meseth U, Wohland T, Rigler R, Vogel H. (1999). Resolution of fluorescence correlation measurements. *Biophys. J.* 76: 1619-1631.

Morris AJ, Malbon CC. (1999). Physiological regulation of G-protein-linked signaling. *Physiol. Rev.* 79: 1373-1430.

Muntz KH, Sternweis PC, Gilman AG, Mumby SM. (1992). Influence of γ subunit prenylation on association of guanine nucleotide-binding regulatory proteins with membranes. *Mol. Biol. Cell* 3: 49-61.

Murzin AG. (1992). Structural principles for the propeller assembly of β-sheets: the preference for seven-fold symmetry. *Proteins* 14: 191-201.

Neer EJ, Smith TF. (2000). A groovy new structure. *Proc. Natl. Acad. Sci. U. S. A.* 97: 960-962.

Ormö M, Cubitt AB, Kallio K, Gross LA, Tsien RY, Remington SJ. (1996). Crystal structure of the *Aequorea victoria* green fluorescent protein. *Science* 273: 1392-1395.

Parent CA. (2004). Making all the right moves: chemotaxis in neutrophils and *Dictyostelium*. *Curr. Opin. Cell Biol.* 16: 4-13.

Parent CA, Blacklock BJ, Froehlich WM, Murphy DB, Devreotes PN. (1998). G-protein signaling events are activated at the leading edge of chemotactic cells. *Cell* 95: 81-91.

Petersen NO, Höddelius PL, Wiseman PW, Seger O, Magnusson K-E. (1993). Quantitation of membrane receptor distributions by image correlation spectroscopy: Concept and application. *Biophys. J.* 65: 1135-1146.

Politz JC, Browne ES, Wolf DE, Pederson T. (1998). Intranuclear diffusion and hybridization state of oligonucleotides measured by fluorescence correlation spectroscopy in living cells. *Proc. Natl. Acad. Sci. U. S. A.* 95: 6043-6048.

Postma M, Bosgraaf L, Loovers HM, Van Haastert PJ. (2004). Chemotaxis: signalling modules join hands at front and tail. *EMBO Rep.* 5: 35-40.

Potma EO, de Boeij WP, Bosgraaf L, Roelofs J, Van Haastert PJ, Wiersma DA. (2001). Reduced protein diffusion rate by cytoskeleton in vegetative and polarized *Dictyostelium* cells. *Biophys. J.* 81: 2010-2019.

Pramanik A, Thyberg P, Rigler R. (2000). Molecular interactions of peptide with phospholipid vesicle membranes as studied by fluorescence correlation spectroscopy. *Chem. Phys. Lipids* 104: 35-47.

Pronin AN, Gautam N. (1993). Proper processing of a G protein γ subunit depends on complex formation with a β subunit. *FEBS Lett.* 328: 89-93.

Roelofs J, Meima M, Schaap P, Van Haastert PJ. (2001a). The *Dictyostelium* homologue of mammalian soluble adenylyl cyclase encodes a guanylyl cyclase. *EMBO J.* 20: 4341-4348.

Roelofs J, Snippe H, Kleineidam RG, Van Haastert PJ. (2001b). Guanylate cyclase in *Dictyostelium discoideum* with the topology of mammalian adenylate cyclase. *Biochem. J.* 354: 697-706.

Roelofs J, Van Haastert PJ. (2002). Characterization of two unusual guanylyl cyclases from *Dictyostelium*. *J. Biol. Chem.* 277: 9167 - 9174.

Ruan Q, Chen Y, Gratton E, Glaser M, Mantulin WW. (2002). Cellular characterization of adenylate kinase and its isoform: Two-photon excitation fluorescence imaging and fluorescence correlation spectroscopy. *Biophys. J.* 83: 3177-3187.

Rubin H, Ravid S. (2002). Polarization of myosin II heavy chain-protein Kinase C in chemotaxing *Dictyostelium* cells. *J. Biol. Chem.* 277: 36005-36008.

Ruchira, Hink MA, Bosgraaf L, Van Haastert PJM, Visser AJWG. (2004). Pleckstrin homology domain diffusion in *Dictyostelium* cytoplasm studied using fluorescence correlation spectroscopy. *J. Biol. Chem.* 279: 10013-10019.

Savage JR, McLaughlin JN, Skiba NP, Hamm HE, Willardson BM. (2000). Functional roles of the two domains of phosducin and phosducin-like protein. *J. Biol. Chem.* 275: 30399-30407.

Schmidt CJ, Neer EJ. (1991). In vitro synthesis of G protein βγ dimers. *J. Biol. Chem.* 266: 4538-4544.

Schmidt CJ, Thomas TC, Levine MA, Neer EJ. (1992). Specificity of G-protein β and γ subunit interactions. *J. Biol. Chem.* 267: 13807-13810.

Schroder S, Bluml K, Dees C, Lohse MJ. (1997). Identification of a C-terminal binding site for G-protein βγ-subunits in phosducin-like protein. *FEBS Lett.* 401: 243-246.

Schroder S, Lohse MJ. (1996). Inhibition of G-protein βγ-subunit functions by phosducin-like protein. *Proc. Natl. Acad. Sci. U. S. A.* 93: 2100-2104.

Schwille P, Haupts U, Maiti S, Webb WW. (1999). Molecular dynamics in living cells observed by fluorescence correlation spectroscopy with one- and two-photon excitation. *Biophys. J.* 77: 2251-2265.

Schwille P, Meyer-Almes FJ, Rigler R. (1997). Dual-color fluorescence cross-correlation spectroscopy for multicomponent diffusional analysis in solution. *Biophys. J.* 72: 1878-1886.

Schwindinger WF, Robishaw JD. (2001). Heterotrimeric G-protein βγ-dimers in growth and differentiation. *Oncogene* 20: 1653-1660.

Shaner NC, Campbell RE, Steinbach PA, Giepmans BNG, Palmer AE, Tsien RY. (2004). Improved monomeric red, orange and yellow fluorescent proteins derived from *Discosoma sp.* red fluorescent protein. *Nat. Biotech.* 22: 1567-1572.

Siegers K, Bolter B, Schwarz JP, Bottcher UM, Guha S, Hartl FU. (2003). TRiC/CCT cooperates with different upstream chaperones in the folding of distinct protein classes. *EMBO J.* 22: 5230-5240.

Simonds WF, Butrynski JE, Gautam N, Unson CG, Spiegel AM. (1991). G-protein βγ dimers. Membrane targeting requires subunit coexpression and intact gamma C-A-A-X domain. *J. Biol. Chem.* 266: 5363-5366.

Skakun VV, Hink MA, Digris AV, Engel R, Novikov EG, Apanasovich VV, Visser AJ. (2005). Global analysis of fluorescence fluctuation data. *Eur. Biophys. J.* 34: 323-334.

Smith TF, Gaitatzes C, Saxena K, Neer EJ. (1999). The WD repeat: a common architecture for diverse functions. *Trends Biochem. Sci.* 24: 181-185.

Sondek J, Bohm A, Lambright DG, Hamm HE, Sigler PB. (1996). Crystal structure of a G-protein βγ dimer at 2.1 angstrom resolution. *Nature* 379: 369-374.

Sprang SR. (1997). G-protein mechanisms: insights from structural analysis. *Annu. Rev. Biochem.* 66: 639-678.

Starr TE, Thompson NL. (2001). Total internal reflection with fluorescence correlation spectroscopy: Combined surface reaction and solution diffusion. *Biophys. J.* 80: 1575-1584.

Straume M, Frasier-Cadoret SG, Johnson ML. (1991). Least-Squares Analysis of Fluorescence Data. In: Lakowicz JR, editor. Topics in Fluorescence. New York: Kluwer Academic Publishers. p 177-240.

Swanson JA, Lansing Taylor D. (1982). Local and spatially coordinated movements in *Dictyostelium discoideum* amoebae during chemotaxis. *Cell* 28: 225-232.

Thelen M. (2001). Dancing to the tune of chemokines. *Nat. Immunol.* 2: 129-134.

Thibault C, Sganga MW, Miles MF. (1997). Interaction of phosducin-like protein with G protein βγ subunits. *J. Biol. Chem.* 272: 12253-12256.

Traynor D, Milne JL, Insall RH, Kay RR. (2000). Ca(2+) signalling is not required for chemotaxis in *Dictyostelium*. *EMBO J.* 19: 4846-4854.

Tsien RY. (1998). The green fluorescent protein. *Annu. Rev. Biochem.* 67: 509-544.

Uchida KSK, Yumura S. (2004). Dynamics of novel feet of *Dictyostelium* cells during migration. *J. Cell Sci.* 117: 1443-1455.

Ueda M, Sako Y, Tanaka T, Devreotes P, Yanagida T. (2001). Single-molecule analysis of chemotactic signaling in *Dictyostelium* cells. *Science* 294: 864-867.

Ursic D, Culbertson MR. (1991). The yeast homolog to mouse Tcp-1 affects microtubule-mediated processes. *Mol. Cell. Biol.* 11: 2629-2640.

Valpuesta JM, Martin-Benito J, Gomez-Puertas P, Carrascosa JL, Willison KR. (2002). Structure and function of a protein folding machine: the eukaryotic cytosolic chaperonin CCT. *FEBS Lett.* 529: 11-16.

Varnai P, Lin X, Lee SB, Tuymetova G, Bondeva T, Spat A, Rhee SG, Hajnoczky G, Balla T. (2002). Inositol lipid binding and membrane localization of isolated pleckstrin homology (PH) domains - Studies on the PH domains of phospholipase C delta(1) and p130. *J. Biol. Chem.* 277: 27412-27422.

Veltman DM, Roelofs J, Engel R, Visser AJWG, Van Haastert PJM. (2005). Activation of soluble guanylyl cyclase at the leading edge during *Dictyostelium* chemotaxis. *Mol. Biol. Cell* 16: 976-983.

Visser AJWG, vdBerg PAW, Hink MA, Petushkov VN. (2001). Fluorescence correlation spectroscopy of flavins and flavoproteins. In: Rigler R, Elson ES, editors. Fluorescence Correlation Spectroscopy: Theory and Applications. Berlin Heidelberg: Springer-Verlag. p 9 - 24.

Vukojevic V, Pramanik A, Yakovleva T, Rigler R, Terenius L, Bakalkin G. (2005). Study of molecular events in cells by fluorescence correlation spectroscopy. *Cell. Mol. Life Sci.* 62: 535-550.

Wachsmuth M, Waldeck W, Langowski J. (2000). Anomalous diffusion of fluorescent probes inside living cell nuclei investigated by spatially-resolved fluorescence correlation spectroscopy. *J. Mol. Biol.* 298: 677-689.

Wall MA, Coleman DE, Lee E, Iniguez-Lluhi JA, Posner BA, Gilman AG, Sprang SR. (1995). The structure of the G protein heterotrimer Giα1β1γ2. *Cell* 83: 1047-1058.

Wang Q, Mullah BK, Robishaw JD. (1999). Ribozyme approach identifies a functional association between the G protein $\beta_1\gamma_7$ subunits in the beta-adrenergic receptor signaling pathway. *J. Biol. Chem.* 274: 17365-17371.

Wedegaertner PB, Wilson PT, Bourne HR. (1995). Lipid modifications of trimeric G-proteins. *J. Biol. Chem.* 270: 503-506.

Weiss M, Elsner M, Kartberg F, Nilsson T. (2004). Anomalous subdiffusion is a measure for cytoplasmic crowding in living cells. *Biophys. J.* 87: 3518-3524.

Weiss M, Hashimoto H, Nilsson T. (2003). Anomalous protein diffusion in living cells as seen by fluorescence correlation spectroscopy. *Biophys. J.* 84: 4043-4052.

Wessels D, Soll D. (1990). Myosin II heavy chain null mutant of *Dictyostelium* exhibits defective intracellular particle movement. *J. Cell Biol.* 111: 1137-1148.

Widengren J. (2001). Photophysical aspects of FCS measurements. In: Rigler R, Elson ES, editors. Fluorescence correlation spectroscopy: theory and applications. Berlin Heidelberg: Springer-Verlag. p 276-301.

Wiseman PW, Petersen NO. (1999). Image correlation spectroscopy. II. Optimization for ultrasensitive detection of preexisting platelet-derived growth factor-beta receptor oligomers on intact cells. *Biophys. J.* 76: 963-977.

Wu L, Valkema R, Van Haastert PJ, Devreotes PN. (1995). The G protein β subunit is essential for multiple responses to chemoattractants in *Dictyostelium*. *J. Cell Biol.* 129: 1667-1675.

Xiao Z, Zhang N, Murphy DB, Devreotes PN. (1997). Dynamic distribution of chemoattractant receptors in living cells during chemotaxis and persistent stimulation. *J. Cell Biol.* 139: 365-374.

Xu J, Wu D, Slepak VZ, Simon MI. (1995). The N terminus of phosducin is involved in binding of $\beta\gamma$ subunits of G-protein. *Proc. Natl. Acad. Sci. U. S. A.* 92: 2086-2090.

Xu X, Meier-Schellersheim M, Jiao X, Nelson LE, Jin T. (2005). Quantitative imaging of single live cells reveals spatiotemporal dynamics of multistep signaling events of chemoattractant gradient sensing in *Dictyostelium*. *Mol. Biol. Cell* 16: 676-688.

Yanai M, Butler JP, Suzuki T, Kanda A, Kurachi M, Tashiro H, Sasaki H. (1999). Intracellular elasticity and viscosity in the body, leading, and trailing regions of locomoting neutrophils. *Am. J. Physiol. Cell Physiol.* 277: C432-440.

Yanai M, Butler JP, Suzuki T, Sasaki H, Higuchi H. (2004). Regional rheological differences in locomoting neutrophils. *Am. J. Physiol. Cell Physiol.* 287: C603-611.

Yeagle PL, Albert AD. (2003). A conformational trigger for activation of a G-protein by a G-protein-coupled receptor. *Biochemistry* 42: 1365-1368.

Yoshida N, Kinjo M, Tamura M. (2001). Microenvironment of endosomal aqueous phase investigated by the mobility of microparticles using fluorescence correlation spectroscopy. *Biochem. Biophys. Res. Commun.* 280: 312-318.

Yumura S, Fukui Y. (1998). Spatiotemporal dynamics of actin concentration during cytokinesis and locomotion in *Dictyostelium*. *J. Cell Sci.* 111: 2097-2108.

Zhang FL, Casey PJ. (1996). Protein prenylation: molecular mechanisms and functional consequences. *Annu. Rev. Biochem.* 65: 241-269.

Zhang N, Long Y, Devreotes PN. (2001). Gγ in *Dictyostelium*: Its role in localization of Gβγ to the membrane is required for chemotaxis in shallow gradients. *Mol. Biol. Cell* 12: 3204-3213.

List of Abbreviations

ACA	Adenylyl Cyclase A
cAMP	Adenosine 3′,5′-cyclic monophosphate
cAR	cAMP Receptor
CCT	Chaperonin Containing T-complex Polypeptide 1
cGMP	Guanosine 3′,5′-cyclic monophosphate
CLSM	Confocal Laser Scanning Microscopy
CRAC	Cytosolic Regulator of Adenylyl Cyclase
DIC	Differential Interference Contrast
eGFP	Enhanced GFP
F-Actin	Filamentous Actin
FCCS	Fluorescence Cross Correlation Spectroscopy
FCS	Fluorescence Correlation Spectroscopy
FFS	Fluorescence Fluctuation Spectroscopy
FIDA	Fluorescence Intensity Distribution Analysis
FMN	Flavin MonoNucleotide
FRAP	Fluorescence Recovery After Photobleaching
FRET	Förster Resonance Energy Transfer
FSPIM	Fluorescence Spectral Imaging Microscopy
GC	Guanylyl Cyclase
GFP	Green Fluorescent Protein
GPCR	G-Protein Coupled Receptor
G-protein	Guanosine Triphosphate Binding Protein
ICS	Image Correlation Spectroscopy
mRFP	Monomeric Red Fluorescent Protein
PCH	Photon Counting Histogram
PH	Pleckstrin Homology
PhLP1	Phosducin Like Protein 1
PI3K	Phophoinositide 3-Kinase
PLC	Phospholipase C
PTEN	PI3 phosphotase
TIR-FCS	Total Internal Reflection FCS
WD repeat	Tryptophan-Aspartate repeat

Education Statement of the Graduate School

Experimental Plant Sciences

Issued to: Ruchira
Date: 20 September 2005
Group: Wageningen University, Laboratory of Biochemistry

1. Start-up Phase	Date
First presentation of the project	
• "Fluidity in Different Areas of a *Dictyostelium* Cell during Chemotaxis"	Nov 2000
Writing a project proposal	
Writing literature study chapter for Thesis	
• "General Introduction"	Start: Mar 2001
MSc courses	
Laboratory use of isotopes	
Subtotal Start-up Phase	*4 credits**

2. Scientific Exposure	Date
EPS PhD student days	
• Wageningen University	Jan 25, 2001
EPS theme symposia	
• Leiden University	Feb 6, 2003
Attendance regular research discussions of the laboratory	2000 - 2004
National meetings	
• Studiegroep Eiwitonderzoek Lunteren	Dec 11-12, 2000
• The first DFG/NWO Meeting: 'Entering the Living Cell'	Sep 28-30, 2001
• Studiegroep Eiwitonderzoek Lunteren	Dec 10-11, 2001
• Studiegroep Eiwitonderzoek Lunteren	Dec 09-10, 2002
• Studiegroep Eiwitonderzoek Lunteren	Dec 08-09, 2003
• Studiegroep Lipiden en Biomembranen	Mar 08-09, 2004
Seminars (series), workshops and symposia	
• Biocentrum Amsterdam-NVBM fall symposium: 'Into the Living Cell and Beyond'	Nov 17, 2000
• Biocentrum Amsterdam: 'Diffusion, Active Transport and Traffic Jams in Biology'	Dec 14, 2000
• Biocentrum Amsterdam: 'Confocal Light Microscopy - Fundamentals and Biological Applications'	May 07-11, 2001

• Biocentrum Amsterdam-NVBM fall symposium: 'Protein-Protein Interactions in Cells: the Biochemistry of Signalling'	Nov 05, 2003
International symposia and conferences	
• 7th Conference on Methods and Applications of Fluorescence, Amsterdam	Sep 16-19, 2001
• 46th Annual Biophysical Society Meeting, San Francisco, USA	Feb 23-27, 2002
• 47th Annual Biophysical Society Meeting, San Antonio, USA	Mar 01-05, 2003
Presentations (Oral)	
• Introduction to Fluorescence Correlation Microscopy, NWO meeting Lunteren	Oct 2002
• Investigating Protein Dynamics in *Dictyostelium* cells, NWO meeting Lunteren	Dec 2002
• Investigating Protein Dynamics in *Dictyostelium* cells, EPS Theme day, Leiden	Feb 2003
• Protein Dynamics in *Dictyostelium* cells, Biophysical Society Meeting, San Antonio, USA	Mar 2003
• Protein Diffusion in *Dictyostelium* cells, Altleiningen, Germany	Apr 2003
• G-protein Dynamics & Ligand-Receptor Interaction in *Dictyostelium* cells characterized using FCS, NWO meeting Lunteren	Mar 2004
• Introduction to Fluorescence Correlation Spectroscopy; Course for PhD students, Erasmus MC, Rotterdam	Nov 2004
Excursion	
Subtotal Scientific Exposure	*15 credits**

3. In-Depth Studies	Date
EPS courses or other PhD course	
• FEBS Advanced Course: Microspectroscopy in Biology	Oct 29 - Nov 03, 2000
• Focus on Microscopy, Amsterdam	Apr 01-04, 2001
• 5th International Carl Zeiss Workshop on FCS and Related Methods	Apr 25-27, 2001
• Post-doc and PhD Student Workshop on Single Molecule Detection in living Cells, Altleiningen	Apr 27-May 01, 2003
• Advanced Practical Course on Optical Spectroscopy in Biology, Juelich, Germany	Oct 10-14, 2004
Journal club	
Individual research training	
• Training on working with *Dictyostelium* cells in lab of Prof. P.J.M. van Haastert	Dec 2000
• Visit to Prof. P. Devreotes' lab at John Hopkins University School of Med, Baltimore, USA, to learn about *Dictyostelium*	Mar 2002
Subtotal In-Depth Studies	*6 credits**

4. Personal Development	Date
Skill training courses	
Organisation of PhD students day, course or conference	
Membership of Board, Committee or PhD council	
Subtotal Personal Development	*credits**
TOTAL NUMBER OF CREDIT POINTS*	25

* A credit represents a normative study load of 42 hours of study

Publications

R. Engel, J.C. Knol, M. Blaauw, P.J.M. van Haastert and A.J.W.G. Visser. (2005) Characterization of G-protein βγ complex diffusion in chemotaxing *Dictyostelium* cells. *Manuscript in preparation*

R. Engel, P.J.M. van Haastert and A.J.W.G. Visser. (2005) Characterization of *Dictyostelium* autofluorescence using fluorescence microscopy. *Submitted*

J.C. Knol[#], **R. Engel**[#], M. Blaauw, A.J.W.G. Visser and P.J.M. van Haastert. (2005) The phosducin like protein PhLP1 is essential for Gβγ dimer formation in *Dictyostelium*. *Mol. Cell. Biol.* In press ([#] both authors contributed equally).

L. Bosgraaf, A. Waijer, **R. Engel**, A.J.W.G. Visser, D. Wessels, D. Soll and P.J.M. van Haastert. (2005) RasGEF-containing proteins GbpC and GbpD have differential effects on cell polarity and chemotaxis in *Dictyostelium*. *J. Cell Sci.* 118: 1899-1910.

V.V. Skakun, MA. Hink, A.V. Digris, **R. Engel**, E.G. Novikov, V.V. Apanasovich and A.J.W.G. Visser. (2005) Global analysis of fluorescence fluctuation data. *Eur. Biophys. J.* 34: 323-334.

D.M. Veltman, J. Roelofs, **R. Engel**, A.J.W.G. Visser and P.J.M. van Haastert. (2005) Activation of soluble guanylyl cyclase at the leading edge during *Dictyostelium* chemotaxis. *Mol. Biol. Cell* 16: 976-983.

Ruchira, M.A. Hink, L. Bosgraaf, P.J.M. van Haastert and A.J.W.G. Visser. (2004) Pleckstrin homology domain diffusion in *Dictyostelium* cytoplasm studied using fluorescence correlation spectroscopy. *J. Biol. Chem.* 279: 10013-10019

M. Blaauw, J.C. Knol, A. Kortholt, J. Roelofs, **Ruchira**, M. Postma, A.J.W.G. Visser and P.J.M. van Haastert. (2003) Phosducin-like proteins in *Dictyostelium* discoideum: implications for the phosducin family of proteins. *EMBO J.* 22: 5047-5057

About the author

Ruchira, the author of this thesis, was born in Bangalore, India on the 3rd of October 1976. She finished her schooling in May 1994 from Kendriya Vidyalaya, Mumbai and then joined the Ramnarain Ruia College at the University of Mumbai. There she followed a bachelor's course in botany, zoology and chemistry, and graduated with a specialization in chemistry in 1997. The same year she joined the Department of Chemistry at the University of Pune for a master's course in chemistry. During this period she worked on a 6-months research project, under the supervision of Dr. L. S. Prabhumirashi, to study the excited state dissociation constant of various substituted benzoic acids using UV-visible spectrophotometry. In 1999, she was awarded an M.Sc. in physical chemistry. From June 1999 till May 2000 Ruchira was employed as a research officer at Unilever Research India, Bangalore. There she studied the binding and removal of composite environmental soil from commercial textiles. In October 2000, the author began work on the PhD project, the results of which are described in this thesis, in the Department of Biochemistry at Wageningen University, The Netherlands. The research work was carried out under the supervision of Prof. Dr. A.J.W.G. Visser (Wageningen University) and Prof. Dr. P.J.M. van Haastert (Groningen University). Since March 2005, the author is working as a post-doctoral researcher in the Department of Biochemistry at Wageningen University, on a project titled "Protein (un)folding studied by single molecule optical detection techniques". The research on this project is supervised by Prof. Dr. A.J.W.G. Visser and Dr. C.P.M. van Mierlo.

Ruchira
Dictyostelium chemotaxis studied with fluorescence fluctuation spectroscopy
Title in Dutch:
Dictyostelium chemotaxis bestudeerd met fluorescentie fluctuatie spectroscopie
Thesis Wageningen University, The Netherlands
With references – with summary in Dutch
ISBN: 90-8504-263-1

Cover: Chemotaxing *Dictyostelium* cells and cartoon representation of a model of GFP tagged G-protein.

The research described in this thesis was performed in the Laboratory of Biochemistry of Wageningen University, The Netherlands. The investigations were (in part) supported by the Research Council for Earth and Life Sciences (ALW) with financial aid from Netherlands Organisation for Scientific Research (NWO).